

**GENETIC DISSECTION OF HEART DEVELOPMENT IN  
THE FRUIT FLY *DROSOPHILA MELANOGASTER***

APPROVED BY SUPERVISORY COMMITTEE

---

Eric N. Olson, Ph.D.

---

Alfred G. Gilman, M.D., Ph.D.

---

John M. Abrams, Ph.D.

---

Jin Jiang, Ph.D.

**TO MY BELOVED WIFE**

**WEI ZHANG**

**AND MY PARENTS**

## **ACKNOWLEDGEMENTS**

I am extremely grateful to my mentor, Dr. Eric Olson, who has been the greatest mentor to me. His great insights and passions in science really inspired me throughout my graduate study. The questions he asked in lab meetings and the discussions with him about the projects always keep me in the right track. I think I am super lucky to have the chance to work under the guidance of Eric in the past four years.

My deepest gratitude also goes to Dr. Rhonda Bassel-Duby for her everyday help. She has always been so patient to help me prepare all the presentations.

I'd like to thank my committee members, Dr. Alfred Gilman, Dr. John Abrams and Dr. Jin Jiang for their advices.

I want to thank Dr. Zhe Han, who is now Assistant Professor in University of Michigan. He taught me how to do the fly works from the very beginning in every detail. I really enjoyed the time when we discussed our projects and worked together on the paper. I wish all the best for his own lab. I want to thank Rene Garlindo and Aaron Johnson for their insightful and encouraging discussion. I also thank Xiumin Li for her great technical support making transgenic flies, and Jiang Wu for his kind help every day for caring the fly stocks and setting crosses.

My gratitude also goes to Alisha Tizenor for her beautiful graphic work and teaching me how to do all the fancy graphic tricks.

I'd like to thank my roommates Kunhua Song, Andrew Williams, Ning Liu, Guo Huang, Drazen Susic, Jens Fielitz, Mark Hatley and Ana Barbosa for discussions and help every day. I'd like to thank my basketball teammates, Matt Potthof, Shusheng Wang, Chad Grueter, Andrew Williams. I enjoyed the time so much playing balls in the gym with them. I also want to thank all the other members of the Olson lab for their support and friendship, and for making such a pleasant environment.

I'd like to thank the great *Drosophila* research community for sharing mutant flies, reagents and ideas. They have made the *Drosophila* the best model system to work with.

Finally, I want to give my greatest thanks to my wife Wei Zhang, my father Xianwei Yi and my mother Guohua Ding. They have always been there supporting me and believing in me. Without their love and support, I could never be able to finish my graduate study.

**GENETIC DISSECTION OF HEART DEVELOPMENT IN  
THE FRUIT FLY *DROSOPHILA MELANOGASTER***

by

**PENG YI**

**DISSERTATION**

Presented to the Faculty of the Graduate School of Biomedical Sciences

The University of Texas Southwestern Medical Center at Dallas

In Partial Fulfillment of the Requirements

For the Degree of

**DOCTOR OF PHILOSOPHY**

The University of Texas Southwestern Medical Center at Dallas

Dallas, Texas

August, 2007

Copyright

by

PENG YI, 2007

All Rights Reserved

# **GENETIC DISSECTION OF HEART DEVELOPMENT IN THE FRUIT FLY *DROSOPHILA MELANOGASTER***

Peng Yi, Ph.D.

The University of Texas Southwestern Medical Center at Dallas, 2007

Mentor: Eric N. Olson, Ph.D.

The early morphogenetic mechanisms involved in heart formation are evolutionarily conserved. The *Drosophila* heart, known as the dorsal vessel, functions as a pulsatile tube-like organ containing an inner layer of contractile cardiac cells that adhere tightly to an adjacent layer of pericardial cells. A genetic screen for genes that control *Drosophila* heart development revealed a cardiac defect in which pericardial and cardiac cells dissociate causing loss of cardiac function and embryonic lethality. This phenotype resulted from mutations in the genes encoding HMG-CoA Reductase, downstream enzymes in the mevalonate pathway, and G-protein G $\gamma$ 1, which is geranylgeranylated, thus representing an endpoint of isoprenoid biosynthesis. These findings reveal a cardiac cell-autonomous requirement of G $\gamma$ 1 geranylgeranylation for heart formation and suggest the involvement of the mevalonate pathway in congenital heart disease. In

addition, we found that the heterotrimeric G proteins G $\beta$ 13F and G- $\alpha$ 47A together with the RGS (regulator of G protein signaling) protein Loco function in the same pathway as G $\gamma$ 1 to regulate septate junction formation in cardiac cells of the *Drosophila* heart. We also present evidence that the septate junction protein Sinuous interacts with Pericardin, a matrix protein secreted by pericardial cells, providing the molecular basis for cardiac-pericardial cell adhesion and serving as a mediator of the actions of the mevalonate pathway and heterotrimeric G protein signaling in *Drosophila* heart development.



## TABLE OF CONTENTS

<i>Title</i> .....	<i>i</i>
<i>Dedication</i> .....	<i>ii</i>
<i>Acknowledgement</i> .....	<i>iii</i>
<i>Abstract</i> .....	<i>vii</i>
<i>List of publications</i> .....	<i>x</i>
<i>List of figures</i> .....	<i>xi</i>
<i>List of tables</i> .....	<i>xiv</i>
<i>List of abbreviations</i> .....	<i>xv</i>
 <b>Chapter I: Introduction</b> .....	 <b>1</b>
Overview of <i>Drosophila</i> embryogenesis .....	3
Overview of <i>Drosophila</i> heart development .....	20
Purpose of study and strategy .....	31
 <b>Chapter II: Materials and methods</b> .....	 <b>33</b>
 <b>Chapter III: The mevalonate pathway controls heart formation in <i>Drosophila</i> by isoprenylation of G<math>\gamma</math>1</b> .....	 <b>40</b>
Genetic screen for cardiac genes .....	40
Identification of <i>broken hearted</i> phenotype .....	50
The mevalonate pathway genes and G $\gamma$ 1 control heart formation .....	54
Discussions .....	70
 <b>Chapter IV: Heterotrimeric G proteins control cardiac integrity in <i>Drosophila</i> by regulating septate junction formation</b> .....	 <b>72</b>
Heterotrimeric G proteins control cardiac integrity .....	72
Septate junction plays an important role in heart formation .....	78
Heterotrimeric G proteins regulate septate junction formation in the heart .....	83
Discussions .....	88
 <b>Chapter V: Summary and future directions</b> .....	 <b>97</b>
Summary .....	97
Future directions .....	101
 <b>References</b> .....	 <b>107</b>

## LIST OF PUBLICATIONS

1. **Yi P**, Zhang W, Zhai Z, Miao L, Wang Y, Wu M. Bcl-rambo  $\beta$ , a special splicing variant with an insertion of an Alu-like cassette, promotes etoposide- and Taxol-induced cell death. *FEBS Lett.* 2003 Jan 16; 534(1-3): 61-8.
2. Miao L, **Yi P**, Wang Y, Wu M. Etoposide upregulates Bax-enhancing tumour necrosis factor-related apoptosis inducing ligand-mediated apoptosis in the human hepatocellular carcinoma cell line QGY-7703. *Eur J Biochem.* 2003 Jul; 270(13): 2721-31.
3. Han Z, **Yi P**, Li X, Olson EN. Hand, an evolutionarily conserved bHLH transcription factor required for *Drosophila* cardiogenesis and hematopoiesis. *Development.* 2006 Mar; 133(6): 1175-82.
4. **Yi P**, Han Z, Li X, and Olson EN. The Mevalonate Pathway Controls Heart Formation in *Drosophila* by Isoprenylation of G $\gamma$ 1. *Science*, 2006 Sep 1;313(5791):1301-3. Epub 2006 Jul 20.
5. Han Z, **Yi P**, Wu J, Li X and Olson EN. A large-scale genetic screening for cardiogenic genes using new heart cells marker *Hand-GFP* in *Drosophila* embryos. in preparation, 2007.
6. **Yi P**, Han Z, Johnson AN, Wu J, Li X, Olson EN. Heterotrimeric G proteins control cardiac integrity in *Drosophila* by regulating heart cell polarity and septate junction formation. Submitted to *Developmental Cell*, 2007.

## LIST OF FIGURES

Figure 1.1. The life cycle of the fruit fly, <i>Drosophila melanogaster</i> .....	4
Figure 1.2. Developmental stages of <i>Drosophila</i> embryogenesis .....	6
Figure 1.3. Anterior-posterior axis is determined by maternal genes .....	11
Figure 1.4. The expression of the gap genes in the early embryo.....	13
Figure 1.5. <i>Drosophila</i> homeotic genes expression pattern.....	15
Figure 1.6. Mesoderm dorsal-ventral patterning in <i>Drosophila</i> embryo .....	17
Figure 1.7. Genes involved in <i>Drosophila</i> embryo dorsal-ventral axis determination .....	17
Figure 1.8. <i>Drosophila</i> heart in different developmental stages .....	21
Figure 1.9. Schematic drawing of a mature <i>Drosophila</i> heart .....	23
Figure 1.10. <i>Drosophila</i> heart development during embryogenesis .....	25
Figure 1.11. Transcriptional network for <i>Drosophila</i> heart development .....	28
 Figure 3.1. The expression of <i>hand</i> in <i>Drosophila</i> embryo .....	41
Figure 3.2. Mapping the cardiac enhancer (HCH) of <i>Hand</i> .....	43
Figure 3.3 <i>Hand-GFP</i> transgenic fly .....	45
Figure 3.4. Cross scheme in <i>Hand-GFP</i> heart forward genetic screen.....	47
Figure 3.5. Different cardiac defects discovered in our genetic screen .....	49
Figure 3.6. Discovering of a new cardiac defect, <i>broken hearted (bro)</i> .....	51

<b>Figure 3.7. <i>HMGCR</i> is mutated in <i>bro1</i> mutant .....</b>	<b>55</b>
<b>Figure 3.8. Mevalonate pathway.....</b>	<b>57</b>
<b>Figure 3.9. The heart phenotype of the mevalonate pathway enzymes mutants .....</b>	<b>58</b>
<b>Figure 3.10. Heterotrimeric G protein <math>G\gamma 1</math> is required for heart cells adhesion .....</b>	<b>60</b>
<b>Figure 3.11. Geranylgeranylation of <math>G\gamma 1</math> is required for heart formation....</b>	<b>62</b>
<b>Figure 3.12. Mevalonate pathway regulates the cellular localization of <math>G\gamma 1</math></b>	<b>64</b>
<b>Figure 3.13. Specification and alignment of cardioblasts and pericardial cells during development .....</b>	<b>66</b>
<b>Figure 3.14. <i>HMGCR</i> and <math>G\gamma 1</math> are specifically required in cardioblasts to maintain cardiac integrity .....</b>	<b>67</b>
<b>Figure 3.15. Characterization of <i>Sar1 (bro5)</i> locus.....</b>	<b>69</b>
<b>Figure 4.1. <i>G<math>\beta</math>13F</i> mutants show the same <i>bro</i> defect as a <i>G<math>\gamma</math>1</i> mutant .....</b>	<b>73</b>
<b>Figure 4.2. Loss-of-function and gain-of-function heart phenotype of <i>Gas</i>..</b>	<b>76</b>
<b>Figure 4.3. Requirement of <i>Nrx-IV</i> for maintenance of cardiac integrity .....</b>	<b>79</b>
<b>Figure 4.4. Septate junction protein mutants have <i>bro</i> defect .....</b>	<b>82</b>
<b>Figure 4.5. Septate junction localization in the heart in wild type or <i>G<math>\gamma</math>1</i> mutant embryos .....</b>	<b>84</b>

<b>Figure 4.6. A model for the role of Sinuous-Pericardin in cardinal-pericardial cell adhesion .....</b>	<b>86</b>
<b>Figure 4.7. A hypothetic model for cardinal-pericardial cell adhesion.....</b>	<b>89</b>
<b>Figure 5.1. Summary of <i>broken hearted</i> genes.....</b>	<b>98</b>
<b>Figure 5.2. The final model for <i>broken hearted</i> genes in mediating the cardinal-pericardial cell adhesion .....</b>	<b>100</b>
<b>Figure 5.3. <i>bro</i> genes in <i>Drosophila</i> germ cell migration.....</b>	<b>102</b>
<b>Figure 5.4. Mapping of the <i>bro</i> gene in <i>bro11</i> locus.....</b>	<b>104</b>

## LIST OF TABLES

<b>Table 1.1. Developmental activities in different <i>Drosophila</i> embryogenesis stages</b>	<b>7</b>
<b>Table 3.1. The <i>broken hearted</i> mutants discovered in our genetic screen</b>	<b>52</b>
<b>Table 4.1. Heterotrimeric G proteins in <i>Drosophila</i> genome</b>	<b>74</b>
<b>Table 4.2. <i>broken hearted</i> genes are evolutionarily conserved</b>	<b>95</b>

## LIST OF ABBREVIATIONS

<b><math>\alpha</math>-FT</b>	$\alpha$ subunit of farnesyl transferase
<b>A-P</b>	Anterior-posterior
<b>BDGP</b>	Berkeley <i>Drosophila</i> Genome Project
<b><math>\beta</math>-FT</b>	$\beta$ subunit of farnesyl transferase
<b><math>\beta</math>GGT-I</b>	$\beta$ subunit of type I geranylgeranyl transferase
<b>bHLH</b>	basic-helix-loop-helix
<b>BMP</b>	Bone morphogenetic protein
<b><i>bro</i></b>	<i>broken hearted</i>
<b>cDNA</b>	complementary DNA
<b>CNS</b>	Central nervous system
<b>COPII</b>	Coat protein complex type II
<b>COUP</b>	Chicken ovalbumin upstream promoter
<b>DGRC</b>	<i>Drosophila</i> Genomics Resource Center
<b>DNA</b>	Deoxyribonucleic acid
<b>dsRNA</b>	Double-stranded RNA
<b>EMS</b>	Ethyl methane sulphonate
<b>ER</b>	Endoplasmic reticula
<b>farnesyl-PP</b>	farnesyl-pyrophosphate
<b>FGF</b>	Fibroblast growth factor

<b>FPP</b>	farnesyl-pyrophosphate
<b>G<math>\alpha</math></b>	Heterotrimeric G protein $\alpha$ subunit
<b>GAP</b>	GTPase activating protein
<b>GAPDH</b>	Glyceraldehyde 3-phosphate dehydrogenase
<b>G<math>\beta</math></b>	Heterotrimeric G protein $\beta$ subunit
<b>G<math>\beta</math>13F</b>	Heterotrimeric G protein $\beta$ subunit at 13F locus
<b>G<math>\beta</math>76C</b>	Heterotrimeric G protein $\beta$ subunit at 76C locus
<b>GDP</b>	Guanosine 5'-diphosphate
<b>GEF</b>	Guanine nucleotide exchange factor
<b>geranylgeranyl-PP</b>	geranylgeranyl-pyrophosphate
<b>GFP</b>	Green fluorescent protein
<b>G<math>\gamma</math></b>	Heterotrimeric G protein $\gamma$ subunit
<b>GGPP</b>	geranylgeranyl-pyrophosphate
<b>GGPPS</b>	Geranylgeranyl-pyrophosphate (GGPP) synthase
<b>Gi</b>	Heterotrimeric G protein $\alpha$ subunit, i class
<b>G-<math>\alpha</math>65A</b>	Heterotrimeric G protein $\alpha$ subunit, i class, at 65A locus
<b>Go</b>	Heterotrimeric G protein $\alpha$ subunit, o class
<b>G-<math>\alpha</math>47A</b>	Heterotrimeric G protein $\alpha$ subunit, o class, at 47A locus
<b>GPCR</b>	G protein-coupled receptor
<b>GST</b>	Glutathione S-transferase



<b>GTP</b>	Guanosine triphosphate
<b>Hand</b>	Heart and neural crest derivatives expressed
<b>HCH</b>	Hand cardiac enhancer
<b>HMGCR</b>	3-hydroxy-3-methyl-glutaryl-CoA reductase
<b>LPP3</b>	Lipid phosphate phosphohydrolase-3
<b>Mef2</b>	Myocyte enhancer factor 2
<b>mRNA</b>	messenger ribonucleic acid
<b>NLS</b>	Nuclear localization signal
<b>PBS</b>	Phosphate buffered saline
<b>PCR</b>	Polymerase chain reaction
<b>PGC</b>	Primordial germ cell
<b>PNS</b>	Peripheral nervous system
<b>RGS</b>	Regulators of G-protein Signaling
<b>RNAi</b>	RNA interference
<b>RT-PCR</b>	Reverse transcriptase polymerase chain reaction
<b>SJ</b>	Septate junction
<b>TGF-<math>\beta</math></b>	Transforming growth factor beta
<b>UAS</b>	Upstream Activation Sequence

## CHAPTER I

### Introduction

*Those of us who are at work on Drosophila find a particular point to the question. For the genetic material available is all that could be desired, and even embryological experiments can be done...It is for us to make use of these opportunities. We have a complete story to unravel, because we can work things from both ends at one.*

JACK SCHULTZ (1935)

To understand how animal is developed from a single fertilized egg to multi-cellular complex organism is the biggest challenge and the most intriguing question in biology research. Although the morphology of animals looks so much different, the regulation of their development is amazingly conserved in both molecular and cellular level. In the past decades, the developmental biology has been greatly facilitated by the usage of various genetic models, including both invertebrate and vertebrate models. The fruit fly, *Drosophila melanogaster*, is one of the greatest genetic models ever used in developmental biology. It helped developmental biologist understand a lot of important questions such as patterning

in early embryogenesis and basic signal pathways involved in development. In 1995, Edward Lewis and Christiane Nusslein-Volhard shared the Nobel Prize in Medicine for their concerning the genetic control of early embryonic development using *Drosophila* as model.

*Drosophila* is not only a good model system to study the early embryogenesis, it is also proved to be an excellent tool for the organogenesis research. For example, *Drosophila* dorsal vessel (heart) serves as an excellent model for heart development study. Using forward genetic screen in *Drosophila*, many genes and signaling pathways have been identified to control the cardiac mesoderm differentiation (reviewed by (Bodmer and Venkatesh, 1998; Cripps and Olson, 2002)). However, the mechanism of *Drosophila* heart tube morphogenesis in later stages still remains poorly known, partially due to lack of good genetic markers for the whole heart structure. *Drosophila* heart resembles the vertebrate linear heart tube prior to heart looping and chambers formation. So, to study the mechanism for *Drosophila* heart morphogenesis will help us gain better understanding how vertebrate heart is formed, defects in which in humans are the major causes of congenital heart disease. The focus of my graduate study is to tackle this complicated developmental process of *Drosophila* heart morphogenesis using the powerful genetic approach in *Drosophila* and our new heart marker, *Hand-GFP* (Han and Olson, 2005), which enable us to observe the whole heart structure even in living embryos for the first time.

## *Overview of Drosophila embryogenesis*

### (1) *Drosophila* life cycle

One reason that scientists used *Drosophila* as a model system is that *Drosophila* has a very short life (14 days only), reproduction cycle and amazing reproduction ability. As an insect, the fruit flies undergo a complete metamorphosis, where the young form of fruit flies looks completely different with the adults. Like most of species, the female fruit flies produce eggs and the male flies provide sperms. Sperms are deposited from the male into the female. Eggs are fertilized on their way through the oviduct to being laid on a food source.

The whole life cycle of the fruit fly, *Drosophila melanogaster*, is shown in Figure 1.1. Fruit flies start their lives from an embryo in an egg. The embryogenesis of fruit flies only takes about 22 hours. During this time, the embryo undergoes a massive change and hatch into a larva at the end. There are three stages of larva, namely 1<sup>st</sup> instar, 2<sup>nd</sup> instar and 3<sup>rd</sup> instar. The larva goes from 1<sup>st</sup> instar to 2<sup>nd</sup> instar and 3<sup>rd</sup> instar by molting. Their bodies become larger and larger. After the last molting, the larva stops moving and form a pupa. During this time, the metamorphosis from larva to adult is occurring. The adult structures, such as wings, legs, compound eyes develop. When the adult flies emerge from the pupas, they become fully formed. They start mating after about ten hours.

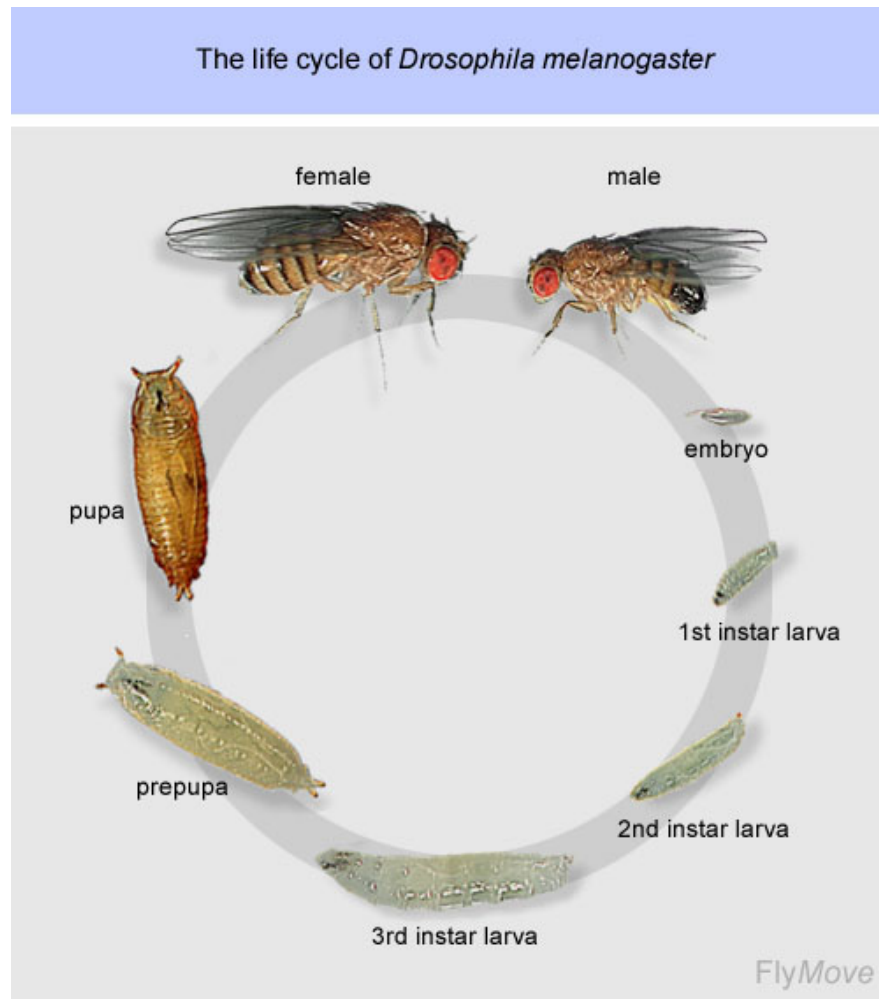


**Figure 1.1. The life cycle of the fruit fly, *Drosophila melanogaster*. (Adapted from Flymove.com).** The life cycle of *Drosophila melanogaster* starts from an embryo. They spend the first day for embryogenesis, and hatch into 1st instar larva. After 4 days and molting for three times, they start their pupa stage. They use another 5 days to develop into adult flies. 10 hours after they emerge from the pupa, they start mating and laying eggs, so the new cycle begins again.

The females lay eggs, and the new cycle begins again. This whole life cycle takes about 12-14 days (reviewed in (Wiggleworth, 1984)).

## (2) *Drosophila* embryogenesis overview

The *Drosophila* embryogenesis can be divided into 17 developmental stages (reviewed in (Hartenstein, 1995)). Figure 1.2 shows the stage 5-17, where the stage 1-4 is a rapid cleavage phase, and stage 17 is a transition stage from embryo to 1<sup>st</sup> instar larva. From stage 4, the *Drosophila* embryos undergo dramatic change in each stage. The main developmental activities occurring in these different stages are summarized in Table 1.1.

*Drosophila* embryogenesis starts with rapid cleavage (stage 1-4). The nuclear of the fertilized egg undergoes 13 divisions. Most of nuclei migrate to the periphery of the embryo and are arranged into a single layer. After that, cell membranes start to form around the nuclei. Embryo is then developed into the cellular blastoderm (stage 5), with a homogeneous cellular sheet surrounding the yolk. At the same time, the germ cells, also called pole cells, form a cluster of 34-37 round cells at the posterior pole of the embryo.

Embryos start the gastrulation from stage 6. During gastrulation, the cells in the polar caps and the mid-ventral part of the blastoderm invaginate, which generate three germ layers: ectoderm, mesoderm and endoderm. The cells that

### Overview of the Stages of Development

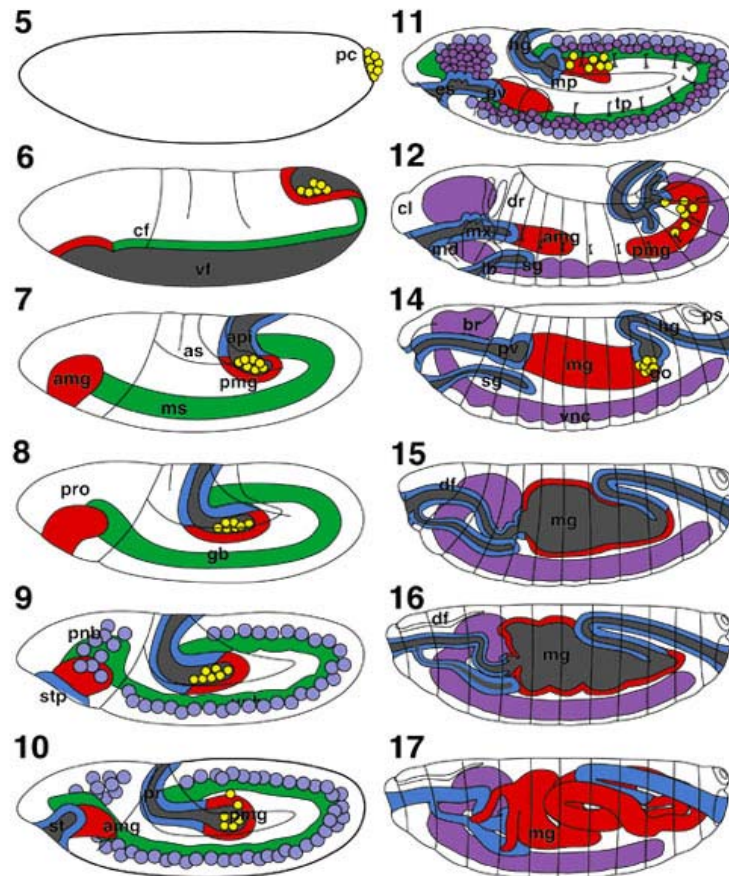


**Figure 1.2. Developmental stages of *Drosophila* embryogenesis. (Adapted from Atlas of *Drosophila* by Volker Hartenstein).** (*amg*) (Anterior midgut rudiment; (*br*) brain; (*cf*) cephalic furrow; (*cl*) clypeolabrum; (*df*) dorsal fold; (*dr*) dorsal ridge; (*es*) esophagus; (*gb*) germ band; (*go*) gonads; (*hg*) hindgut; (*lb*) labial bud; (*md*) mandibular bud; (*mg*) midgut; (*mg*) Malpighian tubules; (*mx*) maxillary bud; (*pc*) pole cells; (*pmg*) posterior midgut rudiment; (*pnb*) procephalic neuroblasts; (*pro*) procephalon; (*ps*) posterior spiracle; (*po*) proventriculus; (*sg*) salivary gland; (*stp*) stomodeal plate; (*st*) stomodeum; (*tp*) tracheal pits; (*vf*) ventral furrow; (*vnb*) ventral neuroblasts; (*vnc*) ventral nerve

Stage number	Minutes after fertilization	Developmental activity
1	0-15	Pronuclear fusion
2	15-70	Preblastoderm (mitotic cycles 1-9) - early cell division - start of cleavage
3	70-90	Pole bud formation - nuclear division 9
4	90-130	Syncytial blastoderm (mitotic cycles 10-13) - end of cleavage divisions
5	130-180	Cellularization of the blastoderm
6	180-195	Gastrulation to form mesoderm and endoderm - pole cells included in posterior midgut primordium
7	195-200	Germ band elongation - lengthening of the ventral epidermis
8	200-230	Rapid germ band elongation - start of first postblastoderm mitosis - ends with mesodermal parasegmentation
9	230-260	Slow germ band elongation - segmentation of neuroblasts - end of first and start of second postblastoderm mitosis - cephalic furrow formation
10	260-320	Gnathal and clypeolabral lobe formation (head features) - stomodeal invagination - end of second and start of third postblastoderm mitosis

**Table 1.1. Developmental activities in different *Drosophila* embryogenesis stages.**

**(Adapted from the Interactive Fly website)**



Stage number	Minutes after fertilization	Developmental activity
12	440-580	Germ band retraction - optic lobe invagination - ventral closure - segment formation - fusion of anterior and posterior midgut
13	560-620	End of germ band retraction - CNS and PNS differentiation
14	620-680	Dorsal closure of midgut and epidermis - head involution begins
15	680-800	End of dorsal closure - head involution - discs invaginate - cuticle deposition begins - dorsal epidermal segmentation
16	800-900	Advanced denticles visible - Shortening of the ventral nerve cord
17	Lasts until hatching	The tracheal tree fills with air - Retraction of the ventral cord continues
Hatch	21-22 hours	Hatch to first instar larva

**Table 1.1. Developmental activities in different *Drosophila* embryogenesis stages (continued).**

remains at the surface of the embryo represent the ectoderm, the invaginated cells become the endoderm and mesoderm. A narrow mid-dorsal partition of the blastoderm gives rise the amnioserosa, which is a thin membrane covering the germ band at the dorsal side.

At the same time of gastrulation, germ band elongation starts. Germ band elongation is a movement that pushes the posterior tip of the germ band upward and then toward anterior. At stage 9-11, the germ band continues to elongate. Meanwhile, the ectoderm begins to split up into many different organ primordia including foregut, hindgut, CNS and epidermis.

Starting from stage 12, germ band begins to retract. The appearance of the ectoderm remains the same from stage 11 to stage 13. During stage 12, important morphogenetic events take place in mesoderm and endoderm. At stage 13, germ band retraction ends, where the cells in most organ primordia begin to differentiate. The main morphogenetic event that shapes the embryonic surface after germ band retraction is dorsal closure. During dorsal closure, the epidermal primordium stretches in the transversal axis, gradually closing the gap in the dorsal germ band. By the end of stage 15, dorsal closure is completed. The amnioserosa is invaginated and then degenerated in this process. By stage 17, the head involution is completed and the embryonic surface reaches its final, larval morphology. The cuticle becomes thicker and the larva is ready to hatch.

### (3) *Patterning and segmentation*

#### (i) *Anterior-posterior axis*

One amazing question in *Drosophila* embryogenesis is how the embryo gets the correct body patterning and segmentation and how they are regulated by the gene networks. Over past decades, genetic approaches have helped us to dissect these complicated processes.

When the ~5000 nuclei are generated after the first 13 rounds of cell cycles (stage 1-4), no apparent difference can be seen in these nuclei. However, their developing fates are already partially determined by their positions. In *Drosophila*, the initial spatial information is provided by the localized maternal gene products during construction of the egg in the ovary, which determine the anterior-posterior and dorsal-ventral axes in the embryo.

Two maternal genes determine the anterior-posterior axis, *bicoid* and *nanos*. In unfertilized egg, *bicoid* mRNA is localized at the anterior end, whereas *nanos* mRNA is located at the posterior end. After fertilization, maternal mRNAs are translated. Bicoid proteins start to diffuse to the posterior end and then form a gradient with the highest level of Bicoid at the most anterior end. In contrast, Nanos protein forms an opposite gradient along the anterior-posterior axis (Namba et al., 1997; Struhl, 1989). Nanos inhibits the translation of both *bicoid* and *hunchback* mRNAs in the posterior end, whereas Bicoid represses the translation of *caudal* maternal mRNA, leading to a Caudal gradient with the

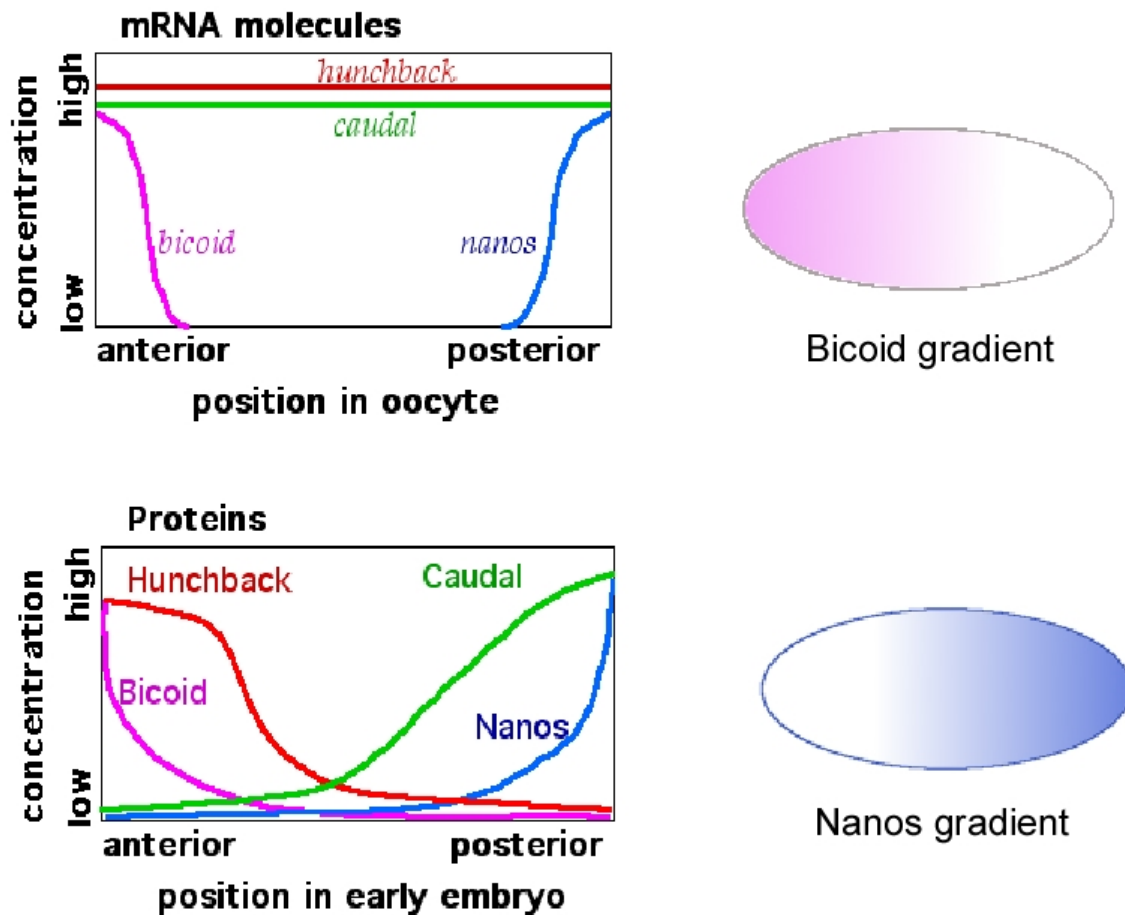


**Figure 1.3. Anterior-posterior axis is determined by maternal genes.** (Adapted and modified from answer.com). In *Drosophila* embryos, the localization of maternal genes, *bicoid* and *nanos*, mRNAs is polarized. Their proteins then form two opposite gradients along the anterior-posterior axis, which leads to the polarization of other maternal proteins such as Hunchback and Caudal.

highest level in the posterior end. Zygotic *hunchback* gene is activated by Bicoid in the anterior but is repressed by Nanos in the posterior, generating a Hunchback gradient from anterior to posterior. Thus, the gradient of Bicoid, Hunchback, Caudal and Nanos set up the initial anterior-posterior axis to guide the next stage of patterning through regulating zygotic genes transcription along the A-P axis (Figure 1.3) (Struhl et al., 1992; Tautz, 1988).

Gap genes are the first zygotic genes expressed along the anterior-posterior axis. Their expression pattern is determined by the maternal genes. Hunchback is the earliest expressed gap genes, which is then required to turn on other gap genes, including *giant*, *Krupple* and *knirps* (Hulskamp et al., 1990; Simpson-Brose et al., 1994). The expression pattern of the gap genes (Figure 1.4) is controlled not only by Bicoid and Hunchback, but also by the gap genes themselves (Kraut and Levine, 1991b; Pankratz et al., 1992; Rivera-Pomar et al., 1995). The interactions between gap genes are often mutual inhibition, which sharpen the boundary of the distinct regions determined by different combinations of gap genes along the anterior-posterior axis (Kraut and Levine, 1991a).

Pair-rule genes are a group of genes that establish the segmental pattern along the anterior-posterior axis. Pair-rule genes divide the embryo into 14 parasegments (Lawrence et al., 1987). They are expressed in a series of seven transverse stripe along the anterior-posterior axis of embryo, each stripe corresponding to every second parasegment. Some pair-rule genes, such as *even-*

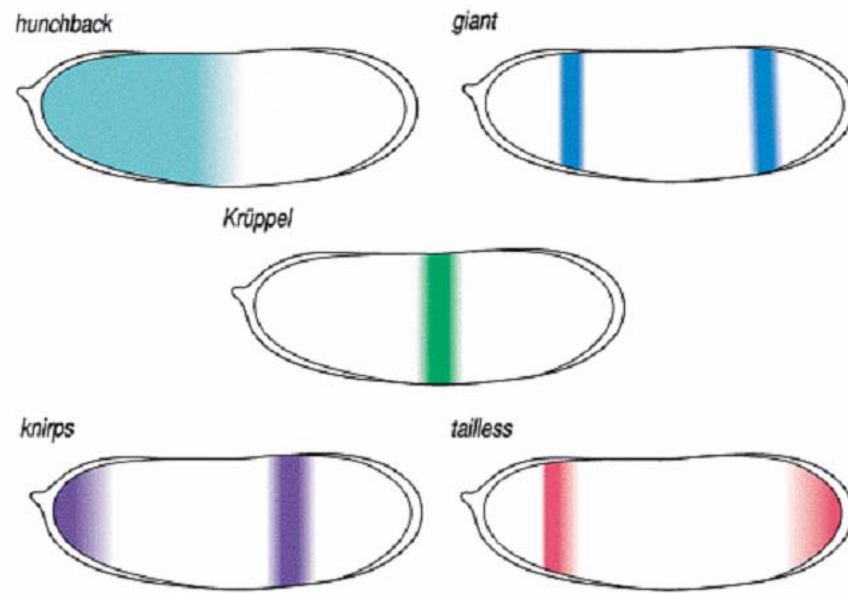


**Figure 1.4. The expression of the gap genes in the early embryo. (Courtesy of Zhe Han).** Gap gene expression at different points along the anterior-posterior axis is controlled by the concentration of Bicoid and Hunchback proteins. The expression pattern of gap genes provides an aperiodic pattern of transcription factors along the anterior-posterior axis, which delimits broad body regions.

-*skipped* (*eve*), define odd-numbered parasegments, where other pair-rule genes, such as *fushi tarazu* (*fzr*), define even-numbered parasegments.

Pair-rule genes define the anterior boundaries of all the 14 parasegments but their activity is only temporary. The parasegment boundaries are fixed by a group of segment polarity genes, including *wingless* and *hedgehog* pathway genes. Maintaining such cell-lineage restriction boundaries depends on an intercellular signaling circuit between adjacent cells on either side of the boundary. On one side of the boundary, *engrailed*-expressing cells secrete Hedgehog protein, which acts on the adjacent cells on the other side of the boundary to maintain *wingless* expression and secretion in those cells. The secreted Wingless protein then provides a signal that feeds back across the boundary to maintain *hedgehog* expression, thus stabilizing and maintaining this parasegment boundary (Hidalgo and Ingham, 1990; Kornberg et al., 1985; Tabata et al., 1992).

After the parasegment is established, the different identity of each parasegment is then determined by a class of master regulatory genes, homeotic genes. Different homeotic genes control parasegments to develop into different structures in the future, for example, some control wing formation, some control eye formation etc. (Figure 1.5). Their expression patterns are defined by both maternal gene and gap gene, and then modulated by the pair-rule genes into a registered series of unique parasegmental patterns (Morata, 1993).

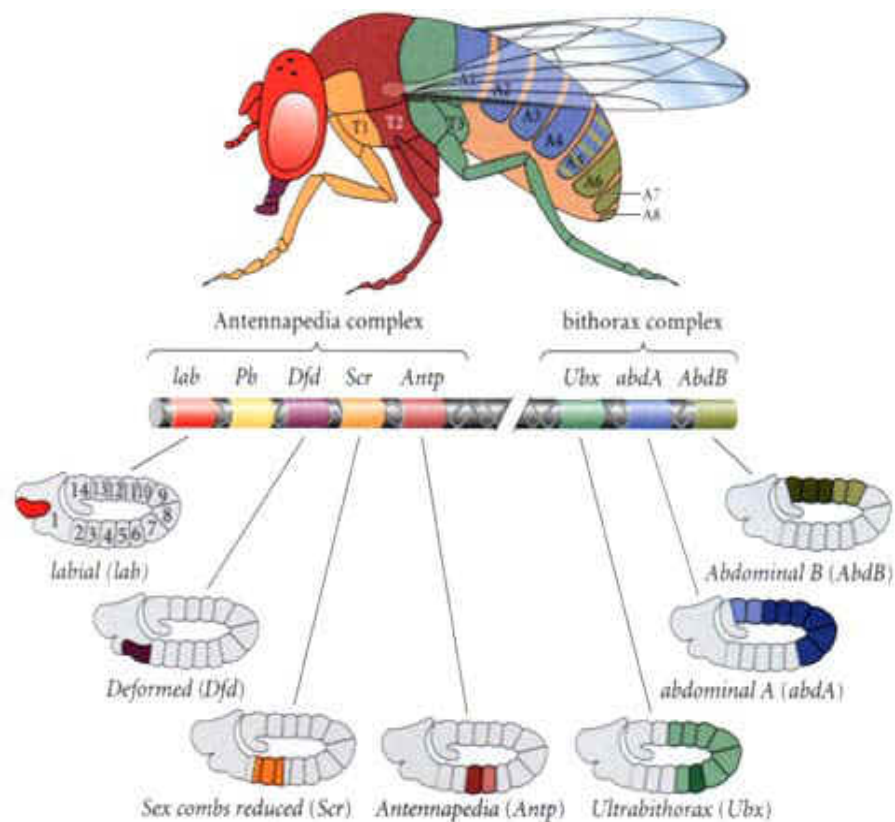


**Figure 1.5. *Drosophila* homeotic genes expression pattern.** (Courtesy of Zhe Han). *Drosophila* homeotic proteins are encoded as a cluster on chromosomes. Different homeotic gene is expressed in different parasegment, corresponding to the development of different body structures.



Each homeotic gene contains a homeobox DNA-binding motif. Mutations in the homeotic genes usually result in the transformation of the corresponding segment from one type to another rather than the elimination of the region in which it is expressed (Lewis, 1978).

In summary, for the embryogenesis along the anterior-posterior axis, after the maternal genes determined the axis, four sets of zygotic genes (gap, pair-rule, segment polarity and homeotic genes) further define the anterior-posterior pattern to determine the fates of cells based on their positions along the anterior-posterior axis.

*(ii) Dorsal-ventral axis*

The dorsal-ventral polarity is defined by a key gene called *pipe*. *pipe* is transcribed only in the follicle cells surrounding the future ventral region of developing egg. Pipe, a secreted enzyme, leads to the processing of Spatzle protein through a series of different proteases. The cleaved Spatzle fragment localizes in the peri-vitelline space on the ventral side of the egg only (Schneider et al., 1994). The Spatzle fragment will then function to activate ubiquitously distributed maternal protein, Toll receptor, only on the ventral plasma membrane of the egg. Activation of Toll signal pathway drive a maternal transcription factor, Dorsal, to go into the cortical nuclei in syncytial blastoderm (Morisato and Anderson, 1994). The greater the activation of Toll signal pathway, the more

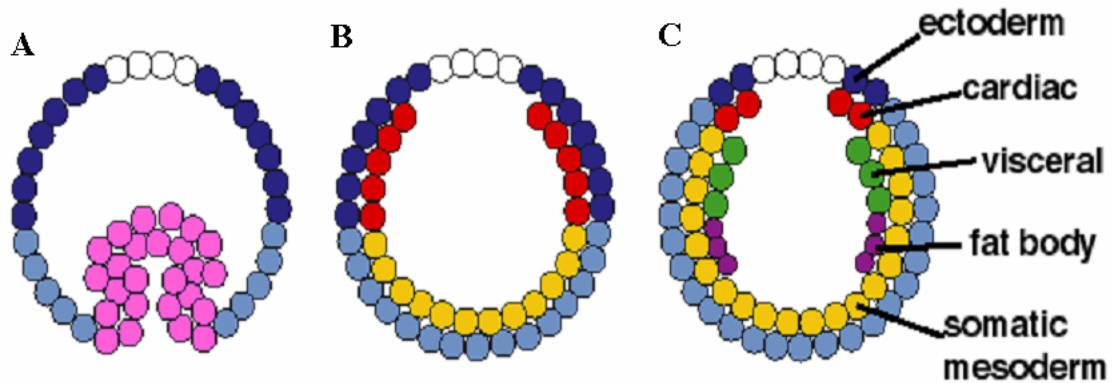


**Figure 1.6. Mesoderm dorsal-ventral patterning in *Drosophila* embryo.** (Courtesy of Zhe Han). (A) Mesoderm invaginates from the ventral midline initiated by Twist. (B) As mesoderm migrates dorsally to ectoderm, *tinman* expression (red) is maintained by the *dpp* signal (deep blue) from the overlying ectoderm, to distinguish the dorsal and ventral mesoderm. (C) As *dpp* expression becomes more dorsally restricted at stage 10, *tinman* expression is also restricted to the cardiac mesoderm (red), the rest of mesoderm differentiates into visceral mesoderm, fat body and somatic mesoderm.

Dorsal enters the nuclei, thereby Dorsal protein in nuclei forms a gradient along the dorsal-ventral axis. The Dorsal gradient will then drive the blastoderm embryo into well-defined regions, namely from ventral to dorsal, mesoderm, ventral ectoderm, dorsal ectoderm and prospective amnioserosa (Figure 1.6).

In the ventral-most region, the zygotic genes *twist* and *snail* are activated by the highest level of Dorsal in a broad stripe. This ventral strip of cells will form the future mesoderm (Figure 1.7). *twist* and *snail* is required for both mesoderm initiation and gastrulation. A gene called *rhomboid* is activated at lower levels of Dorsal in the future neuroectoderm, but is repressed in the mesoderm by the Snail protein (Kosman et al., 1991). On the other hand, the genes *decapentaplegic* (*dpp*), *tolloid* and *zerknüllt* are repressed by Dorsal protein, so that their activity is restricted in the most dorsal regions of the embryo (Figure 1.7) (reviewed in (Ray et al., 1991; Rusch and Levine, 1996)).

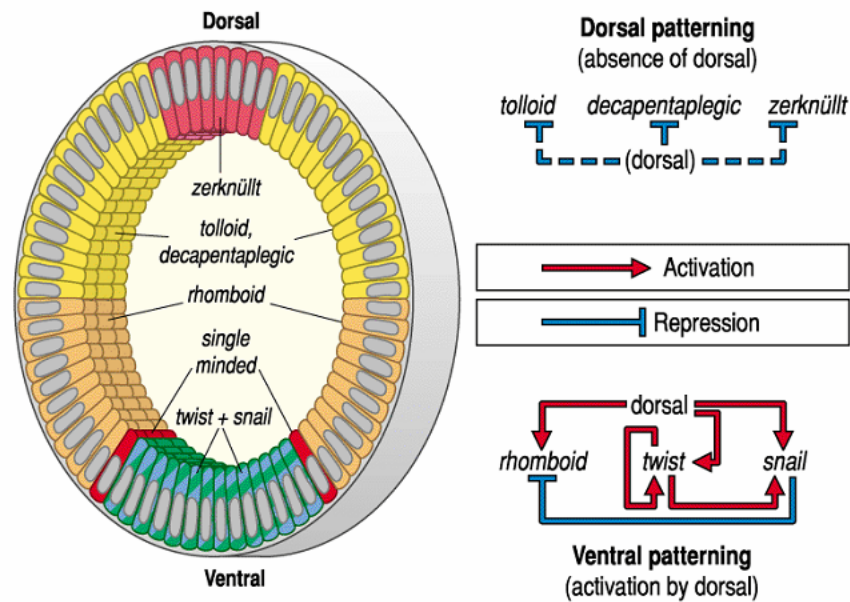


**Figure 1.7. Genes involved in *Drosophila* embryo dorsal-ventral axis determination.** (Courtesy of Zhe Han). In the dorsal region, where nuclear Dorsal is absent, *decapentaplegic* (*dpp*), *tolloid* and *zerknüllt* are expressed to define the ectoderm. In the ventral region, Dorsal protein activates the genes *twist*, *snail* and *rhomboid*. *twist* is autoregulated, maintaining its own expression and also activates *snail*, to specify the mesoderm. *snail* inhibits *rhomboid* and restricts its expression between the ectoderm and mesoderm, where *rhomboid* specifies the neuroectoderm.

### *Overview of Drosophila heart development*

To understand the mechanisms that control the formation of the heart represents a fundamental challenge in developmental biology. Also, any abnormality in the heart development could affect the morphology and function of the mature heart, leading to congenital heart disease, the most common birth defect in humans. Current understanding of the causes of congenital heart defect is that they could be either environmental or genetic. A major part of the environmental cause is drug treatment, which affect certain gene activity, whereas genetic cause is from mutation of genes involved in heart development. Therefore, understanding of the gene regulation during heart development is extremely important for finding the cause, studying the mechanism and looking for potential treatment of congenital heart disease.

A variety of model systems have been used to dissect the complicated mechanism controlling heart development, including *Drosophila*, zebrafish, *Xenopus*, chick and mouse. Study from these model systems indicated that the signal pathway regulating heart development is amazingly revolutionarily conserved through the species (reviewed in (Olson, 2006)). Among these model systems, *Drosophila* has the simplest heart and the most powerful genetics, making it a perfect model system to study the gene networks controlling fundamental developmental processes in heart development, such as cardiac

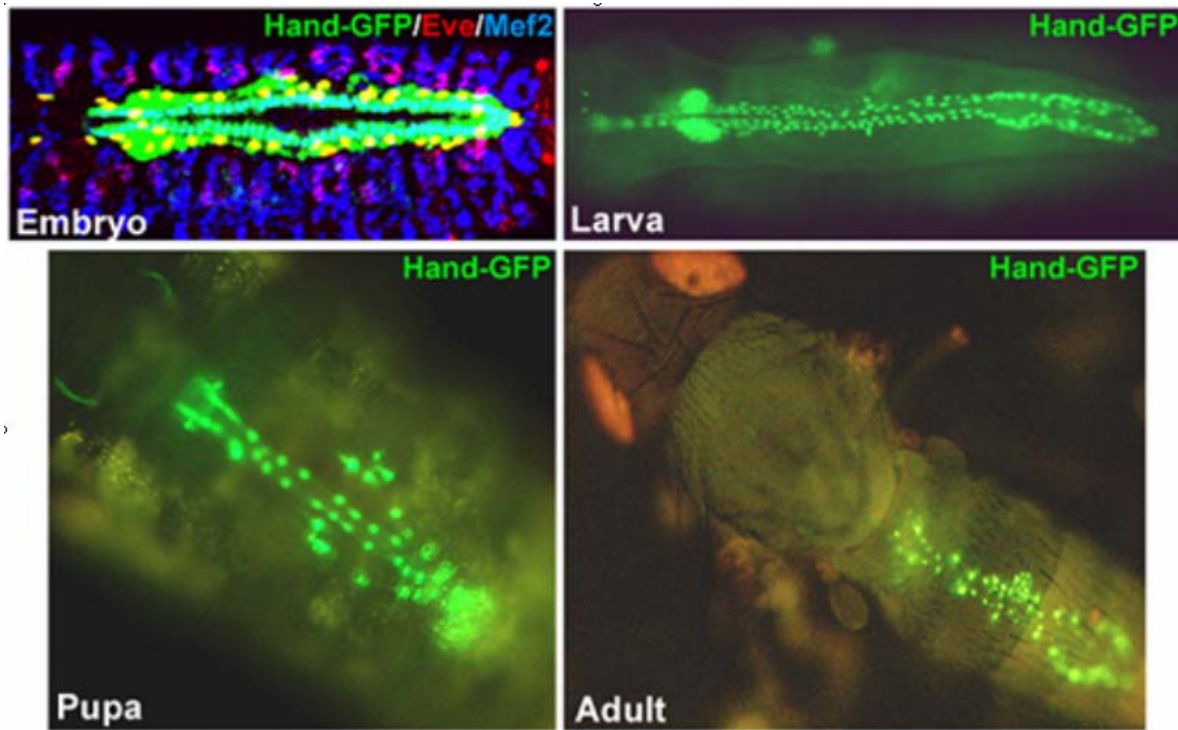


**Figure 1.8. *Drosophila* heart in different developmental stages.** (Courtesy of **Zhe Han**). *Drosophila* heart is labeled either by immunostaining of GFP, Mef2 and Eve in embryo stage, or *Hand-GFP* transgene in larva, pupa and adult stage.

progenitor cell specification, cardiac cell migration, linear heart tube morphogenesis etc. Indeed, the earliest cardiac genes and signaling pathways involved in cardiac progenitor cell specification were first cloned in *Drosophila* system. Nowadays, *Drosophila* is still widely used as model to study linear heart tube assembly, heart disease or heart aging (Ocorr et al., 2007; Wessells and Bodmer, 2007).

*(i) Major events in Drosophila heart development*

*Drosophila* heart, also called dorsal vessel, is a contractile tube structure after embryogenesis on the dorsal side of the larvae, pupae or adult flies. The morphology of *Drosophila* heart in different developmental stages is showed in Figure 1.8 labeled by either immunostaining for heart marker proteins or *Hand-GFP* transgene. The mature heart tube is lined by a layer of myoepithelial cells (cardioblasts) and flanked by two rows of pericardial cells, which provide structural support and also serve an endocrine function. Some pericardial cells at the anterior part are further differentiated into a gland structure, lymph gland, which is a major hematopoiesis organ in larva stage (Cripps and Olson, 2002) (Figure 1.9). Cardioblasts, pericardial cells and the lymph gland, which forms a symmetrical structure at the anterior end of the dorsal vessel, are derived from the cardiac mesoderm (Bodmer and Venkatesh, 1998; Cripps and Olson, 2002; Zaffran and Frasch, 2002).

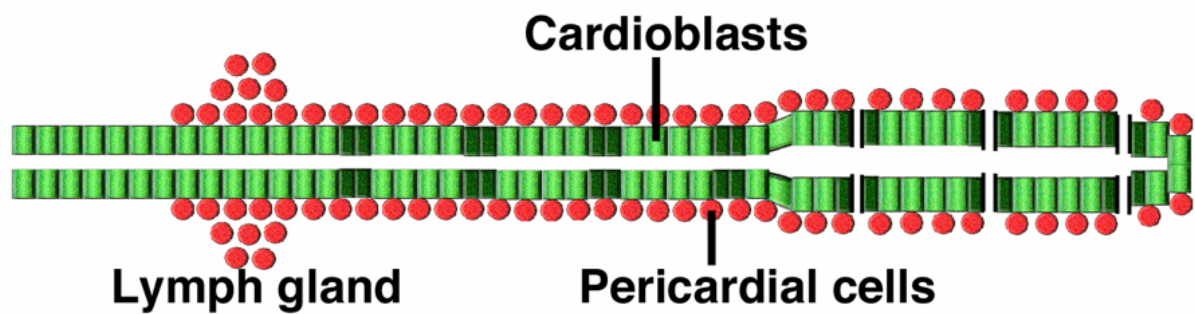


**Figure 1.9. Schematic drawing of a mature *Drosophila* heart. (Dorsal view with anterior to the left).** Cardioblasts are indicated by green, whereas pericardial cells or lymph glands are indicated by red color.



The posterior part of the dorsal vessel becomes dilated, where hemolymph enters the dorsal vessel and is pumped forward from posterior to anterior of the body. The dorsal vessel resembles the primitive vertebrate heart prior to looping and chamber formation.

As shown in Figure 1.10. The primordium of *Drosophila* heart is differentiated shortly after gastrulation. When the mesoderm cells invaginated from the ventral side of the embryos, the cells at the dorsal lateral side of the mesoderm received several signals from overlying ectoderm. These signals drive the dorsal mesoderm cells to differentiate into cardiac primordial cells. During germ band extension and germ band retraction, cardiac progenitor cells undergo several cell divisions, migrate within each parasegment and align themselves into two layers of cells (Cardioblasts and pericardial cells) at the lateral side of the embryo. In the process of dorsal closure, both cardioblasts and pericardial cells migrate together with the overlying ectoderm cells to the dorsal midline, where the cardioblasts from each side meet each other and start to form adhesion. A lumen is then formed between the two cardioblasts and pericardial cells form a tight adhesion with the cardioblasts. At the end of the embryogenesis, the linear heart tube is fully assembled and starts beating to pump hemolymph.

The morphogenesis of the linear heart tube is conserved from *Drosophila* to vertebrate. In vertebrates, the cardiac progenitor cells are also formed at the lateral side the embryo, which is called lateral plate mesoderm.

### Dorsal Vessel

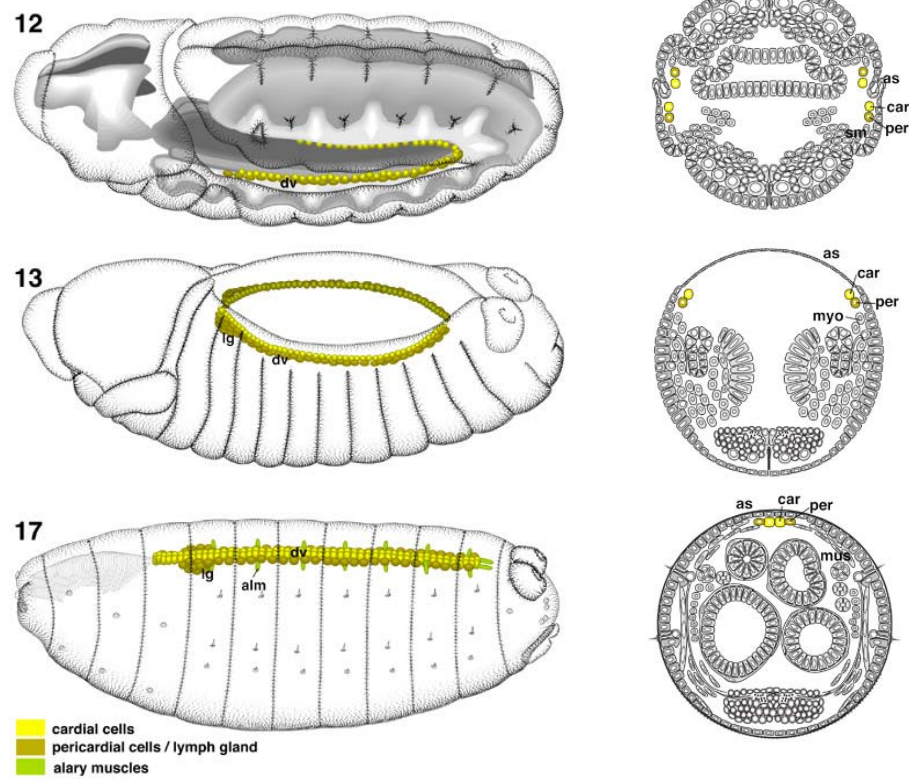


**Figure 1.10. *Drosophila* heart development during embryogenesis. (Adapted from *Atlas of Drosophila Development* by Volker Hartenstein). *Drosophila* heart morphology in stage 12,13 and 17. In the left panel, the anterior end of the embryo is to the left. In the right panel, which is a cross section, the dorsal side of the embryo is upward.**

The cardiac progenitor cells are also specified by evolutionarily conserved signals from overlying ectoderm cells. Similar as *Drosophila*, these cardiac progenitor cells also migrate from the lateral side to the midline of the embryo. In vertebrate, the body plan is opposite to that in *Drosophila*. So the cardiac cells migrate to the ventral midline but not the dorsal midline, where they fuse and form a linear heart tube. Therefore, both the signaling pathways and morphogenesis of the linear heart tube is evolutionarily conserved, *Drosophila* could serve as a perfect model system to study the mechanism regulating these complicated processes.

*(ii) Evolutionarily conserved signaling pathways in Drosophila heart development*

The understanding of the *Drosophila* heart development starts from the analysis of *tinman (tin)*, a homeodomain transcription factor required for the specification of all heart cells. *tin* is broadly expressed in the mesoderm initially, but it is subsequently restricted to the dorsal mesoderm, then the heart precursor cells and finally to an only some of the cardial and pericardial cells. In the absence of *tin*, the cardiac precursor cells are never formed, and the mutant embryos die at the end of embryogenesis, probably from a defect of circulation (Azpiazu and Frasch, 1993; Bodmer, 1993).

The initial pan-mesoderm expression of *tin* is induced by the transcription factor *twist*. During the gastrulation, when the mesoderm cells reach the dorsal

side of the embryo, they received some secreted signals from the overlying ectoderm. One of these signals is *dpp*, a member of the bone morphogenetic protein (BMP) family (Frasch, 1995), which restrict the expression of *tin* to the dorsal mesoderm cells only. Dpp can activate the type I TGF- $\beta$  receptor Thickveins (Tkv), which in turn phosphorylates the Dpp effectors transcription factor Mad and Medea, activating the *tinman* expression (Raftery and Sutherland, 1999; Xu et al., 1998; Yin and Frasch, 1998).

The importance of this dorsal ectoderm signaling in the specification of dorsal mesoderm (heart and visceral muscle) is supported by the mesoderm phenotype of *heartless* (*htl*) mutant. *htl* encodes a *Drosophila* FGF receptor, which is required for the mesoderm migration to the dorsal side during gastrulation. In the mutants of *htl* or its downstream effectors such as *dof*, the mesoderm dorsal migration fails to occur, so the dorsal mesoderm cell fate is not specified, resulting in the lack of cardiac cells and visceral muscle cells (Beiman et al., 1996; Gisselbrecht et al., 1996; Shishido et al., 1997).

After the dorsal mesoderm is established, some other signals secreted from the overlying ectoderm further divide the dorsal mesoderm into cardiac cells and visceral muscle cells. One of these signals is Wingless (Wg), a homolog of vertebrate Wnts, which is secreted from the ectoderm in a series of segmentally repeating stripes, overlying the presumptive dorsal vessel cells (Lawrence et al., 1995).

**Figure 1.11. Transcriptional network for *Drosophila* heart development.**

**(Adapted from (Cripps and Olson, 2002)).** Solid arrowheads indicate direct interactions of transcriptional activators with their target genes. Open arrowheads indicate positive regulatory effects but without no evidence of a direct interaction. Direct or indirect repressive influences are indicated by solid or broken lines. The transcription initiation of target genes is shown as line with rightward pointing arrow. Activation of proteins along a signal transduction pathway is indicated by closed arrows. For the colors: Green indicates Dpp signaling; Purple indicates Wg signaling; Blue indicates interactions that occur specifically in the two Svp-expressing cardiac cells per hemisegment; Red indicates the interactions that occur in the four Tin-positive cardiac cells per hemisegment.

In the *wingless* mutant, heart is not formed, indicating that this signal is essential for heart development (Wu et al., 1995). Mutations in the *wg* downstream effectors, such as *Pangolin* (Pan/dTCF/LEF-1) and Pan target gene *slp-1/2* all lead to the similar cardiac defect as in *wg* mutant (Lee and Frasch, 2000; Park et al., 1998; Park et al., 1996).

After *tin* expression is further restricted into the cardiac mesoderm, *tin* starts to turn on several important cardiac genes. To date, many *tin* target genes have been identified such as *tin* itself, *mef2*, *pnr*, *hand* and  $\beta 3$ -*tubulin* (Cripps et al., 1999; Gajewski et al., 1998; Gajewski et al., 1997; Gajewski et al., 2001; Han and Olson, 2005; Kremser et al., 1999; Xu et al., 1998). *pnr* is one of *Drosophila*

GATA family transcription factor. After *pnr* is turned on by *tin*, *pnr* functions together with *tin* to turn on *mef2* expression in the cardiac cells (Gajewski et al., 1999). The restricted expression of *mef2* in the cardiac cells but not pericardial cells is due to the antagonism of *pnr* by *ush* in pericardial cells (Fossett et al., 2001; Fossett et al., 2000). *mef2* functions to activate a series of muscle specific genes such as myosins, actins, etc. Similar to *mef2*, *hand*, a bHLH family transcription factor, is also activated by *tin* and *pnr* together, but *hand* is expressed in all the cardiac cells as well as pericardial cells and lymph gland (Han and Olson, 2005). So far, the target genes of *hand* have not been found.

In addition to the *dpp* and *wg* signaling from the dorsal ectoderm, the Notch pathway and Hedgehog pathway also have important roles in heart development, especially for the lineage distinction of the cardiac progenitor cells. Notch signaling exerts its function in a lateral inhibition manner. Notch and its ligands function together to distinguish cardiac cells from pericardial cells. Mutations in Notch signaling genes often lead to more cardiac cells at the expense of pericardial cells (Carmena et al., 2002; Zaffran et al., 1995). On the other hand, Hedgehog (Hh) pathway might function to differentiate all the cardiac cells from adjacent cells, as mutations in Hedgehog receptor genes or downstream effector genes lead to either ectopic cardiac cells or less cardiac cells (unpublished data from Zhe Han), probably through regulating Wg signalings in the ectoderm. Also, Hh pathway was reported to regulate *Drosophila* heart inflow tracts development

through regulating *svp*, a COUP family nuclear receptor transcription factor (Ponzielli et al., 2002).

The complex signaling pathways and transcriptional network involved in *Drosophila* heart development (Figure 1.11) are well conserved in vertebrate heart development as well. In vertebrate, the cardiac progenitor cells are also specified by BMP signaling and Wnt signaling from overlying ectoderm. In addition, all the *Drosophila* cardiac transcription factors have close vertebrate homolog and also exert similar functions. For example, Nkx2.5(*Drosophila tin* homolog), GATA4(*Drosophila pnr* homolog), Mef2a/b/c/d (*Drosophila mef2* homolog) and d/eHand (*Drosophila hand* homolog) all have important roles in different stages during vertebrate heart development (reviewed in (Cripps and Olson, 2002; Olson, 2006)).

#### *Purpose of study and strategy*

As described before, the mechanism of early cardiac cells fate specification is well documented, but the mechanism of *Drosophila* heart tube morphogenesis in later stages still remains largely unknown. So to understand how heart tube formation is regulated is my major focus in my graduate study.

One big obstacle for the study of heart tube morphogenesis using *Drosophila* forward genetic screen is the lack of a good genetic marker for the



whole heart structure. Former post-doc in our lab, Zhe Han, generated a perfect fly line with *Hand-GFP* transgene (Han and Olson, 2005), which enable us to observe the whole heart structure even in living embryos for the first time. Together with Dr. Han, I did the forward genetic screen for mutants with heart tube morphological defect. We expected to identify various heart defect caused by cardiac genes mutation in different developmental stages. Here in this thesis, I described my study on one of the heart defects, which later we termed as *broken hearted*. Through mapping all the *broken hearted* mutants, I proposed a model showing how the adhesion between cardiac cells and pericardial cells is mediated by the mevalonate pathway and heterotrimeric G proteins in the *Drosophila* heart.

## CHAPTER II

### Materials and methods

#### *Drosophila strains*

The following mutant stocks were used: HMGCR<sup>clb11.54</sup>, HMGCR<sup>clb26.31</sup> (Van Doren et al., 1998), HMGCR<sup>01152</sup>, G $\gamma$ 1<sup>k08017</sup>, G $\gamma$ 1<sup>N159</sup>, l(2)k07408<sup>k07408</sup>, wun<sup>k10201</sup>, GGPPS/qm<sup>L14.4</sup>,  $\beta$ GGT-I<sup>S-2554</sup>, G $\beta$ 13F <sup>$\Delta$ 15</sup>, G $\beta$ 13F<sup>f261</sup> (gift from Matsuzaki F.), G- $\alpha$ 47A<sup>007</sup> (gift from Semeriva M), G- $\alpha$ 47A<sup>0611</sup> (gift from Tomlinson A), loco <sup>$\Delta$ 13</sup> (gift from Gaul U.), cont<sup>ex956</sup> (gift from Bhat M.A.), sinu<sup>nwu7</sup> (gift from Beitel G. J.), Nr $\alpha$ -IV<sup>EY06647</sup>, Nr $\alpha$ -IV<sup>EP604</sup>, nrv2<sup>k13315</sup>, nrv2<sup>ZCL1649</sup>, cora<sup>14</sup>, Gli<sup>1</sup>, Lac<sup>BG01462</sup>, Nrg<sup>G0488b</sup>, Df(3L)Exel6116, Df(3L)vin5, Df(3L)vin4, Df(3L)BK9, Df(3L)F10, Df(3R)Exel9013, Df(2R)H3E1, Df(3L)Exel6084, Df(2L)Exel6010, Df(3R)Exel6269 and Df(3R)Exel6190 (the Bloomington stock center).

Overexpression of transgenes was accomplished by using the UAS-GAL4 system (Brand and Perrimon, 1993). The following fly lines were used: Hand-GAL4 (Han et al., 2006), Mef2-GAL4 (from Cripps R. M.), Dot-GAL4 (Kimbrell et al., 2002), UAS-HMGCR (Van Doren et al., 1998), UAS-G- $\alpha$ 47A and UAS-G- $\alpha$ 47A(G203T) (gift from Tomlinson A.), UAS-G- $\alpha$ 65A and UAS-G- $\alpha$ 65A(Q203L) (gift from Gaul U.). The UAS-Flag-G $\gamma$ 1, UAS-Flag-G $\gamma$ 1 (C67S)

and UAS-Flag-G $\gamma$ 1- $\Delta$ CAAX constructs were generated by cloning the corresponding cDNAs into pUAST followed by standard transformation.

#### *Genetic screen for cardiogenic genes*

We introduced the *Hand-GFP* transgene, which labels the entire heart (Han and Olson, 2005), into ~3000 homozygous lethal mutation lines (including P-element or PiggyBac insertions, EMS mutants and deficiencies) from the Bloomington Stock Center. Cardiac defects were examined at the 1<sup>st</sup>-instar larvae stage using fluorescent microscopy (Han et al., in preparation).

#### *Examine Hand-GFP in living embryos and larva*

Wild type or mutant flies bearing *Hand-GFP* transgene were used as the source of the embryos we examined. Embryos were collected over an eight hours period at 25°C during daytime. These embryos were then aged overnight at 25°C. The final age of the flies is 16-24 hours, which are mixtures of late stage embryos and early 1<sup>st</sup> instar larva. These embryos/larvas were dechorionized using 50% bleach for 2.5 minutes and mounted in halo-carbon oil. The images were obtained using a Leica DMRXE compound microscope or a Zeiss LSM510 Meta confocal microscope.

#### *Transfection assay, immunohistochemistry and microscopy*

pAc5.1-Flag-G $\gamma$ 1, pAc5.1-Flag-G $\gamma$ 1 (C67S), pAc5.1-Flag-G $\gamma$ 1- $\Delta$ CAAX and pAc5.1-HMGCR-V5 constructs were generated by cloning the corresponding cDNAs into pAc5.1-HisA vector (Invitrogen). S2R<sup>+</sup> cells (DGRC) were transfected using the Effectene transfection reagent (Qiagen). For HMGCR inhibitor experiments, inhibitors (Atorvastatin 50 $\mu$ M, Mevinolin 25 $\mu$ M, Simvastatin 50 $\mu$ M) were added into the medium 6 hours after transfection with pAc5.1-Flag-G $\gamma$ 1. For the HMGCR double-stranded (ds) RNA experiment, dsRNA was generated as described in (Clemens et al., 2000) and added into the medium 24 hours before transfection with pAc5.1-Flag-G $\gamma$ 1. Cells were fixed and immunostained 48 hours after transfection as described in (Chen et al., 2003). Immunostaining of *Drosophila* embryos was performed as described (Han and Olson, 2005). The following primary antibodies were used: Rabbit-anti-Dmef2 (Lilly et al., 1995), mouse-anti-Pericardin (Chartier et al., 2002) (Developmental Studies Hybridoma Bank), GP-anti-Oddskipped (Ward and Skeath, 2000) and Rabbit-anti-Nrx-IV (gift from Bellen H.J.). To observe the *Hand-GFP* marker in *Drosophila* embryos, stage 16 embryos were dechorionized, mounted in halo-carbon oil. Secondary antibodies conjugated with Cy2, Cy3 and Cy5 were from Jackson Laboratory Inc. Images were obtained with a Zeiss LSM510-meta confocal microscope or a Leica DMRXE compound microscope.

#### *Statin treatment*

0.1 $\mu$ M Mevinolin dissolved in 30% ethanol (mixed with sterile PBS) was injected to syncytial blastoderm stage embryos carrying *Hand-GFP*. For each embryo, ~1nl of solution was injected. The same amount of 30% ethanol in PBS was injected to *Hand-GFP* transgenic embryos as a control. The injected embryos were incubated in halocarbon oil in a moisture chamber at room temperature, and were examined at stage 17 for heart development under fluorescent microscope.

#### *RT-PCR and Real-time PCR*

The *G $\gamma$ 1*<sup>k08017</sup> or *Sar1*<sup>05712</sup> mutant harboring *Hand-GFP* and balanced by an actin-GFP balancer was used for RT-PCR. Stage 16 embryos with actin-GFP were collected as heterozygous embryos, while embryos without actin-GFP and displaying the *bro* defect were collected as homozygous embryos. Twenty embryos were collected as a group for RNA isolation and RT-PCR or real-time PCR. Two independent groups for each genotype were used in the analysis. For real-time PCR, 1 $\mu$ g total RNA was used for each group and real-time PCR was performed using the SYBR Green system (Applied Biosystems). The real-time PCR data for *G $\gamma$ 1* and *Sar1* was normalized by GAPDH expression level.

#### *In vitro prenylation assay*

Recombinant GST or GST-*G $\gamma$ 1* protein was expressed and purified using the pGEX-4T vector (Amersham Biosciences). Purified protein was not eluted and

the protein-bound glutathione sepharose was directly used in the in vitro prenylation assay. Sepharose bound with 1µg protein was then added into 50µl reaction containing either (i) 35µl rabbit reticulocyte lysate (Promega) and 50mM Tris, pH 7.5, 1mM MgCl<sub>2</sub>, 1mM dithiothreitol, 0.1mM ZnCl<sub>2</sub>, 20mM KCl, 2µCi [<sup>3</sup>H]Farnesyl pyrophosphate triammonium salt (Sigma-Aldrich) or (ii) 35µl rabbit reticulocyte lysate and 50mM Tris, pH 7.5, 5mM MgCl<sub>2</sub>, 2mM dithiothreitol, 50µM ZnCl<sub>2</sub>, 2µCi [<sup>3</sup>H]Geranylgeranyl pyrophosphate triammonium salt (PerkinElmer). Reactions were performed in 37°C for 2 hours. GST or GST-Gγ1 bounded Sepharose were then precipitated, washed for 5 times, boiled and subjected to SDS-PAGE analysis and fluorography.

#### *Double-strands RNA injection*

1<sup>st</sup> strand cDNA is synthesized using total RNA prepared from 0-24 hours *Drosophila* embryos. T7 sequence flanked pericardin 3' cDNA fragment (~450bp) is amplified using these 1<sup>st</sup> strand cDNA as template by PCR reactions, in which the following two primers are used:

T7-prec-forward:

TAATACGACTCACTATAGGGAGACCACAGCCAACAGACAGTCGTGGT  
GCCGGTG;

T7-prci-reverse:

TAATACGACTCACTATAGGGAGACCACCTAGCATTTCATTGGTGGG  
CGCCTTGG

*Pericardin* (*prc*) double stranded RNA is synthesized following standard protocol (Kennerdell and Carthew, 1998) using T7 RNA polymerase and 3' *prc* cDNA fragment as template. *prc* RNAi is precipitated and resolved in *Drosophila* injection buffer as different concentration (0.5µM-5µM). The *Hand-GFP* transgene was used as the source of embryos for microinjection of *prc* RNAi. Embryos were collected over a 30-min period at 25°C. The microinjection is preformed following standard procedure. The average injection volume was 50pl. After injection of dsRNA, embryos were incubated at 18°C under oil overnight for further development. The injected embryos at stage 16 were examined for cardiac phenotype under a fluorescence microscope.

#### *Live imaging of Drosophila heart development*

Wild type or *Gγ1*<sup>k08017</sup> homozygous mutant embryos bearing *Hand-GFP* transgene were used for the live imaging. Stage 13 embryos were collected, dechorionized and mounted dorsal side up in halo-carbon oil. The images were obtained using a Zeiss LSM510-meta confocal microscope. Every 5 minutes, a series of pictures were scanned from the top to the middle of the embryos and a Z-stack projection was made. The embryos were recorded for 24 hours at 18°C.

Movies were generated from these time-series of Z-stack projections using the Zeiss LSM510 Meta software.



## CHAPTER III

### **The mevalonate pathway controls heart formation in *Drosophila* by isoprenylation of G $\gamma$ 1**

#### *Genetic screen for cardiac genes*

To do the forward genetic screen to study heart morphogenesis, we must find a way allowing us to see the whole structure of *Drosophila* heart easily and fast. The previous genetic screens for *Drosophila* development all used immunostaining for several heart marker proteins such as *mef2*, *eve* or *tinman*. There are two major disadvantages of these screens: First, immunostaining is a very time-consuming and tedious procedure for large-scale genetic screen. Second, those marker proteins used in previous screens only labels a subset of *Drosophila* heart cells. For example, *mef2* only labels the cardioblasts, while *tinman* only labels two out of six heart cells per hemisegment. Therefore, it is impossible for these screens to discover the genes involved in the heart morphogenesis in a whole organ level. To overcome these obstacles, we decided to generate a transgenic fly

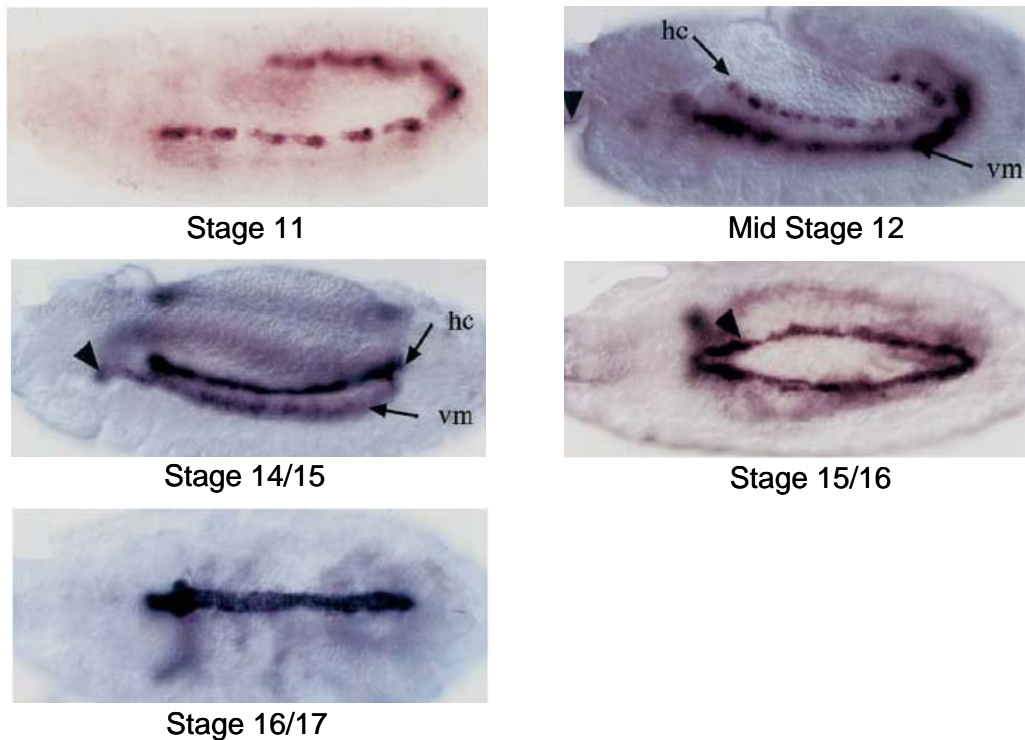


**Figure 3.1. The expression of hand in *Drosophila* embryo.** (adapted from Kolsch V et al.'s paper (Kolsch and Paululat, 2002)). From stage 11 onward, Hand is strongly expressed in all the cardiac cells and visceral muscle cells. The expression of Hand is shown by *in situ* hybridization.

with heart-specific GFP marker which labels all the heart cells. By using the heart GFP transgenic fly, the whole heart structure can be easily examined under a fluorescence microscope without even killing or fixing the animal. Since the GFP marker can be seen in the living animal, we can even monitor how heart is developed into different defects we may find in the genetic screen.

The following is our strategy to generate this heart-GFP transgenic fly:

- (1) Find a candidate gene which is expressed in all the heart cells during the development;
- (2) Map and clone its heart-specific enhancer;
- (3) Use this enhancer to drive the GFP expression and generate the transgenic fly.

Fortunately, there is a perfect candidate gene that fits all our criteria.

*Drosophila hand* is reported to be expressed in all the heart cells and visceral muscles as well during the embryogenesis. The *in situ hybridization* showed the expression of *hand* in the heart in different developmental stages (Figure 3.1) (Kolsch and Paululat, 2002).

Mapping the *Drosophila hand* minimal cardiac enhancer is done by a former post-doc in our lab, Zhe Han (Han and Olson, 2005). He cloned various and overlapped DNA fragments from ~5.7 kb upstream to ~6.9 kb downstream of the *hand* gene (Figure 3.2). These DNA fragments were then cloned to 5' of a GFP gene with NLS at the N-terminus, and injected in the blastocyst stage of

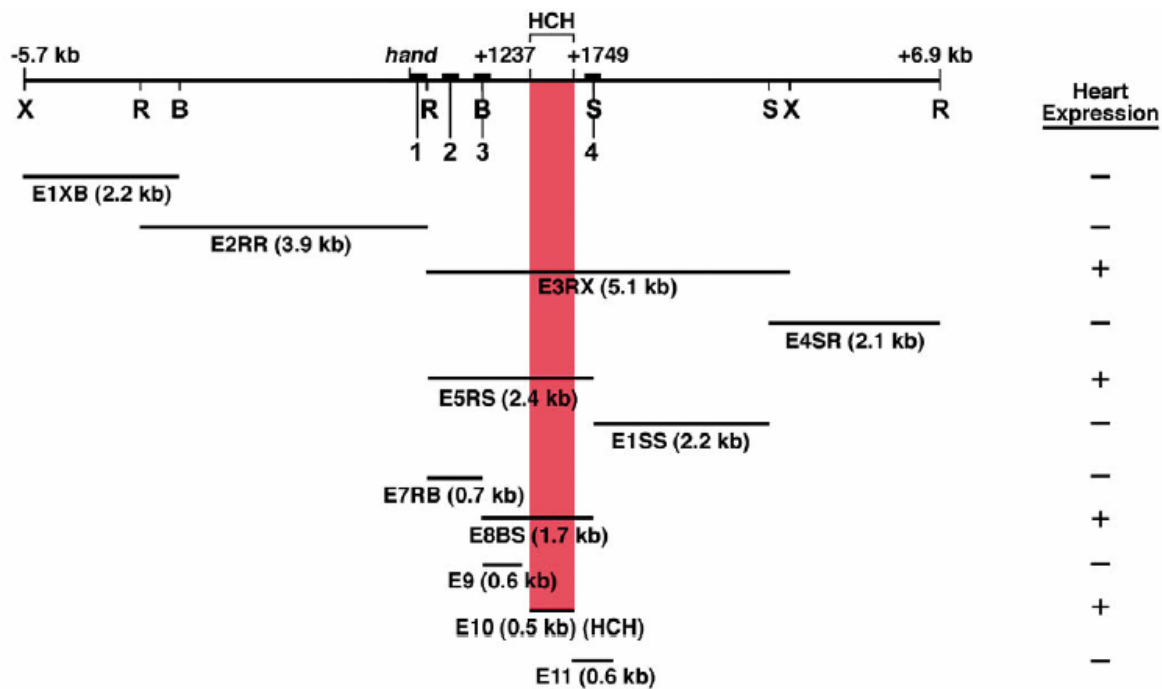


**Figure 3.2. Mapping the cardiac enhancer (HCH) of *Hand* (Han and Olson, 2005).** The *Hand* gene is on chromosome 2, containing 4 exons. The 13 kb genomic region containing *Hand* gene was screened for expression in the embryonic heart using a GFP reporter. A 517 bp minimal cardiac enhancer (called HCH) was identified between exons 3 and 4.

*Drosophila* embryo to generate the transgenic animal. These transgenic animals were then examined to see if their GFP is expressed in the heart cells just as the *hand* gene. The results are summarized in Figure 3.2. The minimal *hand* cardiac enhancer resides in a small region in the 3<sup>rd</sup> intron (+1237~+1742) with 517 base pairs in length (Figure 3.3A). This 517 bp fragment was then cloned to the 5' of NLS-GFP and the transgenic fly was generated (Figure 3.3B).

The GFP labels the nucleus of all the heart cells throughout the embryogenesis. Figure 3.3C shows the GFP expression in the late embryo stage. We can clearly see the different structure of *Drosophila* heart, the lymph gland, two rows of cardioblasts forming the heart tube, and two rows of pericardial cells flanking the heart tube.

There are several strategies to do the forward genetic screens:

- (1) EMS screen;
- (2) P-element (transposon) insertion screen;
- (3) Deficiency screen.

The EMS screen is widely used in the forward genetic screen in different model systems because it can induce the mutation randomly and it is possible to reach the saturation. In theory, we can hit every gene by EMS screen. But the biggest disadvantage of EMS screen is that it is very difficult to map the mutation, which usually takes half year to one year and huge amount of work to know which gene the mutation affects.

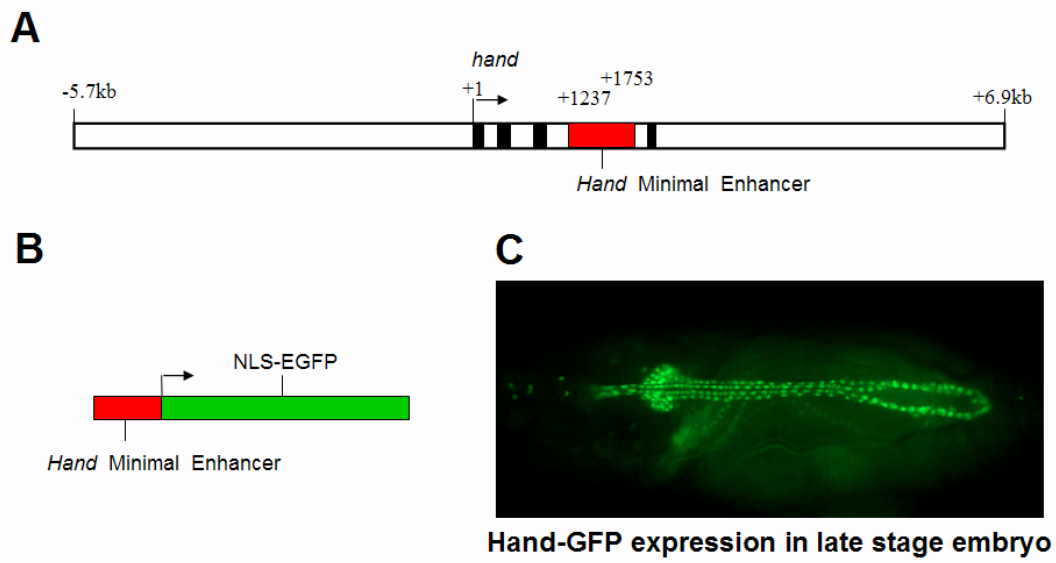


**Figure 3.3 *Hand-GFP* transgenic fly.** The 517bp minimal enhancer of *Hand* (A) can drive GFP expression (B) in all the heart cells, including cardioblasts, pericardial cells and lymph gland (C).

In *Drosophila*, transposon insertion is also a good way to disrupt a gene. For transposon insertion mutant, it is very easy to know which gene is disrupted by just doing a simple reverse PCR experiment, which will tell us the flanking sequence of the transposon insertion and then we can get the position of the transposon on the chromosome by genome blast. The Berkeley *Drosophila* Genome Project (BDGP), the Exelixis stock center and other individual *Drosophila* genetists have generated many transposon insertion mutants and contributed them to the public stock center. The flanking sequence and their positions on chromosome are also published in the stock center. To date, the transposon insertion has hit over 53% of the genes and over 25% vital genes in *Drosophila* genome (Bellen et al., 2004; Spradling et al., 1999; Thibault et al., 2004).

Deficiency screen, on the other hand, is to screen all the deletion mutants instead of the mutant for a single gene. A deficiency line usually deletes tens or over one hundred genes. But the advantage of this screen is only that several hundreds of deficiency lines can cover almost the entire genome. For some of the deficiency collections, such as Exelixis and DroDel collection, the deletion breakpoint is molecularly mapped, so we know exactly what genes are deleted in these deficiency lines. Considering these advantages and disadvantages of different screen strategies, we decided not to do the EMS screen, but combine the

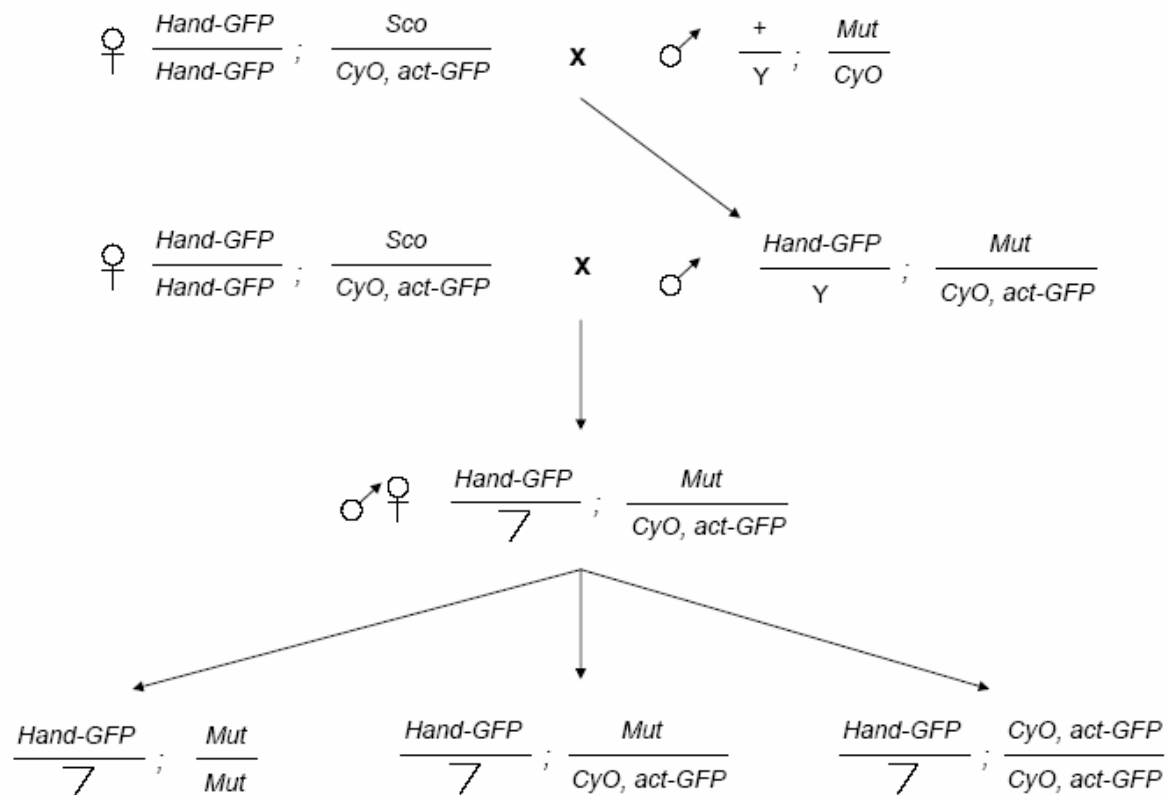


**Figure 3.4. Cross scheme in *Hand-GFP* heart forward genetic screen.** Screen for chromosome 2 is indicated here as an example. The cross scheme for chromosome 3 is similar to that for chromosome 2. The final fly stocks used in the screen have *Hand-GFP* on chromosome X and are balanced with a balancer bearing *act-GFP* transgene, which expresses GFP in gut cells.



transposon insertion screen and deficiency screen in our study. We expected to get a whole picture of what kind of heart morphology defects we can get, and to get a brief idea what pathways contribute to those morphology defects very quickly. If we want to study a certain heart defect in details, we can do the candidate genes search based on the genes coming out from our screen or do an EMS saturated screen later.

We decided to first do screens for 2<sup>nd</sup> and 3<sup>rd</sup> chromosome because the crosses are easier to do and it is more convenient to examine the homozygous embryo phenotype than the screen for X chromosome. Since the heart function is essential for the viability of the flies, we expected every mutants leading to heart defect should be lethal. Therefore, we only collect all the lethal transposon insertion lines and Exelixis deficiency lines on chromosome 2 and 3 for our screen. We put our *Hand-GFP* transgene marker on chromosome X. The cross scheme is indicated in Figure 3.4, as the mutation (transposon insertion or deficiency) on chromosome 2 is shown as an example. We generated a stable line for each mutant we want to screen with *Hand-GFP* on the X chromosome and balanced with a balancer chromosome bearing an *act-GFP* transgene on it. We then collected the embryos of these stable lines and examine the *Hand-GFP* expression in the homozygous mutant embryo at stage 16-17. As shown in Figure 3.4, there are three genotypes for the progenies of the stable lines, homozygous mutant, heterozygous mutant and homozygous balancer chromosome. *Act-GFP* expresses

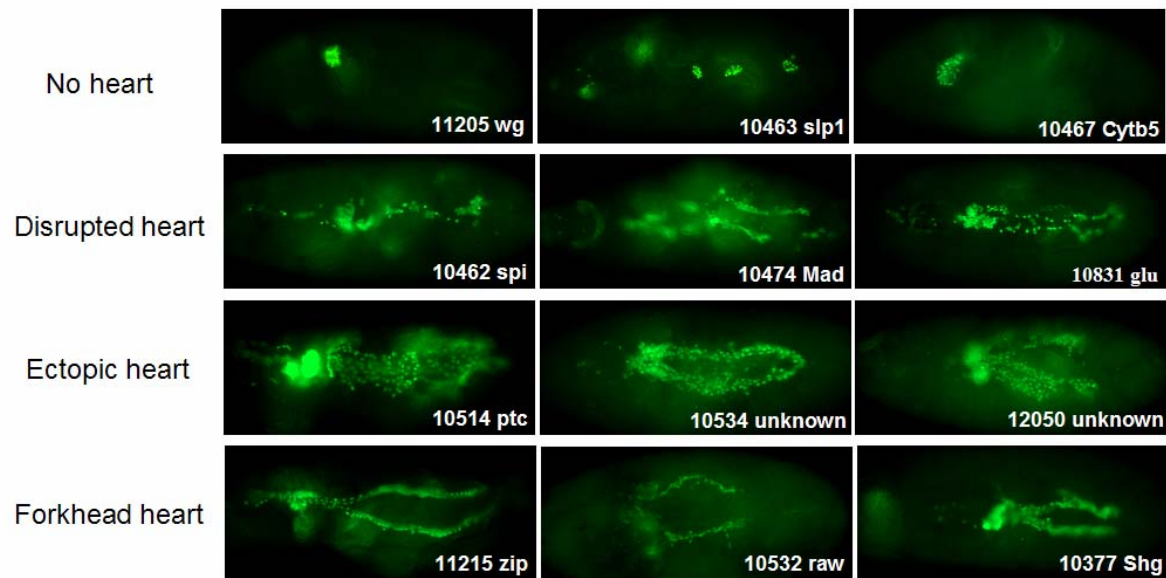


**Figure 3.5. Different cardiac defects discovered in our genetic screen.** The heart defect we found in the screen can be categorized into different classes. Here shows several examples for the classes of “no heart”, “disrupted heart”, “ectopic heart” and “forkhead heart”.

the GFP in the gut cells. Therefore, all the heterozygous mutant will have GFP expression in the gut, and the homozygous balancer chromosome embryos show a very early embryonic lethality and ubiquitous GFP expression. These two genotypes are very easy to be distinguished from the homozygous mutant, in which the GFP is only expressed in the heart but not the gut cells.

#### *Identification of broken hearted phenotype*

We screened ~3000 P-element (transposon) insertion lines and discovered many heart defects. These heart defects can be categorized into different groups. For example, we discovered groups of mutants with the defect of “*no heart*”, “*disrupted heart*”, “*ectopic heart*”, “*forkhead heart*” (Figure 3.5) or “*pericardial cells dissociated heart*” which we later term it “*broken hearted*” (Figure 3.6). In *Drosophila* genetics, showing the same or similar phenotype indicates the genes that are mutated may function in a same pathway. For example, in the “*no heart*” group, *Wg* and *Slp1* were previously reported to regulate the early cardiac mesoderm differentiation. Another example is that in the “*forkhead heart*” group, *zip*, *shg* and *raw* were reported to function together to regulate dorsal closure.

The most interesting heart defect category that we found in our screens is the “*pericardial cells dissociated heart*”, which we later termed *broken hearted (bro)*. As shown in Figure 3.6, compared to the wild type heart, in which the pericardial cells and the cardioblasts are very close to each other and form tight adhesion, the

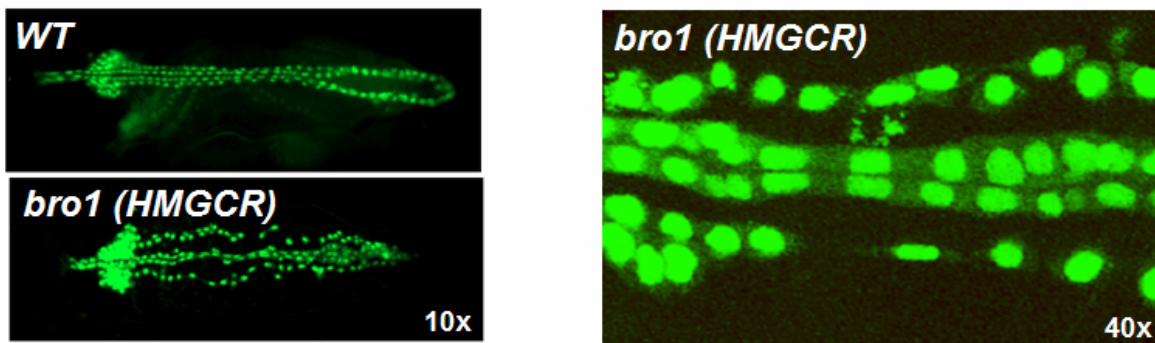


**Figure 3.6. Discovering of a new cardiac defect, *broken hearted (bro)*.** *bro* heart defect is the most popular defect found in our screen. *bro1(HMGCR)* is shown as an example, where pericardial cells fail to attach to cardioblasts to form adhesion.

<u><i>broken hearted mutants</i></u>	<u>Genes or locus</u>
<i>bro1</i>	<i>HMGCR</i>
<i>bro4</i>	<i>G<math>\gamma</math>1</i>
<i>bro5</i>	<i>Sar1</i>
<i>bro6</i>	Deficiency BL7595 (68F2-69A2)
<i>bro10</i>	<i>Wunen/Wunen2</i>
<i>bro11</i>	Deficiency BL7563 (61B2-61C1)

**Table 3.1. The *broken hearted* mutants discovered in our genetic screen.**

hearts in *broken hearted* mutants have the dorsal-midline-localized cardioblasts (heart tube) but have dissociated and dispersed pericardial cells. In the enlarged picture (40x), we can see that the adhesion between the pericardial cells and cardiac cells is lost, but the adhesion between the cardioblasts seems still fine. The relative positions of pericardial cells and cardioblasts changed with each heartbeat. All these *broken hearted* mutants are embryonic lethal. The heart function in the *broken hearted* mutants is compromised, as the heart is hardly beating in the mutant embryos. The other organs such as epidermis, tracheal system and muscles are well formed, suggesting that the heart defect is less likely due to the side effect of ubiquitous embryonic defect.

This *broken hearted* phenotype has never been described before, partially because no genetic screens have been done using a marker for the entire heart. It also turns out to be the most frequently seen heart defect in our genetic screens. We identified six mutants showing the *broken hearted* defect, four of which are P-element insertion mutants, while two are deficiency mutant deleting ~30 genes (Table 3.1). In the following chapters, we found more *bro* mutants through candidate genes approach. We name them *bro1-14* because they all show the very similar *broken hearted* defect. As we discussed before, having the same phenotype often suggests their genetic interaction or functioning together in the same pathway. We expected the genes mutated in these *bro* mutants represent a new pathway involved in *Drosophila* heart morphogenesis, mediating the

adhesion between pericardial cells and cardiac cells (cardioblasts). Therefore, my focus in this thesis study is to answer the following two questions:

- (1) How are these genes possibly linked to each other and functioning together in the same pathway?
- (2) How do these genes mediate the adhesion between the pericardial cells and the cardiac cells?

I first start from study of the *bro1* mutant, in which a gene called *HMG-CoA reductase (HMGCR)* is mutated. We discovered an important role that the mevalonate pathway plays in *Drosophila* heart development.

#### *The mevalonate pathway genes and Gγ1 control heart formation*

The P-element in the *bro1* locus (l(3)01152) is located in the first exon of the hydroxymethyl-glutaryl (HMG)-CoA reductase gene (*HMGCR*) (Fig. 3.7A) which is expressed in the dorsal vessel and the gonadal mesoderm, where it is required for migration of primordial germ cells (Van Doren et al., 1998). Mutants trans-heterozygous for *HMGCR*<sup>01152</sup> and a deficiency line Df(3R)Exel9013, which deletes the *HMGCR* gene, or two EMS mutants, *HMGCR*<sup>clb26.31</sup> and *HMGCR*<sup>clb11.54</sup> (Van Doren et al., 1998), showed similar, but more severe, cardiac defects than homozygous *HMGCR*<sup>01152</sup> mutants (Figure 3.7B-D). Injection of 0.1μM mevanolin, a HMG-CoA reductase specific inhibitor, into the blastocysts

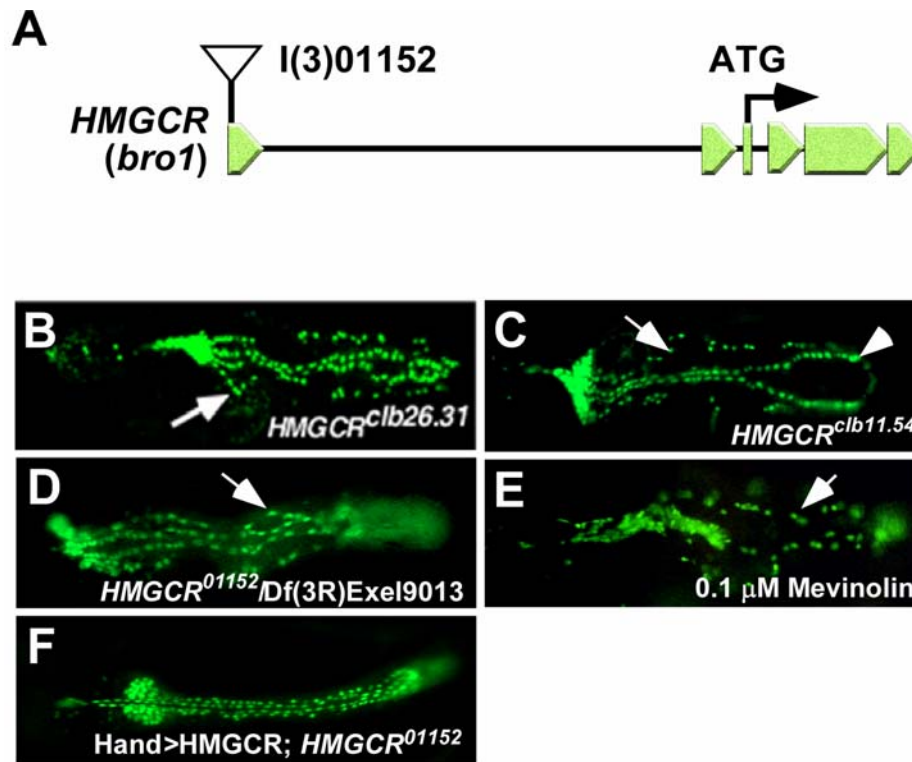


**Figure 3.7. *HMGCR* is mutated in *bro1* mutant.** (A) A schematic presentation of the *HMGCR (bro1)* locus. P-element insertion I(3)01152 in the *bro1* locus is inserted into the first exon of the *HMGCR* gene, where the starting ATG of *HMGCR* is in the third exon. (B and C) *HMGCR* EMS mutants *HMGCR<sup>clb26.31</sup>* and *HMGCR<sup>clb11.54</sup>* showed a more severe cardiac defect in which the posterior region of the heart tube was abnormally dilated (arrowhead). (D) Trans-heterozygous mutant *HMGCR<sup>01152</sup>/Df(3R)Exel9013* showed a severe *bro* defect. (E) Embryos injected with 0.1 μM Mevinolin showed cardiac defects similar to those of *HMGCR* null mutants at stage 17. (F) Expression of *HMGCR* specifically in the heart using *Hand-GAL4* and *UAS-HMGCR* is sufficient to rescue the *bro* defect in *HMGCR<sup>01152</sup>* embryos.



stage embryos also causes cardiac defects at stage 17 similar to those of the *HMGCR* mutants (Figure 3.7E). Expression of HMGCR in the heart, using a *Hand-GAL4* driver and *UAS-HMGCR* transgene, rescued the cardiac defects in the *HMGCR*<sup>01152</sup> mutant (Figure 3.7F), confirming the heart autonomous function of HMGCR.

HMG-CoA reductase (HMGCR) controls a rate-limiting step in the conversion of HMG-CoA into mevalonate, a precursor for the synthesis of cholesterol and isoprene derivatives (Figure 3.8). There are two major types of isoprene derivatives, namely farnesyl and geranylgeranyl. These two isoprenyls are used to modify the C-termini of proteins containing a CAAX motif (C, cysteine; A, aliphatic amino acid; X, any amino acid) (Der and Cox, 1991). In contrast to mammalian cells, *Drosophila* does not use the HMGCR pathway to synthesize cholesterol because several enzymes catalyzing the chemical reaction from squalene to cholesterol are missing (Santos and Lehmann, 2004b). To investigate whether either of the two major isoprenoids (Figure 3.8) - farnesyl pyrophosphate (farnesyl-PP) and geranylgeranyl pyrophosphate (geranylgeranyl-PP) - might be required for heart formation, we examined whether mutants in the genes encoding geranylgeranyl pyrophosphate synthase (GGPPS) and geranylgeranyl transferase type I  $\beta$  subunit ( $\beta$ GGT-I), which act downstream of HMGCR and are required for the biosynthesis of geranylgeranyl-PP or transfer of geranylgeranyl-PP to protein, might also cause cardiac defects. Indeed, GGPPS

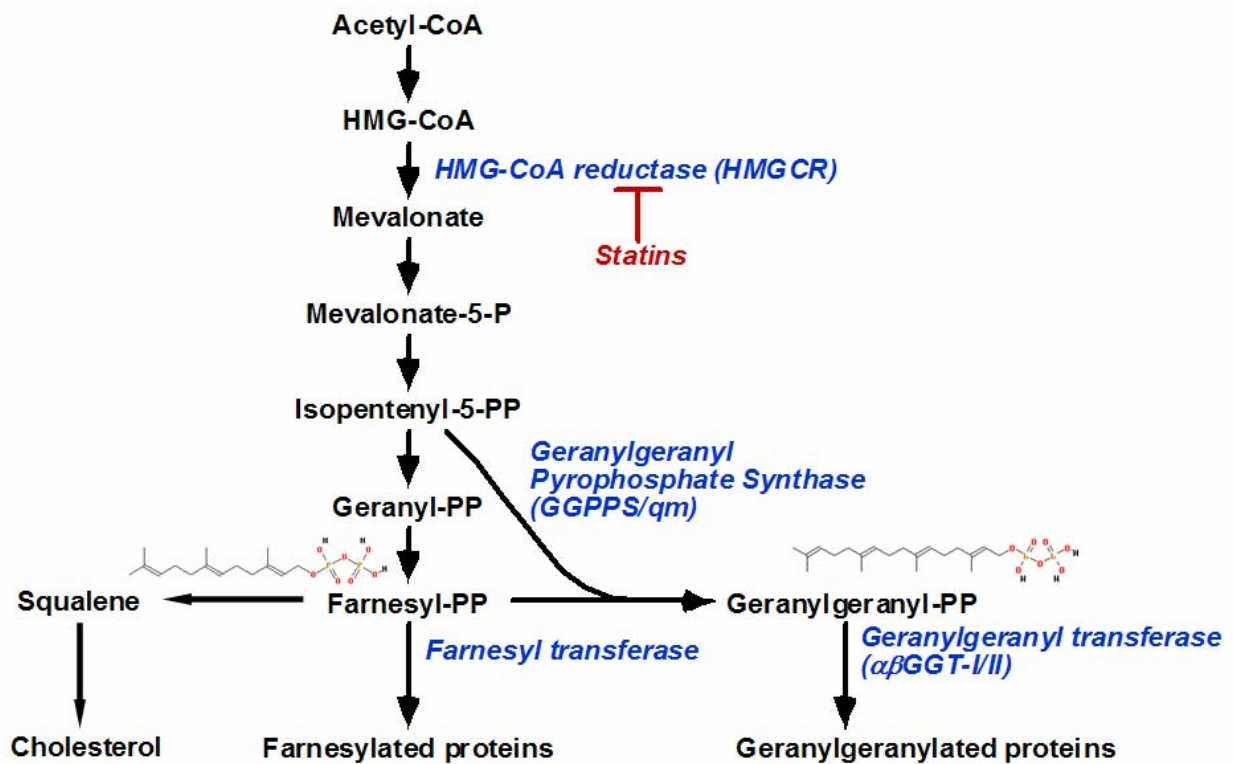


**Figure 3.8. Mevalonate pathway.** HMG-CoA reductase (HMGCR) is the rate-limiting enzyme in this pathway, which can be inhibited by statins, widely used cholesterol lowering drugs. Mevalonate pathway is used to synthesize three major lipid molecules, cholesterol, farnesyl and geranylgeranyl. Different from vertebrate, *Drosophila* does not use this pathway to synthesize cholesterol.

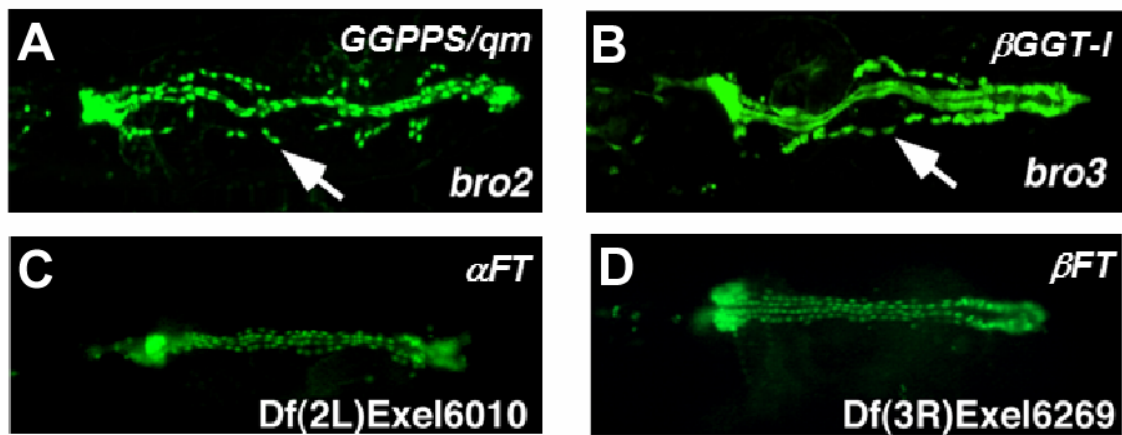


**Figure 3.9. The heart phenotype of the mevalonate pathway enzymes mutants.**

The mutants of *GGPPS(qm)* and *βGGT-I*, *GGPPS/qm<sup>L14.4</sup>* (**A**) and *βGGT-I<sup>S-2554</sup>* (**B**), showed the *bro* heart defect with 100% penetrance. (**C and D**) Deficiency lines Df(2L)Exel6010 or Df(3R)Exel6269 deleting either the farnesyl transferase  $\alpha$ (CG2976) or  $\beta$ (CG17565) subunit did not display similar cardiac defects as the other *bro* mutants.

(also called *qm*) mutant embryos showed 100% penetrance for the *bro* phenotype, just like *HMGCR* mutants (Figure 3.9A), and at least 30% of the  $\beta$ GGT-I mutants displayed the same phenotype (Figure 3.9B). In contrast, two deficiency lines (Df(2L)Exel6010 or Df(3R)Exel6269) deleting either the farnesyl transferase  $\alpha$  (CG2976) or  $\beta$  (CG17565) subunit did not display similar cardiac defects (Figure 3.9 C and D). These findings suggested that the cardiac defects of *HMGCR* mutant embryos resulted from a failure of geranylgeranylation of a target substrate protein required for the adhesion between cardioblasts and pericardial cells.

Analysis of another *bro* mutant (*bro4*) (Figure 3.10 D) suggested the G protein  $\gamma$  subunit 1 (*G $\gamma$ 1*), which contains a C-terminal CAAX motif, to be the substrate of this geranylgeranylation modification required for heart formation. The P-element in the *bro4* locus l(2)k08017 is inserted into the splice donor site after the first exon of the *G $\gamma$ 1* gene (Figure 3.10 A). *G $\gamma$ 1* expression level was reduced over 50% in homozygous l(2)k08017 embryos (Figure 3.10 B and C), suggesting that l(2)k08017 is a hypomorphic mutant allele of the *G $\gamma$ 1* gene. The homozygous embryos of *G $\gamma$ 1*<sup>k08017</sup>, the null mutant *G $\gamma$ 1*<sup>N159</sup> and heterozygous mutant *G $\gamma$ 1*<sup>N159</sup>/Df(2R)H3E1 all show similar *broken hearted* defect (Figure 3.10 D-F). The double mutants of the hypomorphic *HMGCR* and *G $\gamma$ 1* alleles showed a more severe cardiac defect than either single mutant, suggesting their

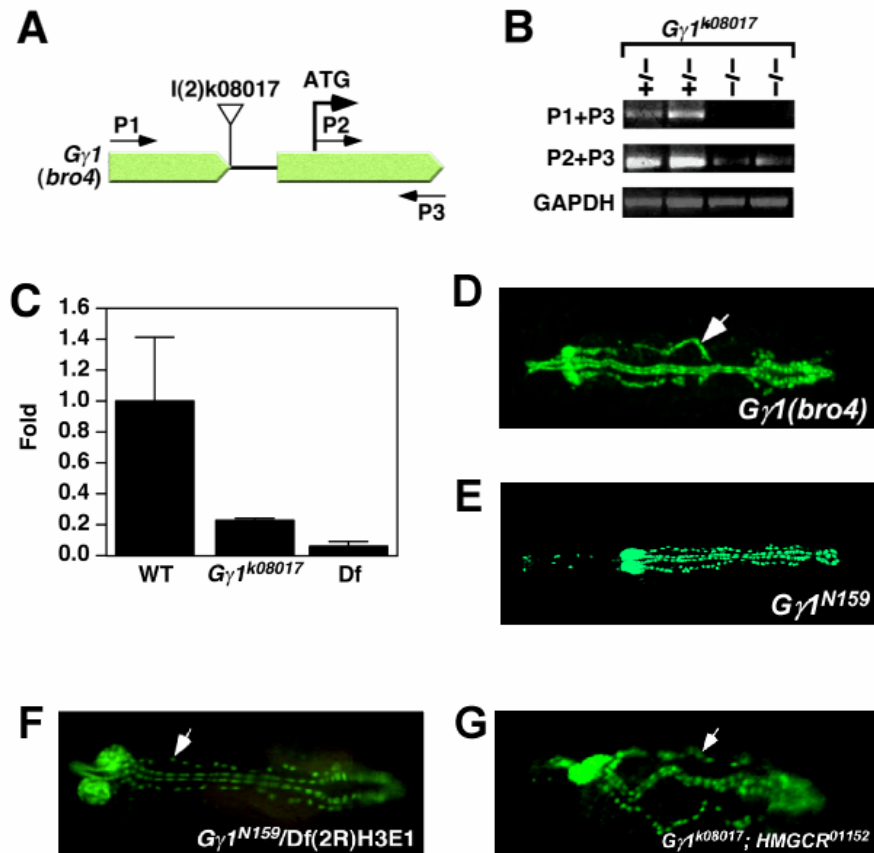


**Figure 3.10. Heterotrimeric G protein *Gγ1* is required for heart cells adhesion.**

(A) Schematic representation of the *Gγ1 (bro4)* locus. Primers P1 and P3 were used to amplify the full-length transcript, and P2 and P3 were used to amplify the coding region. (B) RT-PCR for *Gγ1<sup>k08017</sup>* embryos. Compared to *Gγ1<sup>k08017</sup>* heterozygous embryos, the *Gγ1<sup>k08017</sup>* homozygous embryos have no full-length transcript (P1+P3), but generate a weak PCR product for the coding region (P2+P3). GAPDH serves as loading control. (C) Real-time PCR shows that the expression level of *Gγ1* in homozygous *l(2)k08017* embryos is reduced over 50% compared to wildtype is still more than *Gγ1* deficiency homozygous embryos. The expression level of *Gγ1* for wild type is considered as 1 fold. Two *Gγ1* mutants, *Gγ1<sup>k08017</sup>* (D) and *Gγ1<sup>N159</sup>* (null) (E), and heterozygous mutant of *Gγ1<sup>N159</sup>* with *Df(2R)H3E1* all have very similar *bro* heart defect. (G) Double mutant of *Gγ1<sup>k08017</sup>* and *HMGCR<sup>01152</sup>* have more severe heart defect than either of the single mutants, suggesting their genetic interaction.

genetic interreaction (Figure 3.10 G)..

The final C-terminal residues of all G protein  $\gamma$  subunits contain a CAAX motif (Clapham and Neer, 1997) in which the variable amino acid X determines the type of lipid modification: If X is Ser, Met, Ala or Gln, the Cysteine is modified by farnesylation, whereas if X is Leu or Val, it is modified by geranylgeranylation (Kinsella et al., 1991; Reiss et al., 1991). Using an in vitro prenylation assay, we found that *Drosophila* G $\gamma$ 1 protein, which contains a CAAX motif of –CTVL, was modified by geranylgeranylation, but not by farnesylation (Figure 3.11A), in agreement with the requirement of GGPPS/qm and  $\beta$ GGT-I for cardiac development.

To determine directly if geranylgeranylation of G $\gamma$ 1 is essential for heart development, we tested whether wild type and mutant forms of G $\gamma$ 1 protein could rescue the cardiac defect of the G $\gamma$ 1 mutant. Targeted expression of wild type G $\gamma$ 1 in the heart was sufficient to rescue the cardiac defects of G $\gamma$ 1 mutants (Figure 3.11B), whereas mutant forms of G $\gamma$ 1, in which geranylgeranylation was abolished by either a substitution of Cysteine-67 in the CAAX box by Serine (G $\gamma$ 1-C67S) or a deletion of the CAAX box (G $\gamma$ 1- $\Delta$ CAAX), failed to rescue the cardiac defects in G $\gamma$ 1 mutants (Figure 3.11 C and D). We conclude that geranylgeranylation of the CAAX motif of G $\gamma$ 1 is required for its normal activity during *Drosophila* heart formation.

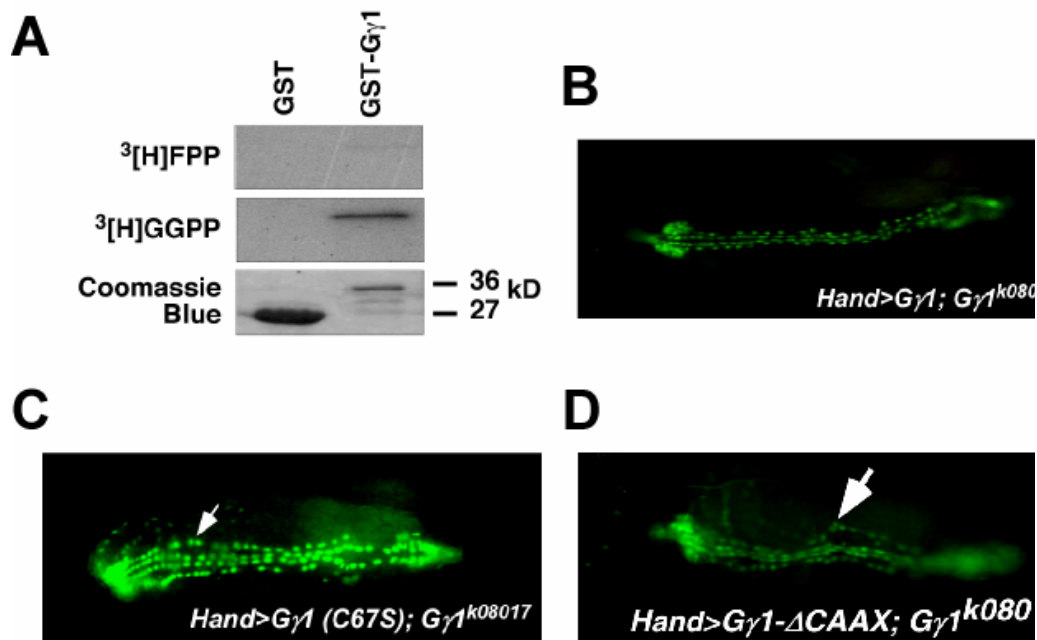


**Figure 3.11. Geranylgeranylation of Gγ1 is required for heart formation.** (A) Gγ1 can be efficiently geranylgeranylated, as labeled by [ $^3\text{H}$ ]geranylgeranyl pyrophosphate ([ $^3\text{H}$ ]GGPP) (middle panel), but cannot be farnesylated by [ $^3\text{H}$ ]farnesyl pyrophosphate ([ $^3\text{H}$ ]FPP) (top panel). Recombinant GST (27kD) and GST-Gγ1 (36kD) proteins are shown by coomassie blue staining in the bottom panel. (B) Expression of Gγ1 in the heart using Hand-GAL4 driving UAS-Gγ1 is sufficient to rescue the *Gγ1<sup>k08017</sup>* mutant cardiac defects, but targeted expression of Gγ1 (Gγ1(C67S) (C) or Gγ1-ΔCAAX (D) mutants in the heart failed to rescue the *Gγ1<sup>k08017</sup>* cardiac defects.

Lipid modification of the CAAX motif facilitates the association of proteins with membranes (Clapham and Neer, 1997; Maltese and Robishaw, 1990; Muntz et al., 1992; Ohguro et al., 1991). To further explore how geranylgeranylation of G $\gamma$ 1 affects its biological function, we examined the subcellular localization of the G $\gamma$ 1 protein in *Drosophila* S2R<sup>+</sup> cells. Wild type G $\gamma$ 1 protein was always excluded from the nucleus in S2R<sup>+</sup> cells (Figure 3.12 a and a'), whereas the two mutant forms of G $\gamma$ 1 (G $\gamma$ 1(C67S) and G $\gamma$ 1- $\Delta$ CAAX), which were not geranylgeranylated, were located throughout the cytoplasm and nucleus (Figure 3.12 b and b', c and c'). Since G $\gamma$ 1 is a small protein and can enter the nucleus freely, the specific localization of wild type G $\gamma$ 1 protein to the cytoplasm likely reflects its interaction with membranous structures, which requires modification by geranylgeranylation.

In S2R<sup>+</sup> cells treated with three HMGCR inhibitors (Atorvastatin, Mevinolin and Simvastatin) as well as *HMGCR* double-stranded RNA, the wild type G $\gamma$ 1 protein displayed the same abnormal subcellular distribution as the two mutant forms of G $\gamma$ 1 (Figure 3.12 d, d', e, e', f, f', g and g'). These findings suggest that abnormal subcellular localization of G $\gamma$ 1 accounts for the cardiac defects in the HMGCR pathway mutants and G $\gamma$ 1 mutants.



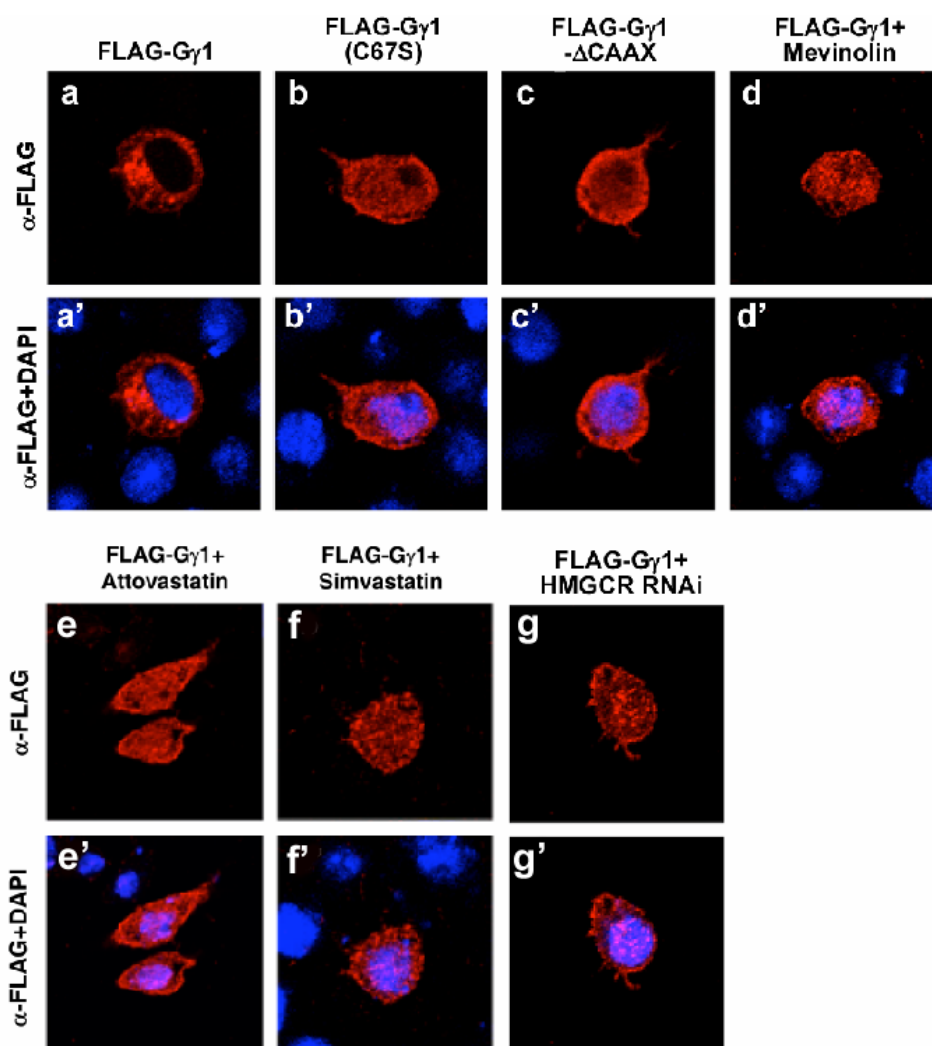


**Figure 3.12. Mevalonate pathway regulates the cellular localization of G $\gamma$ 1.** (a and a') In S2R<sup>+</sup> cells, G $\gamma$ 1 is localized to the cytosolic compartment, whereas the two mutant forms show nuclear and cytoplasmic localization (b, b', c, c'). In the presence of HMGCR inhibitors, mevinolin (d and d'), Atrovastatin (e and e'), Simvastatin (f and f') or *HMGCR* double-stranded RNA treatment, G $\gamma$ 1 shows a ubiquitous localization as seen with the two mutant forms (g and g').

The developmental onset of cardiac defects was identical in the *HMGCR*, *G $\gamma$ 1*, *GGPPS/qm* and  $\beta$ GGT-I mutants. Cardioblasts and pericardial cells were properly specified, aligned and migrated to dorsal midline until stage 16 (Figure 3.13 A-D). However, at stage 17, pericardial cells dissociated from the dorsal vessel and the posterior region of the heart tube became abnormally dilated, suggesting that these genes are required to maintain cardiac integrity. The phenotypes of the different mutants were also comparable, except for the two *HMGCR* EMS mutants or the *HMGCR*<sup>01152</sup>/Df(3R)Exel9013 mutant, which was more severe and showed distortion of the shape of the dorsal vessel (Figure 3.7 B-D).

Cardiac defects of *HMGCR* or *G $\gamma$ 1* mutants could be completely rescued by targeted expression of *UAS-HMGCR* and *-G $\gamma$ 1* transgenes, respectively, using a Hand-GAL4 driver, which directs expression in both cardioblasts and pericardial cells, or a Mef2-GAL4 driver, which is expressed in cardioblasts but not in pericardial cells (Figure 3.14 A and B). In contrast, targeted expression of *HMGCR* or *G $\gamma$ 1* using Dot-GAL4, which only drives expression in pericardial cells, failed to rescue the cardiac defects in either mutant (Figure 3.14 C and D).

These results demonstrate that *HMGCR* and *G $\gamma$ 1* function specifically in cardioblasts to adhere with pericardial cells and exclude the possibility that the *bro* cardiac phenotype arises secondarily from general metabolic abnormalities.

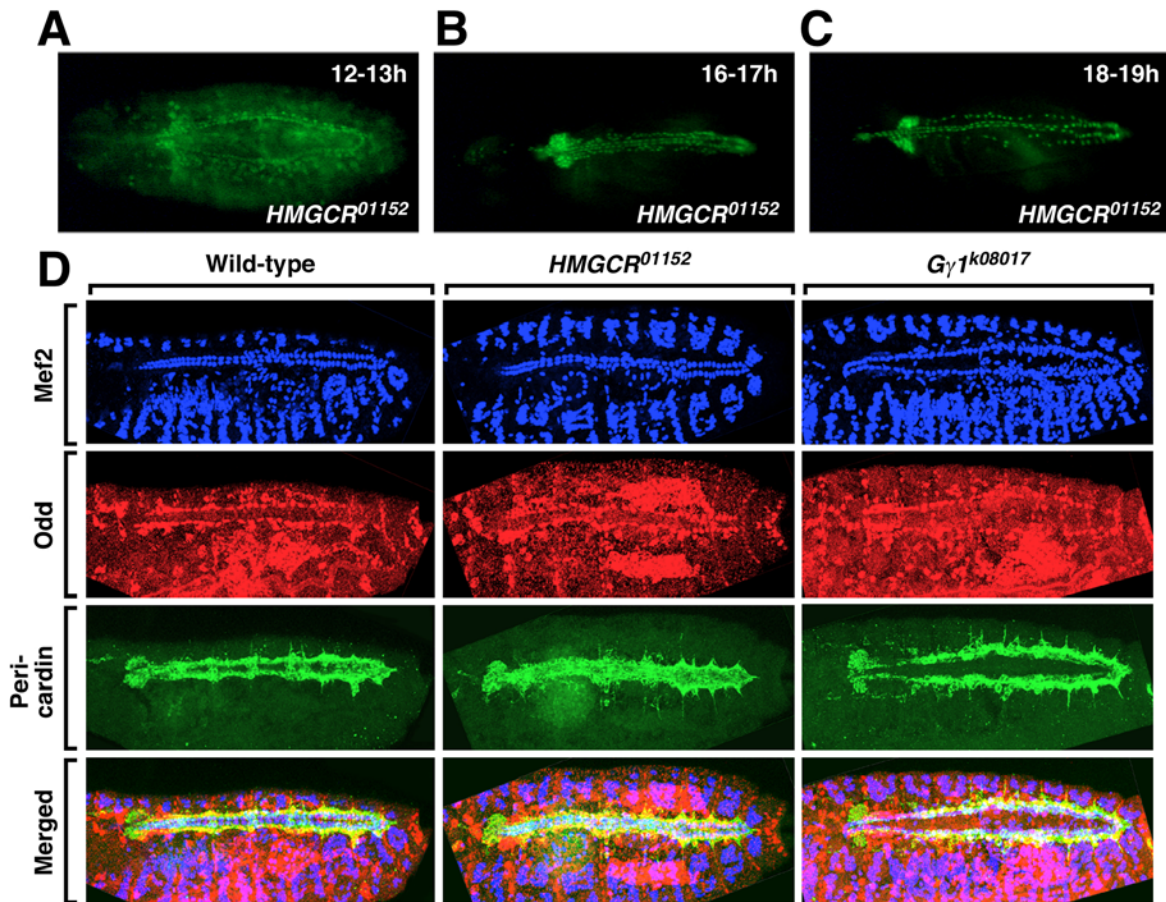


**Figure 3.13. Specification and alignment of cardioblasts and pericardial cells during development.** (A-C) Cardioblasts and pericardial cells (labeled by Hand-GFP) were properly specified and aligned until stage 16. (A) Stage 14 (12-13 hours) *HMGCR*<sup>01152</sup> embryo. (B) Stage 16 (16-17 hours) *HMGCR*<sup>01152</sup> embryo. (C) Stage 17 (18-19 hours) *HMGCR*<sup>01152</sup> embryo. (D) *HMGCR*<sup>01152</sup> and *Gγ1*<sup>k08017</sup> embryos showed normal cardiac and pericardial cell specification and alignment compared to wildtype. Stage 16 embryos were labeled by antibodies against Dmef2 (blue, labels cardioblasts), Odd-skipped (red, labels pericardial cells) and Pericardin (green, labels the general morphology of the heart).

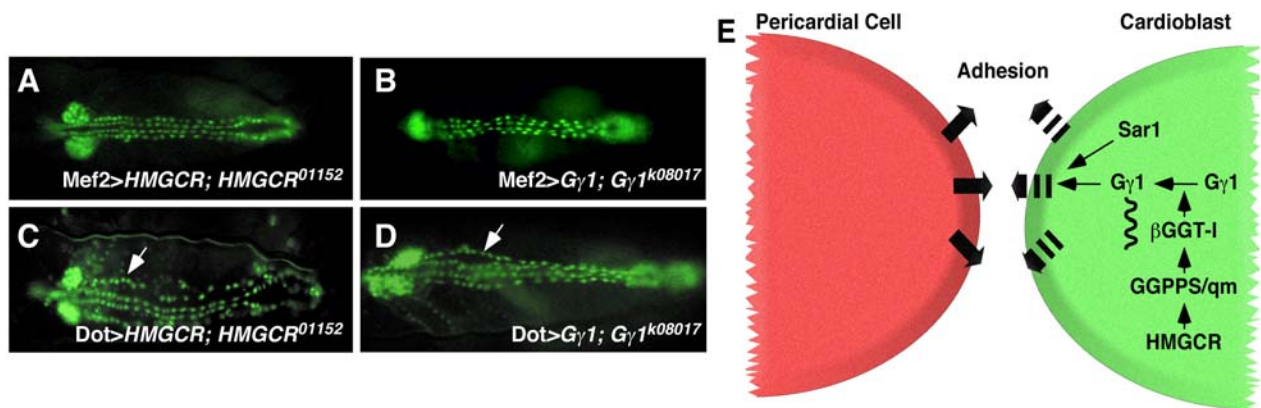


**Figure 3.14. HMGCR and G $\gamma$ 1 are specifically required in cardioblasts to maintain cardiac integrity.** (A and B) Expression of HMGCR or G $\gamma$ 1 in cardioblasts is sufficient to rescue the *bro* defect in *HMGCR*<sup>01152</sup> or *Gγ1*<sup>k08017</sup> mutants, respectively. (C and D) Expressing HMGCR (C) or G $\gamma$ 1 (D) in pericardial cells cannot rescue the *bro* defect in *HMGCR*<sup>01152</sup> or *Gγ1*<sup>k08017</sup> mutants. (E) A model summarizing the function of the Mevalonate pathway, G $\gamma$ 1, and Sar1 during *Drosophila* heart formation.

A fifth *bro* mutation was mapped to the *Sar1* gene (Figure 3.15 A), which encodes a GTPase that controls budding of COPII coated vesicles from the ER to the Golgi network (Aridor et al., 2001). The *Sar1* mutant we used in the screen is a hypomorph mutant and it shows the similar *broken hearted* phenotype as the other *bro* mutants (Figure 3.15 B and C).

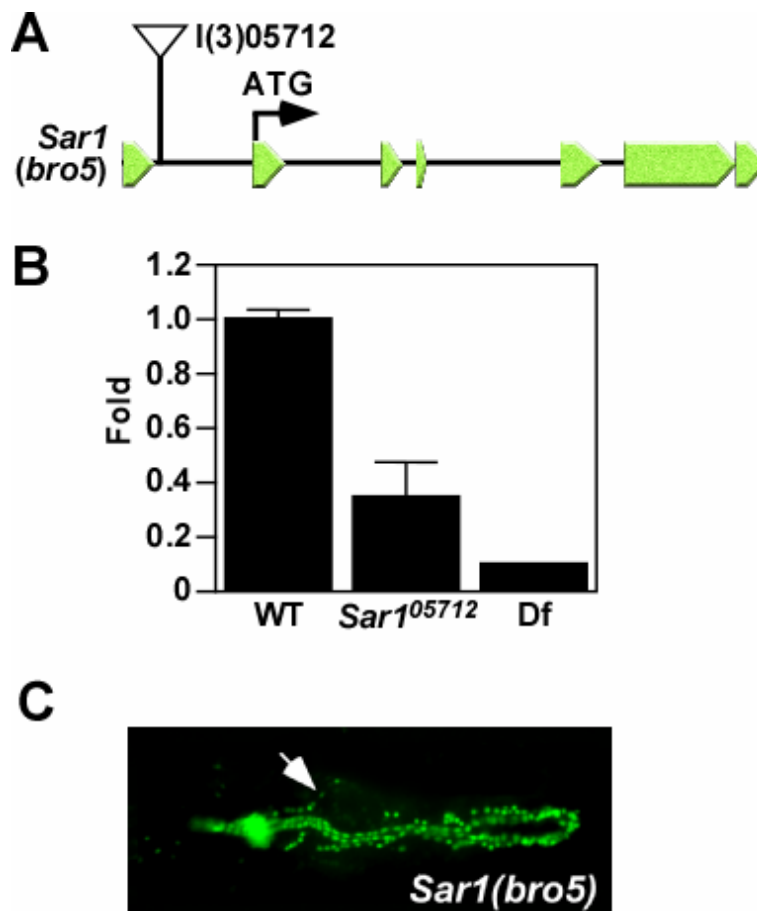


**Figure 3.15. Characterization of *Sar1 (bro5)* locus.** (A) Schematic representation of the *Sar1 (bro5)* locus. P-element insertion l(3)05712 in the *bro5* locus is inserted into the first intron of the *Sar1* gene, where the starting ATG of *Sar1* is in the second exon. (B) Real-time PCR shows that the expression level of *Sar1* in homozygous l(3)05712 embryos is greatly reduced compared to wild type but is still more than *Sar1* deficiency (Df(3R)Exel6190) homozygous embryos. The expression level of *Sar1* for wild type is considered as 1 fold. (C) *Sar1(bro5)* mutant shows *bro* heart defect with 100% penetrance.

### *Discussions*

HMGCR and downstream enzymes in the biochemical pathway leading to the synthesis of geranylgeranyl-PP are specifically required in cardioblasts to modify G $\gamma$ 1 (Fig. 3.14E). We propose that geranylgeranylation, which is required for the proper intracellular localization of G $\gamma$ 1, is in turn required for generating a signal for pericardial cells to adhere to cardioblasts throughout heart formation. Indeed, G $\beta$  $\gamma$  has been shown to control Golgi apparatus organization and vesicle formation during exocytosis in mammalian cells (Jamora C. et al., 1997; Ohashi and Huttner, 1994). The finding that a mutation in Sar1 causes the same cardiac phenotype as the G $\gamma$ 1 mutation further supports the possibility that this collection of mutations perturbs the secretion of a factor required for maintenance of cardiac integrity.

Interestingly, the essential function of the mevalonate pathway in heart tube morphogenesis seems to be conserved from *Drosophila* to vertebrates, as it was recently reported that zebrafish with a mutation in the *hmgcr1b* gene show abnormal heart morphology, defects in myocardial cell migration and pericardial edema (D'Amico et al., 2007). Although the specific target of the mevalonate pathway that controls zebrafish heart formation remains to be defined, the evolutionary conservation of basic cardiogenic regulatory mechanisms suggests

that heterotrimeric G proteins may serve as targets for the mevalonate pathway during vertebrate heart morphogenesis.

Inhibition of this pathway with statins results in cardiac defects similar to those resulting from mutations in HMGCR and downstream genes required for isoprenoid biosynthesis, raising the possibility that congenital heart defects reportedly associated with the use of statins (Edison and Muenke, 2004, 2005), which are contraindicated during pregnancy, may reflect perturbation in a similar developmental pathway.

HMGCR has also been shown to be required for recruitment of primordial germ cells (PGCs) to the gonad in *Drosophila* (Van Doren et al., 1998), but the protein target of the mevalonate pathway that mediate this process have not been identified. Perhaps G $\gamma$ 1 functions in the gonad mesoderm to guide PGC migration. We speculate that lipid modifications mediated by the mevalonate pathway contribute to directed cell migration and subsequent cell-cell adhesion in diverse cell types. Given the conservation of cardiac developmental control mechanisms, it will be of interest to investigate the potential involvement of the mevalonate pathway in mammalian heart development and congenital heart disease.



## CHAPTER IV

### **Heterotrimeric G proteins control cardiac integrity in *Drosophila* by regulating septate junction formation**

#### *Heterotrimeric G proteins control cardiac integrity*

At the end of *Drosophila* embryogenesis, cardiac and pericardial cells must adhere tightly to maintain the structural integrity of the dorsal vessel (Figure 4.1A). The *bro* defect is characterized by morphological abnormalities in the dorsal vessel due to a failure in adhesion between cardiac and pericardial cells, resulting in dilation of the dorsal vessel, loss of cardiac function and early larval lethality (Yi et al., 2006). The *bro* phenotype can be readily visualized by perturbation in the ordered expression pattern of a *Hand-GFP* marker in cardiac and pericardial cells. Mutations in mevalonate pathway genes as well as *Gγ1* all result in a similar *bro* heart defect (compare Figures 4.1 B and C).

Because G proteins function as heterotrimers, we sought to identify the  $\alpha$  and  $\beta$  subunits that functioned together with *Gγ1* to mediate cell adhesion in the dorsal vessel. There are 6 annotated *Gα* subunits, 3 *Gβ* subunits, and 2 *Gγ* subunits encoded by the *Drosophila* genome (Table 4.1). *Gα49B*, *Gβ76C* and *Gγ30A* (also called *Gαq*, *Gβe* and *Gγe*, respectively) function specifically in

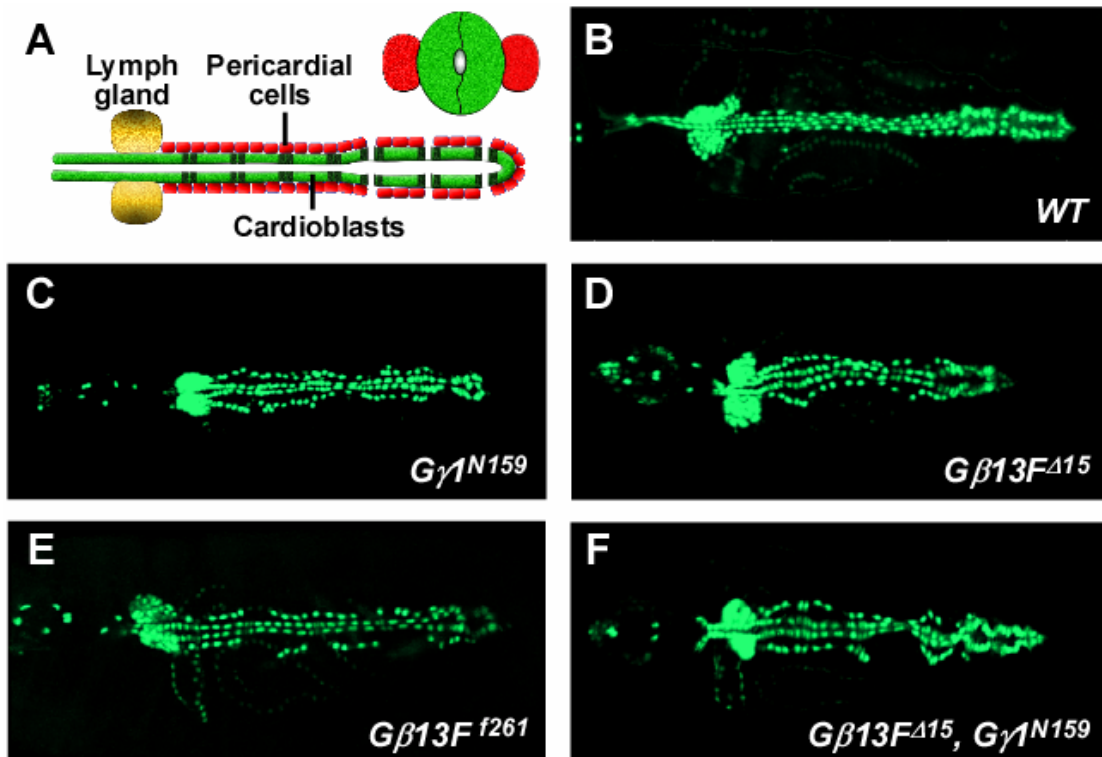


**Figure 4.1.  $G\beta 13F$  mutants show the same *bro* defect as a  $G\gamma 1$  mutant.** (A) Schematic drawing of a stage 17 embryonic heart (Dorsal view with anterior to the left and a cross section view). Cardioblasts, pericardial cells and lymph glands are indicated by green, red and yellow color, respectively. (B-F) Stage 17 embryonic heart labeled by *Hand-GFP* in wild type embryo (B), null mutant of  $G\gamma 1$  ( $G\gamma 1^{N159}$ ) (C), null mutant of  $G\beta 13F$  ( $G\beta 13F^{\Delta 15}$ ) (D), protein null mutant of  $G\beta 13F$  ( $G\beta 13F^{f261}$ ) (E), and double mutant of  $G\beta 13F^{\Delta 15}$  and  $G\gamma 1^{N159}$  (F).

<b>G<math>\alpha</math></b>	<b>G<math>\beta</math></b>	<b>G<math>\gamma</math></b>
<i>concertina</i>	<i>G<math>\beta</math>5</i>	<i>G<math>\gamma</math>1</i>
<i>G-i<math>\alpha</math>65A</i>	<i>G<math>\beta</math>13F</i>	<i>G<math>\gamma</math>30A (G<math>\gamma</math>e)</i>
<i>G-o<math>\alpha</math>47A</i>	<i>G<math>\beta</math>76C (G<math>\beta</math>e)</i>	
<i>G-s<math>\alpha</math>60A</i>		
<i>G<math>\alpha</math>49B (G<math>\alpha</math>q)</i>		
<i>G<math>\alpha</math>73B</i>		

**Table 4.1. Heterotrimeric G proteins in *Drosophila* genome.**

phototransduction and are unlikely to function in the heart (Lee et al., 1990; Schulz et al., 1999; Yarfitz et al., 1991). Two mutants for *Gβ13F*, referred to as *Gβ13F<sup>f261</sup>* and *Gβ13F<sup>Δ15</sup>* (Fuse et al., 2003), both showed a *bro* heart defect similar to the *Gγ1* mutant (Figures 4.1 D and E), whereas a deficiency line deleting either *Gβ5* or *Gβ76C* did not show a *bro* defect (data not shown). A double null mutant of *Gβ13F<sup>Δ15</sup>* and *Gγ1<sup>N159</sup>* displayed the same *bro* heart defect as either single mutant (Figure 4.1F), suggesting that *Gβ13F* and *Gγ1* function in the same pathway during dorsal vessel development.

Among all the Gα subunits in *Drosophila*, *G-α47A* seemed most likely to function together with *Gβ13F/Gγ1* in the heart because of its cardiac expression (Fremion et al., 1999; Zaffran et al., 1995). Embryos homozygous for a large deficiency, Df(2R)47A, that includes *G-α47A* show a disrupted dorsal vessel lacking a subset of heart cells (Fremion et al., 1999). However, this deficiency deletes many genes in addition to *G-α47A*, which could also be important for heart development. For example, a gene called *lola* is deleted in the Df(2R)47A mutant, and RNAi knockdown of *lola* in *Drosophila* embryos leads to dorsal vessel defects (Kim et al., 2004 and online database of Fly Embryo RNAi Project). Therefore, to more precisely study the function of *G-α47A* in the heart, we examined the structure of the dorsal vessel in two *G-α47A* specific mutants *G-α47A<sup>007</sup>* and *G-α47A<sup>0611</sup>*, a null allele (Katanaev et al., 2005), using the

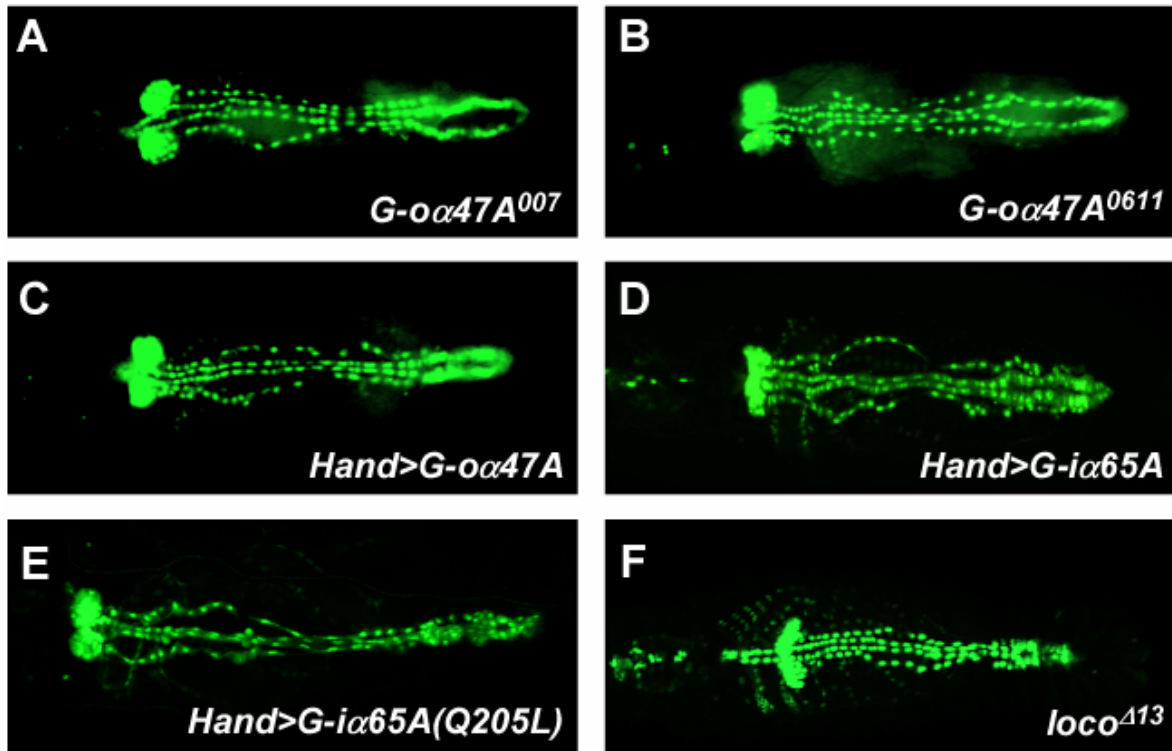


**Figure 4.2. Loss-of-function and gain-of-function heart phenotype of  $G\alpha s$ .**

(A-B) Two mutants of  $G-o\alpha 47A$ ,  $G-o\alpha 47A^{007}$  (A) and null mutant  $G-o\alpha 47A^{0611}$  (B) both show *bro* heart defect similar to that of  $G\beta 13F$  or  $G\gamma 1$  mutants. (C) Overexpression of  $G-o\alpha 47A$  in the heart by *Hand-Gal4* causes the same *bro* defect as in  $G-o\alpha 47A$  mutant embryos. (D) Overexpression of  $G-i\alpha 65A$  in the heart causes the *bro* defect. (E) Overexpression of a constitutive form of  $G-i\alpha 65A$ ,  $G-i\alpha 65A$  (Q205L), in the heart causes the same *bro* defect as overexpression of  $G-i\alpha 65A$  wild type. (F) *loco* mutant  $loco^{\Delta 13}$  shows the same *bro* defect.

*Hand-GFP* marker. As shown in Figures 4.2A and 4.2B, both mutants showed the same *bro* heart defect as in *Gβ13F* or *Gγ1* mutants, in which the normal number of cardioblasts was aligned at the dorsal midline, but there was an obvious failure in adhesion with pericardial cells. Therefore, the more severe heart defect associated with the Df(2R)47A deficiency likely results from deletion of multiple genes that affect cardiac structure. We conclude that *G-α47A* functions together with *Gβ13F/Gγ1* in cardioblasts to mediate cardiac-pericardial cell adhesion.

Gα and Gβγ typically form a trimeric complex when they are inactive, whereas in response to upstream signals, the Gβγ dimer dissociates from Gα and Gβγ and Gα then activate different downstream signaling pathways. In principle, deletion of Gβγ can result in the inactivation of Gβγ targets and the release of Gα with consequent hyperactivation of Gα targets. However, in the dorsal vessel, mutants of *Gβ13F/Gγ1* and *G-α47A* both caused the *bro* defect, suggesting that appropriate G-α47A or Gβ13F/Gγ1 signaling is required for cardiac integrity. Indeed, when we overexpressed G-α47A in the heart using a *Hand-Gal4* driver, we found the same *bro* defect as in the *G-α47A* mutant (Figure 4.2C).

Gi and Go have been reported to couple to the same downstream signaling pathways. Although the *G-iα65A* mutant has a normal heart (data not shown), overexpression of G-iα65A in the heart caused the same *bro* defect as seen in

embryos overexpressing G- $\alpha$ 47A (Figure 4.2D). In addition, overexpression of a G- $\alpha$ 65A(GTP) mutant, which mimics the active GTP-bound protein and cannot bind G $\beta\gamma$ , but not a G- $\alpha$ 65A(GDP) mutant, which mimics the inactive GDP-bound protein and is able to bind G $\beta\gamma$ , caused the *bro* defect (Figure 4.2E), suggesting that this defect is caused by overactivation of a downstream pathway rather than depletion of G $\beta$ 13F/G $\gamma$ 1.

RGS proteins usually function as negative regulators of G $\alpha$  signaling (Dohlman and Thorner, 1997). We found that a mutant form of the RGS protein, *loco*<sup>Al3</sup>, also resulted in the *bro* phenotype (Figure 4.2F). Therefore, G- $\alpha$ 47A, G $\beta$ 13F, G $\gamma$ 1 and *loco* constitute a molecular pathway to regulate heart integrity. Maintenance of heart integrity requires appropriate G- $\alpha$ 47A downstream pathways.

#### *Septate junction plays an important role in heart formation*

One unmapped *bro* mutant in our collection, *bro*6, is an Exelixis deficiency mutant (*Df(3L)Exel6116*) that deletes 25 genes. Homozygous *Df(3L)Exel6116* embryos display the *bro* phenotype with 100% penetrance (Figure 4.3A, a). To identify the gene within this deficiency responsible for the cardiac phenotype, we first narrowed down the critical region by generating flies trans-heterozygous for *Df(3L)Exel6116* and overlapping deficiency chromosomes within this region.

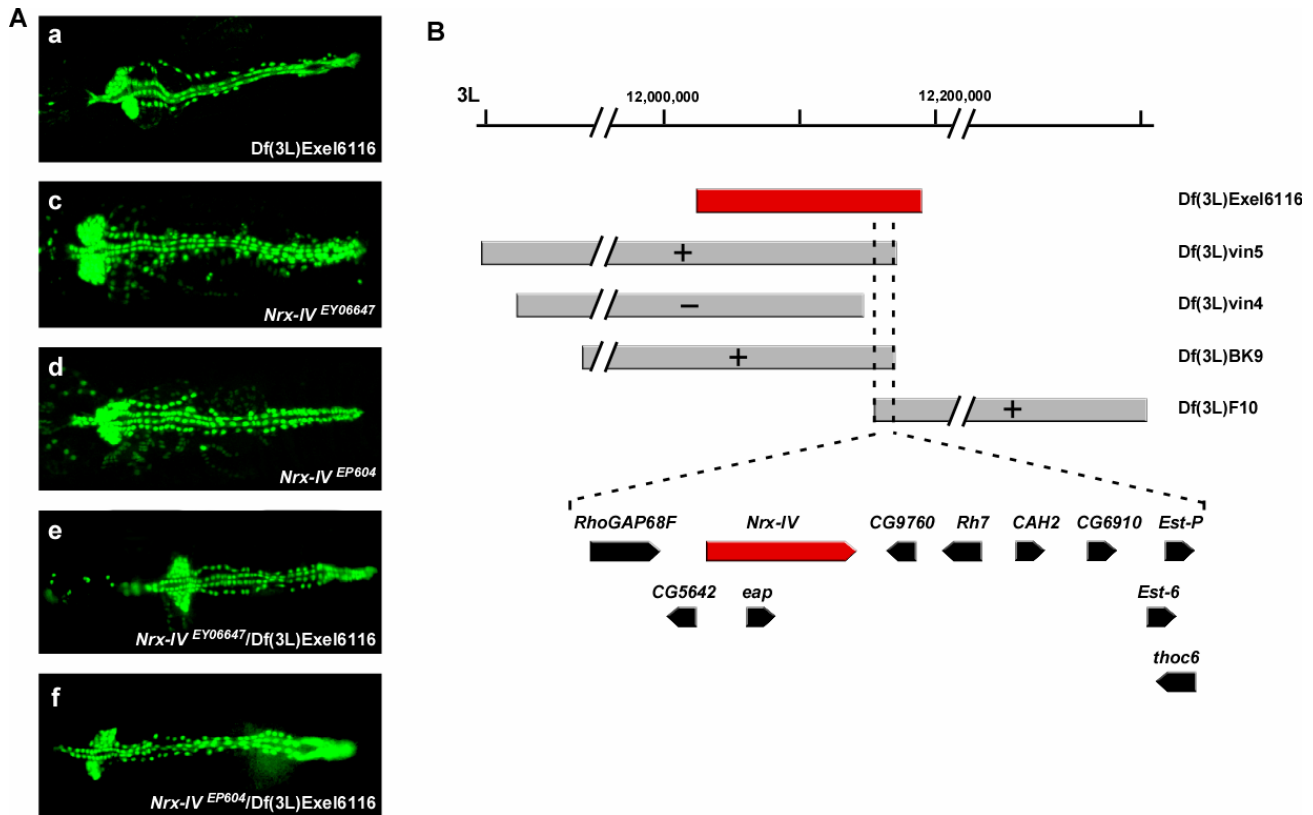


**Figure 4.3. Requirement of *Nrx-IV* for maintenance of cardiac integrity.** (A)

A deficiency mutant Df(3L)Exel6116 showed a *bro* phenotype. (B) Trans-heterozygous mutants were generated for Df(3L)Exel6116 and 4 different overlapping deficiency mutants including Df(3L)vin5, Df(3L)vin4, Df(3L)BK9 and Df(3L)F10. “+” indicates that the trans-heterozygous mutant shows the same *bro* heart defect, and “-” indicates that it has a normal heart. The critical region was narrowed to the region indicated between the two dashed lines, in which 11 genes were deleted. (C and D) Two mutants of *Nrx-IV*, *Nrx*<sup>EY06647</sup> (C) and *Nrx*<sup>EP604</sup> (D), both showed similar *bro* phenotypes. (E and F) Trans-heterozygous mutants for Df(3L)Exel6116 and the two *Nrx-IV* mutants, *Nrx-IV*<sup>EY06647</sup>/Df(3L)Exel6116 (E) and *Nrx-IV*<sup>EP604</sup>/Df(3L)Exel6116 (F) showed the *bro* defect.



Of the four deficiency lines from this region, (Df(3L)vin5, Df(3L)vin4, Df(3L)BK9 and Df(3L)F10), only mutant (Df(3L)vin4/Df(3L)Exel6116) had a normal heart, whereas the other three trans-heterozygous mutants all showed the same *bro* defect as the homozygous mutant of Df(3L)Exel6116. These findings suggested that a ~55kb region of overlap between these three deficiency lines contained a *bro* gene (Figure 4.3B). Among the 11 genes in this region, only *Neurexin-IV* (*Nrx-IV*) and *Est-6* have reported lethal alleles. A UAS-dsRNA transgenic line is available for *RhoGAP68F*, but all the other genes either have no mutant alleles or only have viable mutant alleles. We overexpressed the *RhoGAP68F* dsRNA in the heart using *Hand-Gal4*, and also examined the *Nrx-IV* and *Est-6* mutants for cardiac defects using the *Hand-GFP* marker. Two *Nrx-IV* mutants (*Nrx-IV*<sup>EY06647</sup> and *Nrx-IV*<sup>EP604</sup>) showed a *bro* defect comparable to that of Df(3L)Exel6116 (Figure 4.3A, b and c), whereas the *Est-6* mutant and *RhoGAP68F* dsRNA overexpression flies had normal hearts (data not shown). Trans-heterozygous mutants *Nrx-IV*<sup>EY06647</sup>/Df(3L)Exel6116 and *Nrx-IV*<sup>EP604</sup>/Df(3L)Exel6116 also displayed a *bro* defect indistinguishable from that of homozygous Df(3L)Exel6116 (Figures 4.3, d and e), confirming that *Nrx-IV* is the *bro* gene in (Df(3L)Exel6116) locus.

*Nrx-IV* encodes a key component of septate junctions, which act as the trans-epithelial barrier in most epithelia of non-chordate animals, functionally substituting for the chordate tight junction (Tepass et al., 2001). To further test

whether a septate junction defect underlies the *bro* phenotype, we collected mutants for other septate junction component genes and examined them for heart phenotypes. Indeed, *bro* defects were found with 100% penetrance in homozygous mutants of *contactin* (*cont*<sup>ex956</sup>) (Faivre-Sarrailh et al., 2004), *nervana 2* (*nrv2*<sup>k13315</sup> and *nrv2*<sup>ZCL1649</sup>), *coracle* (*cora*<sup>14</sup>) and *sinuous* (*sinu*<sup>nwu7</sup>) (Wu et al., 2004) (Figure 4.4A-E), which encode essential components of septate junctions. Minor *bro* defects were also found in a homozygous *Glialactin* (*Gli*<sup>1</sup>) mutant with low penetrance (~30%) (Figure 4.4F), *Lachesin* (*Lac*<sup>BG01462</sup>) and *Neuroglian* (*Nrg*<sup>G0488b</sup>) mutants (Figure 4.4 G and H) with about 20% penetrance..

We conclude that the *bro* phenotype can be caused by septate junction defects. Since septate junction proteins mediate cell-cell adhesion and maintain cell polarity, it is possible that the heart defects associated with mutations in the mevolanate pathway genes or heterotrimeric G protein mutants are also caused by septate junction malformation.

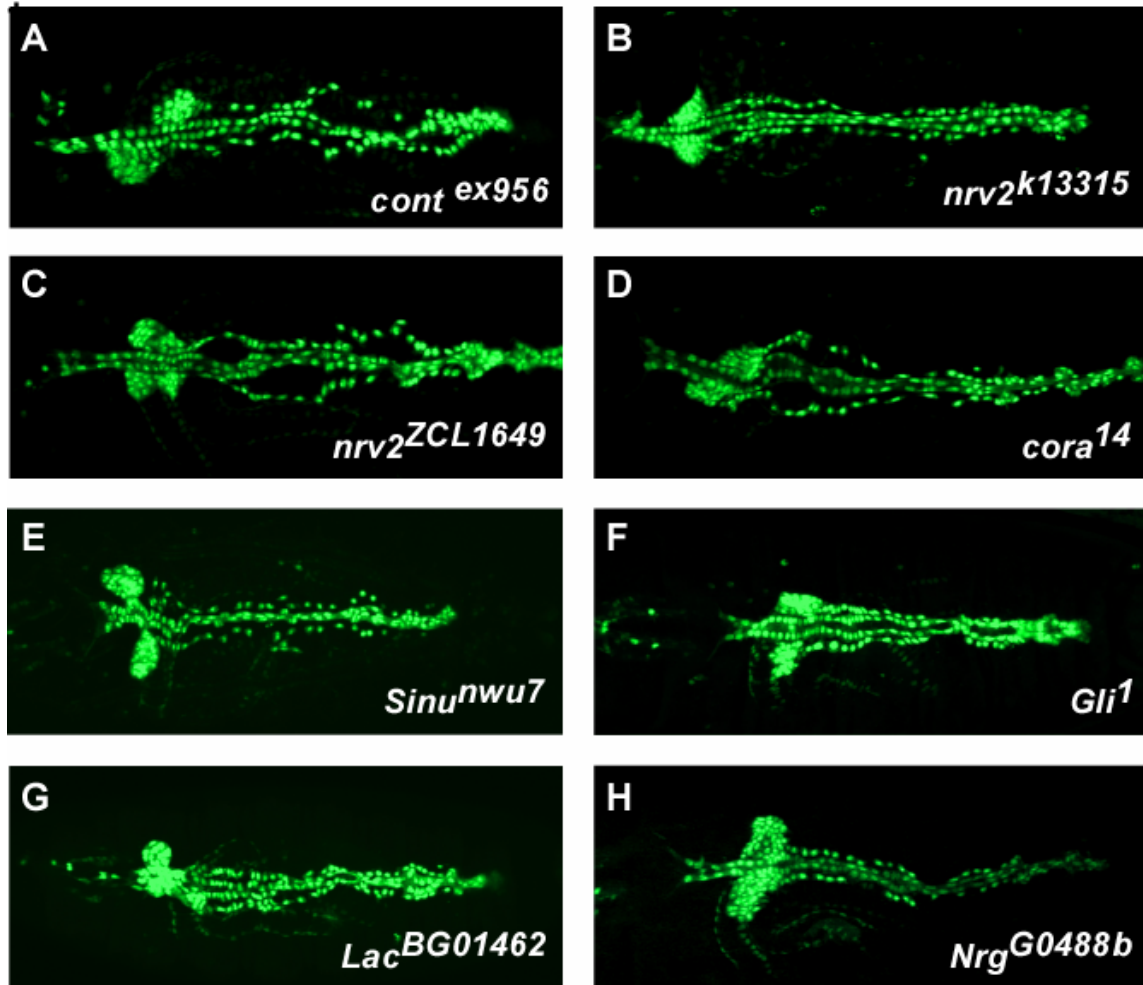


**Figure 4.4. Septate junction protein mutants have a *bro* defect.** (A-E) The *bro* defect is found with 100% penetrance in homozygous embryos of *cont<sup>ex956</sup>* (A), *nrv2<sup>k13315</sup>* (B), *nrv2<sup>ZCL1649</sup>* (C), *cora<sup>14</sup>* (D) and *Sinu<sup>nwu7</sup>* (E). (F-H) *bro* defect is also found with low penetrance (~20%-30%) in homozygous embryos of *Gli<sup>1</sup>* (F), *Lac<sup>BG01462</sup>* (G) and *Nrg<sup>G0488b</sup>* (H).

*Heterotrimeric G proteins regulate septate junction formation in the heart*

Septate junctions are a unique structure of epithelial cells in *Drosophila*. Cardioblasts are myoepithelial cells that adhere at the midline to form a tube-like structure. To visualize septate junctions in the dorsal vessel, we performed immunostaining for the septate junction marker protein, Nr<sub>x</sub>-IV. As shown in Figure 4.5A, Nr<sub>x</sub>-IV is mainly expressed in cardioblasts but not pericardial cells and, in the heart, it is most enriched at the dorsal midline, where cardioblasts attach to each other to form a junctional structure (arrow). Nr<sub>x</sub>-IV staining was also observed along the lateral membranes of cardioblasts (arrow head), where it colocalized with pericardin, an extracellular matrix protein specifically expressed by pericardial cells at the cardial-pericardial cell boundary (Figure 4.5A-C). The septate junction between cardioblasts may function to maintain integrity of the heart tube and cardial cell polarity. Given the defect of cardial-pericardial cell adhesion associated with mutations in components of septate junctions, we propose that the septate junction on the lateral membrane of cardioblasts functions to mediate this adhesion between the two cell layers of the heart, thereby maintaining cardiac integrity.

Since the mevalonate pathway genes and heterotrimeric G proteins function specifically in cardioblasts (Yi et al., 2006), which is consistent with the septate junction localization in the heart, we postulate that these genes function to

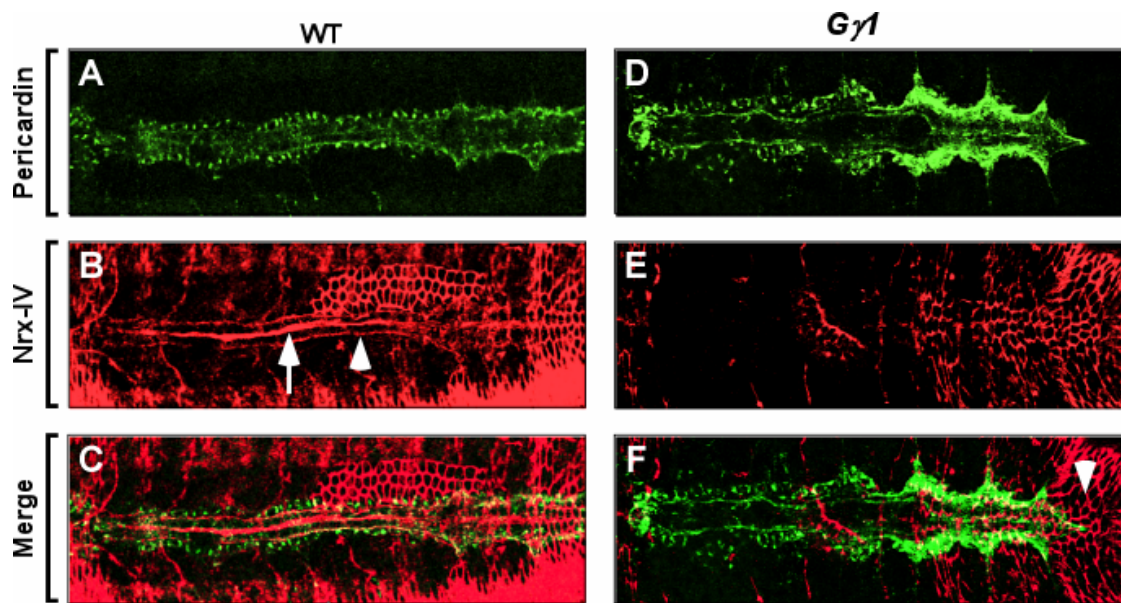


**Figure 4.5. Septate junction localization in the heart in wild type or *Gγ1* mutant embryos.** (A-F) Stage 16 embryos were co-immunostained with anti-pericardin and anti-septate junction marker NrX-IV antibodies. In wild type embryos, septate junctions colocalize with pericardin at the cardiac-pericardial cell boundary (indicated by arrow head). Septate junctions are also enriched at the midline between cardioblasts (arrow) (A-C). In *Gγ1* mutant embryos, septate junctions are hardly detected in the heart, whereas septate junctions in epidermis are still well formed (D-F). The septate junctions in epidermis is indicated by an arrow head (F).

regulate septate junction formation in the heart. To test this possibility, we analyzed the expression pattern of Nr $\alpha$ -IV in homozygous *G $\gamma$ 1* mutant (*bro4*) embryos by immunostaining. In contrast to wild type embryos, in which Nr $\alpha$ -IV staining clearly demarcated the interface between cardioblasts and pericardial cells, Nr $\alpha$ -IV staining was almost undetectable in *G $\gamma$ 1* mutants (Figures 4.5D-F). In contrast, Nr $\alpha$ -IV staining of epithelial cells in the epidermis was unchanged in *G $\gamma$ 1* mutant embryos, indicating a specific role for heterotrimeric G protein signaling in the maintenance of septate junctions in the dorsal vessel.

We hypothesized that septate junction proteins on the lateral membrane of cardioblasts interact with proteins on the surface of pericardial cells to maintain integrity of the dorsal vessel. To identify such interactions, we searched the *Drosophila* protein interaction map (Giot et al., 2003) with septate junction proteins and found that Sinuous, is able to interact with Pericardin (Figure 4.6A). If Pericardin is required for pericardial cells to adhere to cardiac cells through interaction with septate junctions, mutation of *pericardin* might be expected to cause a *bro* defect as seen with septate junction gene mutants. However, Pericardin also attaches cardioblasts to overlying ectoderm cells, and deletion of Pericardin causes detachment of cardioblasts from the ectoderm and a failure in migration to the dorsal midline together with ectoderm leading edge cells (Chartier et al., 2002), which is a more severe and earlier heart defect than the *bro* defect. Because there is no hypomorphic mutant available for *pericardin*, we

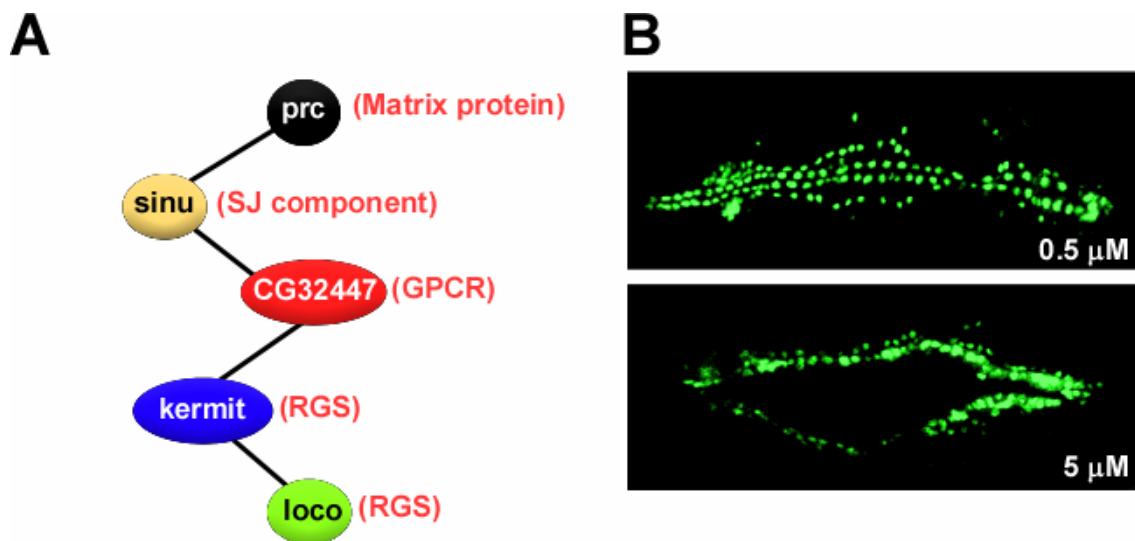


**Figure 4.6. A model for the role of sinuous-pericardin in cardial-pericardial cell adhesion.** (A) Protein-protein interaction searched from *Drosophila* protein interaction database (Giot et al., 2003). (B) Heart phenotype of pericardin RNAi injected embryos. Injection of RNAi in 0.5 $\mu$ M leads to the *bro* phenotype (upper panel), whereas injection in 5 $\mu$ M causes a dorsal opened heart phenotype (lower panel).

investigated the potential role of Pericardin in the late heart phenotype by injecting blastoderm stage *Hand-GFP* transgenic embryos with double-stranded RNA for *pericardin*. As shown in Figure 4.6B, injection of 5 $\mu$ M *pericardin* RNAi recapitulated the severe migration defect seen in pericardin mutant embryos (Chartier et al., 2002). However, when we injected the embryo with 0.5 $\mu$ M *pericardin* RNAi, cardioblasts migrated normally to the dorsal midline and formed the linear heart tube, but pericardial cells failed to adhere with cardioblasts, resulting in the *bro* defect. These findings support the conclusion that pericardin functions, at least in part, to mediate cardiac-pericardial cell adhesion, and the pericardin-septate junction interaction could be the molecular basis for this cell adhesion in *Drosophila* heart.



## *Discussions*

The results of this study show that the heterotrimeric G proteins *G- $\alpha$ 47A*, *G $\beta$ 13F* and *G $\gamma$ 1* function together to maintain integrity of the *Drosophila* heart at the late stage of embryogenesis. Through mapping of a new *bro* mutant (*Nrx-IV*) and additional candidate genes, we discovered a potential role of septate junction proteins in cardiac-pericardial cell adhesion and found that one component of septate junctions, sinuous, can interact with pericardin. These findings suggest that pericardin-septate junction interaction provides the molecular basis for cardiac-pericardial cell adhesion. We also obtained evidence that heterotrimeric G proteins are required for septate junction formation. Therefore, it is possible that in heterotrimeric G protein mutants, septate junctions fail to form or be properly localized, so Pericardin-septate junction interaction cannot occur, leading to a failure in cardiac-pericardial cell adhesion and the *bro* defect (Figure 4.7).

### *(1) GPCR dependent or independent mechanism in Drosophila heart*

The G- $\alpha$ 47A/G $\beta$ 13F/G $\gamma$ 1 complex might function in the heart in either GPCR-dependent or independent manner. No GPCR gene mutant was discovered in our screen *bro* genes. Heterotrimeric G proteins *G- $\alpha$ 47A/G- $\alpha$ 65A*, *G $\beta$ 13F* and *G $\gamma$ 1* have previously been shown to function together with the G protein

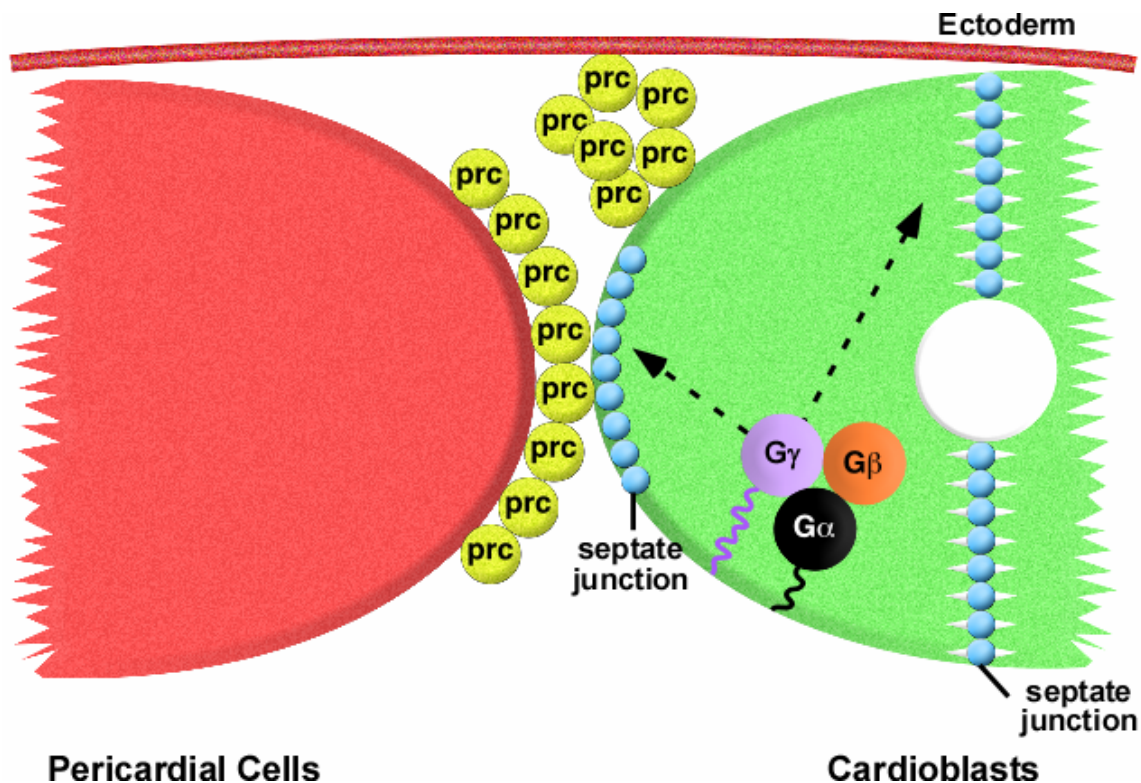


**Figure 4.7. A hypothetical model for cardiac-pericardial cell adhesion.**

Heterotrimeric G proteins regulate septate junctions formation in cardioblasts. The septate junctions on the lateral membrane of cardioblast interact with the pericardin surrounding pericardial cells through Sinuous-Pericardin binding. Mutations in heterotrimeric G proteins and septate junctions genes all cause the defect of septate junctions formation in cardioblasts, so that the Sinuous-Pericardin interaction cannot form, leading to the cardiac-pericardial cell adhesion loss and *bro* defect. Depletion of Pericardin between cardiac-pericardial cell but not between cardioblasts and ectoderm cells also causes adhesion loss and *bro* defect.

coupled receptor (GPCR) *moody* and the RGS protein RGS *loco* to regulate septate junction formation during development of the *Drosophila* brain-blood barrier (Schwabe et al., 2005). Although the *loco* mutant shows the same *bro* heart defect (Figure 4.2F), the *moody* mutant does not cause heart defects, suggesting that heterotrimeric G proteins use another GPCR or act in a GPCR-independent manner, but share the same RGS protein *loco* to regulate cell adhesion in the heart.

By searching the *Drosophila* protein interaction map, we found that sinuous is also able to interact with a GPCR (CG32447) and an RGS protein, called Kermit (Figure 4.6A). We also noticed that Kermit can interact with another RGS protein, *loco*, the mutant of which also displays the *bro* defect. We examined a deficiency line, in which CG32447 is deleted, but did not find any heart defect (data not shown). It is conceivable that a GPCR homologous to CG32447 actually functions in the heart and is also able to interact with sinuous to regulate septate junction formation.

On the other hand, *G- $\alpha$ 65A*, *G $\beta$ 13F*, *G $\gamma$ 1* and *loco* are also found to regulate neuroblasts asymmetric cell division via a GPCR-independent signaling pathway (reviewed in (Knust, 2001)). These heterotrimeric G proteins and RGS proteins regulate the mitosis spindle orientation and polarized membrane protein localization. It was reported that heterotrimeric G proteins can be activated by the GTPase exchange factor (GEF) *ric-8*, but not GPCRs during neuroblasts

asymmetric cell division in both *C. elegans* and *Drosophila* (Afshar et al., 2004; David et al., 2005; Wang et al., 2005). However, a lethal *ric-8* mutant *ric-8*<sup>G0397</sup> does not show any heart defect (data not shown). *ric-8*<sup>G0397</sup> might be a hypomorphic mutant and *ric-8* may also have maternal contributions, so a *ric-8* germ line mutant or a *ric-8* null mutant would need to be generated and checked for a heart phenotype to determine if the function of heterotrimeric G proteins is also *ric-8*-dependent in the dorsal vessel.

Although the same heterotrimeric G proteins and RGS proteins are involved in brain-blood barrier formation, asymmetric cell division of neuroblasts, and heart formation, it seems that they act in rather different ways to regulate these processes. In brain-blood barrier formation, overexpression of wild type Gi, wild type Go or the inactive GDP-bound form of Go (Go-GDP) but not the constitutive active form of Gi or Go (Gi-GTP or Go-GTP) leads to the septate junction defect (Schwabe et al., 2005). Similar results have been obtained in the analysis of heterotrimeric G protein functions in neuroblast cell division (Schaefer et al., 2001; Yu et al., 2003). These results demonstrate that G signaling is essential in these two processes. Defects observed with overexpression of G $\alpha$  are caused by depletion of G $\beta\gamma$  rather than the hyperactivation of G $\alpha$  downstream signaling. However, these heterotrimeric G proteins act in a completely different way in *Drosophila* heart development. Overexpression of the Go, Gi, Gi-GTP form but not the Go-GDP form show the

*bro* defect, suggesting that depletion of G $\beta\gamma$  in heart cells is not essential for cardiac-pericardial cell adhesion. The *bro* defect observed in *G $\beta$ 13F* or *G $\gamma$ 1* mutants is caused by misregulation of G- $\alpha$ 47A signaling.

In this study, we showed that the heterotrimeric G proteins regulate the adhesion of heart cells through controlling septate junction formation in the heart, but the exact mechanism whereby heterotrimeric G proteins function in this process remains to be determined. One possibility is that heterotrimeric G proteins control the polarity of cardioblasts. In the G protein mutants, cardioblasts fail to be properly polarized, so the polarized membrane protein structures including the septate junction can not be formed. Indeed, it has been reported that cardiac cell polarity is probably disrupted in G- $\alpha$ 47A mutant (Fremion et al., 1999). G $\beta$ 13F and G $\gamma$ 1 have also been implicated in maintaining cell polarity, as treating polarized cell with G $\beta$ 13F or G $\gamma$ 1 double-strands RNA causes cells to round up and become depolarized (Kiger et al., 2003). It is also possible that heterotrimeric G proteins regulate septate junction formation or cell polarity through regulating vesicular transport and membrane targeting from the ER to the plasma membrane. In this regard, it has been shown that heterotrimeric G proteins control synaptic vesicle priming in *C. elegans* neurons (Reynolds et al., 2005). We have also shown that mutation in *sar1*, a key regulator of ER-Golgi vesicular transport, leads to the *bro* phenotype (Yi et al., 2006).

(2) *Septate junctions, pericardin and heart formation*

We found that multiple septate junction gene mutants have very similar *bro* phenotypes. In the *G $\gamma$ 1* mutant, septate junction formation is defective specifically in the heart but not in epidermis cells. This could be due to the strong maternal contribution of G- $\alpha$ 65A and G- $\alpha$ 47A because the septate junction in the epidermis cells is formed earlier in embryogenesis. On the other hand, the septate junction in cardioblasts which are myoepithelial cells (Tepass, 1997; Tepass and Hartenstein, 1994), is formed *de novo* after these cells differentiate starting after stage 11, which is less sensitive to maternal effects.

We propose that the interaction of the matrix protein pericardin with sinuous in cardioblast septate junctions is the molecular basis for cardinal-pericardial cell adhesion. This is supported by the co-localization of pericardin and septate junctions at the cardinal-pericardial cells boundary (Figure 4.5). Injection of *pericardin* dsRNA in low dose also caused a *bro* phenotype similar to that of other *bro* mutants. The reason the *bro* defect was observed only at low dose *pericardin* RNAi injection is that pericardin has multiple function including attaching cardioblasts to overlying ectoderm leading edge cells (Chartier et al., 2002). This attachment is required for heart cell migration from the lateral side of the embryo to the dorsal midline. If Pericardin is completely depleted, heart cells fail to migrate together with the ectoderm leading edge cells, resulting in a dorsal-opened-heart defect, which is much earlier and than the *bro* defect which occurs

after heart migration. The adhesion between cardioblasts and ectoderm leading edge cells may be less sensitive to pericardin dose than that between cardinal-pericardial cells. Low dose RNAi injection does not completely deplete Pericardin in the embryos, which enables cardioblasts to migrate normally with ectoderm cells because their adhesion is not completely lost, but pericardial cells fail to attach to cardioblasts due to the adhesion defect.

*(3) broken hearted genes are evolutionally conserved.*

All the *bro* genes have close vertebrate homologs (Table 4.2). Since the function of mevalonate pathway genes in heart development seems to be conserved from *Drosophila* to vertebrates (D'Amico et al., 2007; Edison and Muenke, 2005; Yi et al., 2006), it is reasonable to speculate that the mechanism whereby heterotrimeric G proteins regulate septate junction formation was also evolutionarily conserved. So far there is no evidence showing that heterotrimeric G proteins play a role in vertebrate heart development, but there is abundant evidence for the involvement of heterotrimeric G proteins in heart disease (Zolk et al., 2000). Since these heterotrimeric G proteins are also widely expressed during embryogenesis, it is reasonable to expect they are important regulators for heart development.

<i>Drosophila</i>	Vertebrate
<i>HMGCR</i>	HMG-CoA reductase
<i>qm</i>	geranylgeranyl diphosphate synthase 1
<i><math>\beta</math>GGT-I</i>	Geranylgeranyl transferase type I $\beta$ subunit
<i>G-<math>\alpha</math>47A</i>	G $\alpha$ 2
<i>G<math>\beta</math>13F</i>	G $\beta$ 1
<i>G<math>\gamma</math>1</i>	G $\gamma$ 12
<i>loco</i>	Regulator of G protein signaling 19
<i>Sinuous</i>	Claudin-1
<i>Neurexin-IV</i>	<i>Drosophila</i> Neurexin IV-related protein
<i>contactin</i>	contactin
<i>pericardin</i>	Collagen alpha-1(IV)

**Table 4.2. *broken hearted* genes are evolutionary conserved.**



Septate junctions exist only in invertebrates, but are considered as a functional substitute of tight junctions in vertebrate. All the septate junction genes have close homologs in vertebrate (Table 4.2). For example, *Nrx-IV* and *contactin* homologs are components of paranodal septate junctions formed in myelinated neurons (Boyle et al., 2001; Einheber et al., 1997) and the vertebrate homolog of *sinuous*, claudin-1, is a component of tight junctions (Wu et al., 2004). Interestingly, in chicken, it has been shown that appropriate expression of claudin-1 is required for normal heart looping (Simard et al., 2006). Another member of the claudin family, claudin-5, is expressed at the lateral membrane of cardiomyocytes and has been associated with human cardiomyopathy (Sanford et al., 2005). Moreover, *pericardin* is a *Drosophila* collagen type IV like matrix protein (Chartier et al., 2002). In vertebrate heart, type IV collagen is abundantly expressed in fibroblasts and cardiomyocytes. Mutation in *pericardin* homolog, collagen alpha-1(IV), causes vascular defect in mice and humans (Gould et al., 2005). Thus, it is interesting to speculate that the heterotrimeric G proteins and the septate junction proteins also play an important role in vertebrate heart morphogenesis.

## CHAPTER V

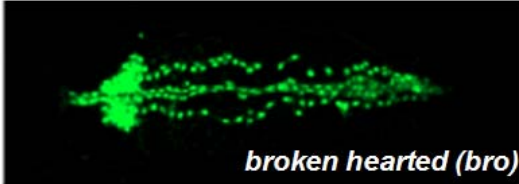
### Summary and future directions

#### *Summary*

Using the powerful *Drosophila* forward genetic screen, we found a unique heart defect where the adhesion between the cardiac cells and pericardial cells is lost at the end of embryogenesis, leading to loss of cardiac function and embryonic lethality (Figure 5.1). We termed this heart defect as *broken hearted* (*bro*). Through the original genetic screen and subsequent candidate genes test, we found 14 genes or loci in total, the mutants of which all show the very similar *broken hearted* defect. These genes or loci are summarized in Figure 5.1.

First, the identification of *bro1-3*, which encode several important enzymes in mevalonate pathway, indicates that the synthesis and transferring of geranylgeranyl to a certain protein by this pathway is essential for the adhesion between the cardiac-pericardial cells. And then, mapping of *bro4* tells us that heterotrimeric G protein  $\gamma$  subunit 1 ( $G\gamma 1$ ) is this important protein to be modified by geranylgeranyl to regulate the heart cells adhesion. We also found that  $G\alpha 47A$  and  $G\beta 13F$  are the other G protein subunits functioning together with  $G\gamma 1$

<i>bro1</i>	<i>HMGCR</i>
<i>bro2</i>	<i>GGPPS/qm</i>
<i>bro3</i>	<i><math>\beta</math>GGT-I</i>
<i>bro4</i>	<i>G<math>\gamma</math>1</i>
<i>bro5</i>	<i>Sar1</i>
<i>bro6</i>	<i>Nrx-IV / BL7595 (Df)</i>
<i>bro7</i>	<i>G<math>\beta</math>13F</i>
<i>bro8</i>	<i>Go<math>\alpha</math>47A</i>
<i>bro9</i>	<i>Sinu</i>

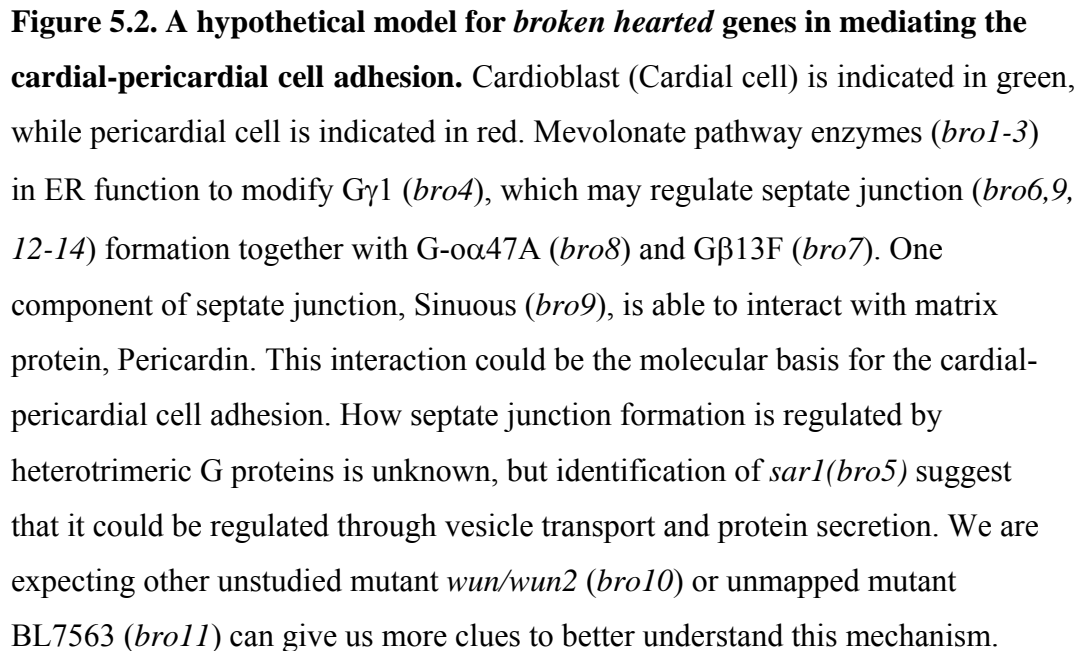


<i>bro10</i>	<i>Wun/wun2</i>
<i>bro11</i>	<i>BL7563 (Df)</i>
<i>bro12</i>	<i>Cont</i>
<i>bro13</i>	<i>Cor</i>
<i>bro14</i>	<i>Nrv2</i>

**Figure 5.1. Summary of *broken hearted* genes.** From the original screen and subsequent candidate genes test, we identified 14 genes or loci, the mutant of which all shows the very similar *broken hearted* defect. Two of them are deficiency mutants deleting multiple genes, while the others are P-element insertion mutant or EMS mutant for a single gene.

in the heart. Appropriate G- $\alpha$ 47A signaling is required in cardioblasts to regulate an intercellular junction structure, so called septate junction, formation by a yet unknown mechanism. We also showed evidence that the interaction of matrix protein Pericardin with Sinuous, a component of septate junction in the heart, may serve as the molecular basis for the cardiac-pericardial cell adhesion. A hypothetical model summarizing how all these genes work is shown in Figure 5.2.

One of the significance of this work is that it indicates that mevalonate pathway genes play an important role in heart development during embryogenesis. The rate-limiting enzyme in mevalonate pathway, HMG-CoA reductase, is an important drug target for high-cholesterol patients treatment. However, there are some cases showing that gestation exposure to statins, the HMG-CoA reductase inhibitors, may associate with heart developmental defect at birth (Edison and Muenke, 2004, 2005). Our study in *Drosophila* model clearly showed that HMG-CoA reductase is essential for the heart development during embryogenesis, and we also provide the mechanism explaining how the mutation or inhibition of HMG-CoA reductase causes heart defect. Interestingly, the study in zebrafish heart development also showed that mutation in *hmgcr1b* gene leads to similar heart developmental defect, probably through the same mechanism as in *Drosophila* (D'Amico et al., 2007).



Another important indication from this study is that these *bro* genes may serve as a general machinery for cell migration or cell-cell adhesion in development. Most of the *bro* genes are not restricted in heart cells. These genes have been shown to regulate germ cell migration, neuroblasts asymmetric cell division and brain-blood barrier formation etc. These processes all involve cell movement and subsequent cell adhesion or intercellular junction formation. Since *Drosophila* heart is such a simple structure, it could be used as a very good model system to study the basic cell biology questions during organogenesis.

#### *Future directions*

This thesis has focused on the study of mevalonate pathway genes, heterotrimeric G proteins and septate junctions. However, how the G proteins work and through what mechanism the septate junction formation is regulated is still unknown. *bro5* mutant is mapped to the gene *sar1*, which encodes a key protein regulating ER-Golgi vesicle transport, suggesting the protein secretion and trafficking may be the linkage between G proteins and the septate junction formation. But to understand the detail mechanism involved in this process, we need to get more *broken hearted* mutants or to gain better understanding of the unstudied or unmapped *bro* mutant found in our screen.

*bro6* is a unstudied *bro* mutant, which is mapped to two *Drosophila* LPP3 homologs *wun* and *wun2*. Interestingly, several *bro* genes, such as *HMGCR*,

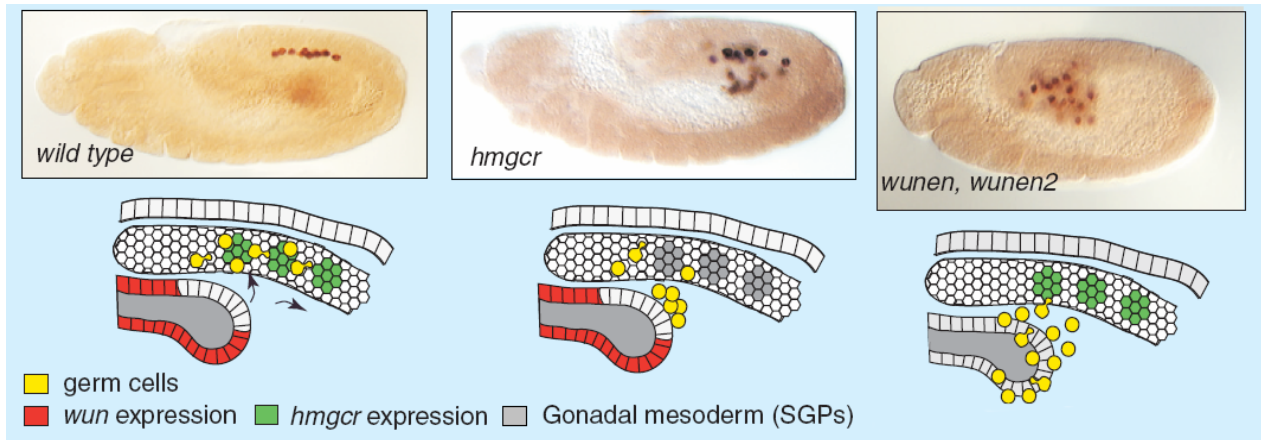


**Figure 5.3. *bro* genes in *Drosophila* germ cell migration.** (Modified from (Santos and Lehmann, 2004a)) *HMGCR* and *wun/wun2* are also involved in *Drosophila* germ cells migration. *HMGCR* is expressed only in the gonad mesoderm to guide the migrating germ cells, whereas *wun/wun2* is expressed in the gut cells to repel the germ cells away from gut toward the gonad mesoderm.

*qm*, *βGGT-I* and *wun/wun2* are also involved in *Drosophila* germ cell migration (reviewed in (Santos and Lehmann, 2004a)). During development, *Drosophila* germ cells need to migrate from the invaginated gut to the gonad mesoderm to form adhesion. HMGCR is specifically expressed in the gonad mesoderm, functioning to send an unknown signal to the migrating germ cells to recruit them to the gonad (Van Doren et al., 1998). On the other hand, *wun/wun2* is expressed in the gut cells but not the gonad mesoderm, functioning to send a repelling signal to the germ cells and drive them away of the gut to the gonad mesoderm (Zhang et al., 1997). *HMGCR* and *wun/wun2* are also expressed in *Drosophila* heart, where HMGCR is expressed in the cardioblasts and *wun2* has been shown to be expressed in pericardial cells (Starz-Gaiano et al., 2001). Their expression pattern in the heart suggests their function may be very similar to that in the germ cells migration. Although there is no evidence showing that pericardial cells need to migrate toward cardioblasts to form adhesion, it is still possible that in *Drosophila* germ cells migration, HMGCR and other enzymes of mevalonate pathway in the gonad mesoderm also function to modify G $\gamma$ 1 and subsequently regulate cell junction structure, where the migrating germ cell will finally attach on. Thus, it could be a good idea to get more indications from the study on *Drosophila* germ migration and study them in the context of *Drosophila* heart development.



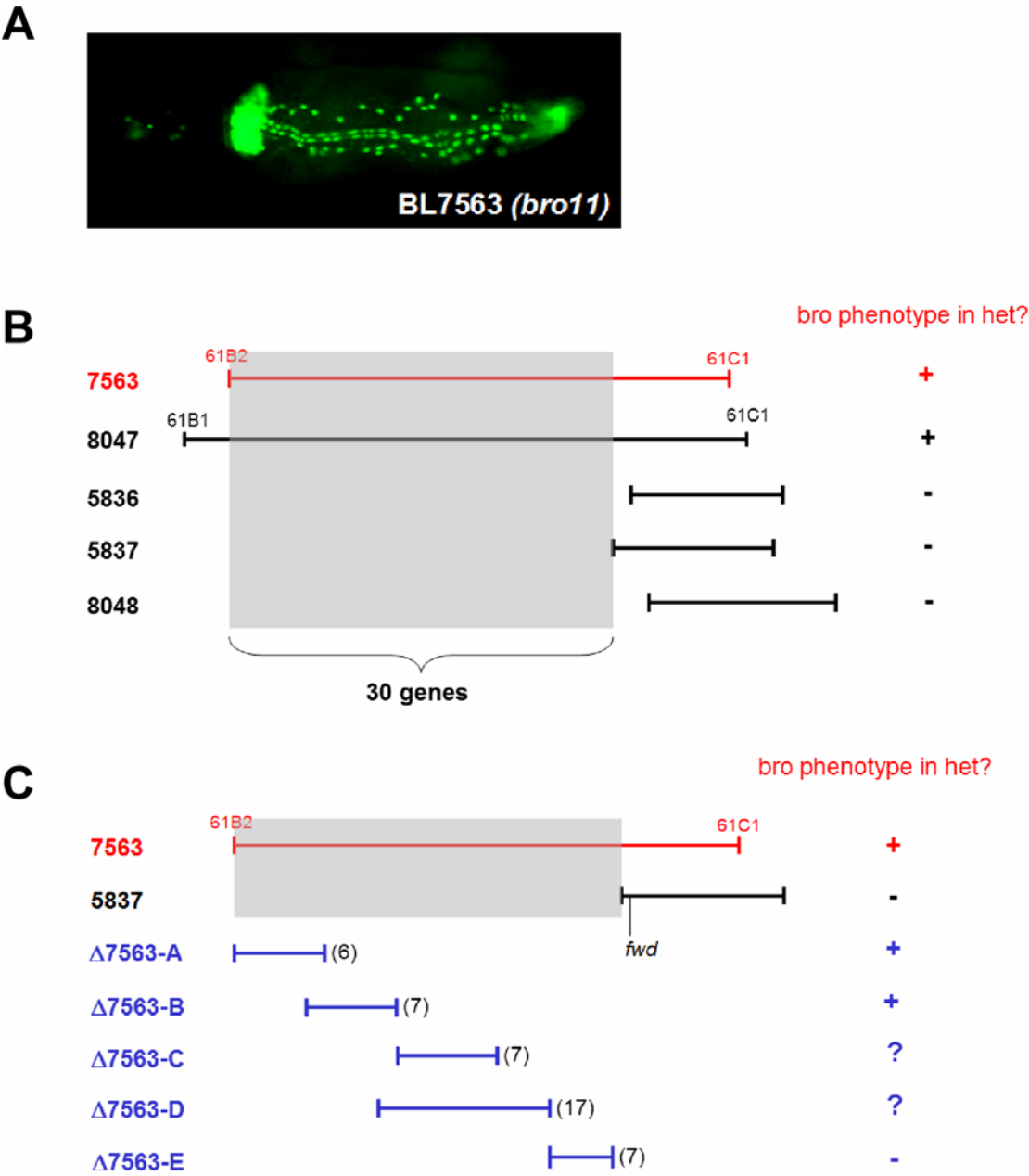


Figure 5.4. Mapping of the *bro* gene in *bro11* locus.

(A) Deficiency mutant *bro11* show bro defect with 100% penetrance. (B) First round overlapping deficiency mapping only eliminate 6 genes. The bro gene resides in the shaded region. (C) Five smaller deficiency mutants were generated and the critical region is further narrowed down to the small region overlapped by  $\Delta 7563A$  and  $\Delta 7563B$ , which only deletes 4 genes.

One unmapped bro mutant is *bro11*, a deficiency mutant deleting 36 genes (Df(3L)Exel6084) (Figure 5.4A). We first tried to narrow down the critical region where the *bro* gene resides in by checking several overlapping deficiency mutants for the heart phenotype. We picked four deficiency mutants in this region, Df(3L)ED201, Df(3L)2D, Df(3L)7C and Df(3L)ED4177. We generated the heterozygous mutants of Df(3L)Exel6084 with these four deficiency mutants and examine if they also have same *bro* defect as seen in *bro11* mutant. The results are summarized in Figure 5.4B. Unfortunately, these four deficiency mutant only helped us to eliminate 6 genes. To further narrow down the critical region for the *bro11* gene, we generated five small deficiency lines ( $\Delta 7563$ -A-E) using FRT-FLIP mediated genome deletion strategy (Parks et al., 2004). Each deficiency line only deletes about 7 genes. We also checked the heterozygous mutants of these deficiency mutants with *bro11*. We found  $\Delta 7563$ -A and  $\Delta 7563$ -B both have similar *bro* heart defect as in the *bro11* mutant. This result narrowed the bro gene down to the small region overlapped by  $\Delta 7563$ -A and  $\Delta 7563$ -B mutants, in which

only four genes are deleted (Figure 5.4C). These four genes are CG6851 (mitochondrial carrier homolog), rhinoceros (transcription regulator), mrityu (voltage-gated potassium channel) and CG18374 (glycerol kinase). To determine which one of these four genes is the *bro* gene we are looking for, one approach I am taking now is to overexpress UAS-dsRNA transgene for all the four genes in the heart to see which one can recapitulate the *bro11* mutant phenotype. This work is still in progress. We are expecting that this *bro11* gene could tell us more clues about how the heterotrimeric G proteins work to regulate septate junction formation and mediate the cardiac-pericardial cell adhesion.

## REFERENCES

- Afshar, K., Willard, F.S., Colombo, K., Johnston, C.A., McCudden, C.R., Siderovski, D.P., and Gonczy, P. (2004). RIC-8 is required for GPR-1/2-dependent Galpha function during asymmetric division of *C. elegans* embryos. *Cell* *119*, 219-230.
- Aridor, M., Fish, K.N., Bannykh, S., Weissman, J., Roberts, T.H., Lippincott-Schwartz, J., and Balch, W.E. (2001). The Sar1 GTPase coordinates biosynthetic cargo selection with endoplasmic reticulum export site assembly. *J Cell Biol* *152*, 213-229.
- Azpiazu, N., and Frasch, M. (1993). tinman and bagpipe: two homeo box genes that determine cell fates in the dorsal mesoderm of *Drosophila*. *Genes & development* *7*, 1325-1340.
- Beiman, M., Shilo, B.Z., and Volk, T. (1996). Heartless, a *Drosophila* FGF receptor homolog, is essential for cell migration and establishment of several mesodermal lineages. *Genes & development* *10*, 2993-3002.
- Bellen, H.J., Levis, R.W., Liao, G., He, Y., Carlson, J.W., Tsang, G., Evans-Holm, M., Hiesinger, P.R., Schulze, K.L., Rubin, G.M., *et al.* (2004). The BDGP gene disruption project: single transposon insertions associated with 40% of *Drosophila* genes. *Genetics* *167*, 761-781.

- Bodmer, R. (1993). The gene *tinman* is required for specification of the heart and visceral muscles in *Drosophila*. *Development* 118, 719-729.
- Bodmer, R., and Venkatesh, T.V. (1998). Heart development in *Drosophila* and vertebrates: conservation of molecular mechanisms. *Dev Genet* 22, 181-186.
- Boyle, M.E., Berglund, E.O., Murai, K.K., Weber, L., Peles, E., and Ranscht, B. (2001). Contactin orchestrates assembly of the septate-like junctions at the paranode in myelinated peripheral nerve. *Neuron* 30, 385-397.
- Brand, A.H., and Perrimon, N. (1993). Targeted gene expression as a means of altering cell fates and generating dominant phenotypes. *Development* 118, 401-415.
- Carmena, A., Buff, E., Halfon, M.S., Gisselbrecht, S., Jimenez, F., Baylies, M.K., and Michelson, A.M. (2002). Reciprocal regulatory interactions between the Notch and Ras signaling pathways in the *Drosophila* embryonic mesoderm. *Dev Biol* 244, 226-242.
- Chartier, A., Zaffran, S., Astier, M., Semeriva, M., and Gratecos, D. (2002). Pericardin, a *Drosophila* type IV collagen-like protein is involved in the morphogenesis and maintenance of the heart epithelium during dorsal ectoderm closure. *Development* 129, 3241-3253.
- Chen, E.H., Pryce, B.A., Tzeng, J.A., Gonzalez, G.A., and Olson, E.N. (2003). Control of myoblast fusion by a guanine nucleotide exchange factor, loner, and its effector ARF6. *Cell* 114, 751-762.

Clapham, D.E., and Neer, E.J. (1997). G protein beta gamma subunits. *Annu Rev Pharmacol Toxicol* 37, 167-203.

Clemens, J.C., Worby, C.A., Simonson-Leff, N., Muda, M., Maehama, T., Hemmings, B.A., and Dixon, J.E. (2000). Use of double-stranded RNA interference in *Drosophila* cell lines to dissect signal transduction pathways. *Proc Natl Acad Sci U S A* 97, 6499-6503.

Cripps, R.M., and Olson, E.N. (2002). Control of cardiac development by an evolutionarily conserved transcriptional network. *Dev Biol* 246, 14-28.

Cripps, R.M., Zhao, B., and Olson, E.N. (1999). Transcription of the myogenic regulatory gene *Mef2* in cardiac, somatic, and visceral muscle cell lineages is regulated by a *Tinman*-dependent core enhancer. *Dev Biol* 215, 420-430.

D'Amico, L., Scott, I.C., Jungblut, B., and Stainier, D.Y. (2007). A mutation in zebrafish *hmgcr1b* reveals a role for isoprenoids in vertebrate heart-tube formation. *Curr Biol* 17, 252-259.

David, N.B., Martin, C.A., Segalen, M., Rosenfeld, F., Schweisguth, F., and Bellaiche, Y. (2005). *Drosophila* Ric-8 regulates *Galphai* cortical localization to promote *Galphai*-dependent planar orientation of the mitotic spindle during asymmetric cell division. *Nature cell biology* 7, 1083-1090.

Der, C.J., and Cox, A.D. (1991). Isoprenoid modification and plasma membrane association: critical factors for ras oncogenicity. *Cancer Cells* 3, 331-340.

- Dohlman, H.G., and Thorner, J. (1997). RGS proteins and signaling by heterotrimeric G proteins. *J Biol Chem* 272, 3871-3874.
- Edison, R.J., and Muenke, M. (2004). Central nervous system and limb anomalies in case reports of first-trimester statin exposure. *N Engl J Med* 350, 1579-1582.
- Edison, R.J., and Muenke, M. (2005). Gestational exposure to lovastatin followed by cardiac malformation misclassified as holoprosencephaly. *N Engl J Med* 352, 2759.
- Einheber, S., Zanazzi, G., Ching, W., Scherer, S., Milner, T.A., Peles, E., and Salzer, J.L. (1997). The axonal membrane protein Caspr, a homologue of neurexin IV, is a component of the septate-like paranodal junctions that assemble during myelination. *J Cell Biol* 139, 1495-1506.
- Faivre-Sarrailh, C., Banerjee, S., Li, J., Hortsch, M., Laval, M., and Bhat, M.A. (2004). *Drosophila* contactin, a homolog of vertebrate contactin, is required for septate junction organization and paracellular barrier function. *Development* 131, 4931-4942.
- Fossett, N., Tevosian, S.G., Gajewski, K., Zhang, Q., Orkin, S.H., and Schulz, R.A. (2001). The Friend of GATA proteins U-shaped, FOG-1, and FOG-2 function as negative regulators of blood, heart, and eye development in *Drosophila*. *Proc Natl Acad Sci U S A* 98, 7342-7347.

- Fossett, N., Zhang, Q., Gajewski, K., Choi, C.Y., Kim, Y., and Schulz, R.A. (2000). The multitype zinc-finger protein U-shaped functions in heart cell specification in the *Drosophila* embryo. *Proc Natl Acad Sci U S A* 97, 7348-7353.
- Frasch, M. (1995). Induction of visceral and cardiac mesoderm by ectodermal Dpp in the early *Drosophila* embryo. *Nature* 374, 464-467.
- Fremion, F., Astier, M., Zaffran, S., Guillen, A., Homburger, V., and Semeriva, M. (1999). The heterotrimeric protein Go is required for the formation of heart epithelium in *Drosophila*. *J Cell Biol* 145, 1063-1076.
- Fuse, N., Hisata, K., Katzen, A.L., and Matsuzaki, F. (2003). Heterotrimeric G proteins regulate daughter cell size asymmetry in *Drosophila* neuroblast divisions. *Curr Biol* 13, 947-954.
- Gajewski, K., Fossett, N., Molkenstin, J.D., and Schulz, R.A. (1999). The zinc finger proteins Pannier and GATA4 function as cardiogenic factors in *Drosophila*. *Development* 126, 5679-5688.
- Gajewski, K., Kim, Y., Choi, C.Y., and Schulz, R.A. (1998). Combinatorial control of *Drosophila* *mef2* gene expression in cardiac and somatic muscle cell lineages. *Development genes and evolution* 208, 382-392.
- Gajewski, K., Kim, Y., Lee, Y.M., Olson, E.N., and Schulz, R.A. (1997). D-*mef2* is a target for Tinman activation during *Drosophila* heart development. *Embo J* 16, 515-522.



- Gajewski, K., Zhang, Q., Choi, C.Y., Fossett, N., Dang, A., Kim, Y.H., Kim, Y., and Schulz, R.A. (2001). Pannier is a transcriptional target and partner of Tinman during *Drosophila* cardiogenesis. *Dev Biol* 233, 425-436.
- Giot, L., Bader, J.S., Brouwer, C., Chaudhuri, A., Kuang, B., Li, Y., Hao, Y.L., Ooi, C.E., Godwin, B., Vitols, E., *et al.* (2003). A protein interaction map of *Drosophila melanogaster*. *Science* 302, 1727-1736.
- Gisselbrecht, S., Skeath, J.B., Doe, C.Q., and Michelson, A.M. (1996). heartless encodes a fibroblast growth factor receptor (DFR1/DFGF-R2) involved in the directional migration of early mesodermal cells in the *Drosophila* embryo. *Genes & development* 10, 3003-3017.
- Gould, D.B., Phalan, F.C., Breedveld, G.J., van Mil, S.E., Smith, R.S., Schimenti, J.C., Aguglia, U., van der Knaap, M.S., Heutink, P., and John, S.W. (2005). Mutations in *Col4a1* cause perinatal cerebral hemorrhage and porencephaly. *Science* 308, 1167-1171.
- Han, Z., and Olson, E.N. (2005). Hand is a direct target of Tinman and GATA factors during *Drosophila* cardiogenesis and hematopoiesis. *Development* 132, 3525-3536.
- Han, Z., Yi, P., Li, X., and Olson, E.N. (2006). Hand, an evolutionarily conserved bHLH transcription factor required for *Drosophila* cardiogenesis and hematopoiesis. *Development* 133, 1175-1182.
- Hartenstein, V. (1995). *Atlas of Drosophila Development*.

- Hidalgo, A., and Ingham, P. (1990). Cell patterning in the *Drosophila* segment: spatial regulation of the segment polarity gene *patched*. *Development* *110*, 291-301.
- Hulskamp, M., Pfeifle, C., and Tautz, D. (1990). A morphogenetic gradient of hunchback protein organizes the expression of the gap genes *Kruppel* and *knirps* in the early *Drosophila* embryo. *Nature* *346*, 577-580.
- Jamora C., Takizawa P.A., Zaarour R.F., Denesvre C., Faulkner D.J., and V., M. (1997). Regulation of Golgi structure through heterotrimeric G proteins. *Cell* *91*, 617-626.
- Katanaev, V.L., Ponzielli, R., Semeriva, M., and Tomlinson, A. (2005). Trimeric G protein-dependent frizzled signaling in *Drosophila*. *Cell* *120*, 111-122.
- Kennerdell, J.R., and Carthew, R.W. (1998). Use of dsRNA-mediated genetic interference to demonstrate that *frizzled* and *frizzled 2* act in the wingless pathway. *Cell* *95*, 1017-1026.
- Kiger, A.A., Baum, B., Jones, S., Jones, M.R., Coulson, A., Echeverri, C., and Perrimon, N. (2003). A functional genomic analysis of cell morphology using RNA interference. *Journal of biology* *2*, 27.
- Kim, Y.O., Park, S.J., Balaban, R.S., Nirenberg, M., and Kim, Y. (2004). A functional genomic screen for cardiogenic genes using RNA interference in developing *Drosophila* embryos. *Proc Natl Acad Sci U S A* *101*, 159-164.

- Kimbrell, D.A., Hice, C., Bolduc, C., Kleinhesselink, K., and Beckingham, K. (2002). The Dorothy enhancer has Tinman binding sites and drives hopscotch-induced tumor formation. *Genesis* 34, 23-28.
- Kinsella, B.T., Erdman, R.A., and Maltese, W.A. (1991). Posttranslational modification of Ha-ras p21 by farnesyl versus geranylgeranyl isoprenoids is determined by the COOH-terminal amino acid. *Proc Natl Acad Sci U S A* 88, 8934-8938.
- Knust, E. (2001). G protein signaling and asymmetric cell division. *Cell* 107, 125-128.
- Kolsch, V., and Paululat, A. (2002). The highly conserved cardiogenic bHLH factor Hand is specifically expressed in circular visceral muscle progenitor cells and in all cell types of the dorsal vessel during *Drosophila* embryogenesis. *Development genes and evolution* 212, 473-485.
- Kornberg, T., Siden, I., O'Farrell, P., and Simon, M. (1985). The engrailed locus of *Drosophila*: in situ localization of transcripts reveals compartment-specific expression. *Cell* 40, 45-53.
- Kosman, D., Ip, Y.T., Levine, M., and Arora, K. (1991). Establishment of the mesoderm-neuroectoderm boundary in the *Drosophila* embryo. *Science* 254, 118-122.

- Kraut, R., and Levine, M. (1991a). Mutually repressive interactions between the gap genes giant and Kruppel define middle body regions of the *Drosophila* embryo. *Development* *111*, 611-621.
- Kraut, R., and Levine, M. (1991b). Spatial regulation of the gap gene giant during *Drosophila* development. *Development* *111*, 601-609.
- Kremser, T., Gajewski, K., Schulz, R.A., and Renkawitz-Pohl, R. (1999). Tinman regulates the transcription of the beta3 tubulin gene (betaTub60D) in the dorsal vessel of *Drosophila*. *Dev Biol* *216*, 327-339.
- Lawrence, P.A., Bodmer, R., and Vincent, J.P. (1995). Segmental patterning of heart precursors in *Drosophila*. *Development* *121*, 4303-4308.
- Lawrence, P.A., Johnston, P., Macdonald, P., and Struhl, G. (1987). Borders of parasegments in *Drosophila* embryos are delimited by the fushi tarazu and even-skipped genes. *Nature* *328*, 440-442.
- Lee, H.H., and Frasch, M. (2000). Wingless effects mesoderm patterning and ectoderm segmentation events via induction of its downstream target sloppy paired. *Development* *127*, 5497-5508.
- Lee, Y.J., Dobbs, M.B., Verardi, M.L., and Hyde, D.R. (1990). dgq: a *drosophila* gene encoding a visual system-specific G alpha molecule. *Neuron* *5*, 889-898.
- Lewis, E.B. (1978). A gene complex controlling segmentation in *Drosophila*. *Nature* *276*, 565-570.

- Lilly, B., Zhao, B., Ranganayakulu, G., Paterson, B.M., Schulz, R.A., and Olson, E.N. (1995). Requirement of MADS domain transcription factor D-MEF2 for muscle formation in *Drosophila*. *Science* 267, 688-693.
- Maltese, W.A., and Robishaw, J.D. (1990). Isoprenylation of C-terminal cysteine in a G-protein gamma subunit. *J Biol Chem* 265, 18071-18074.
- Morata, G. (1993). Homeotic genes of *Drosophila*. *Current opinion in genetics & development* 3, 606-614.
- Morisato, D., and Anderson, K.V. (1994). The *spatzle* gene encodes a component of the extracellular signaling pathway establishing the dorsal-ventral pattern of the *Drosophila* embryo. *Cell* 76, 677-688.
- Muntz, K.H., Sternweis, P.C., Gilman, A.G., and Mumby, S.M. (1992). Influence of gamma subunit prenylation on association of guanine nucleotide-binding regulatory proteins with membranes. *Mol Biol Cell* 3, 49-61.
- Namba, R., Pazdera, T.M., Cerrone, R.L., and Minden, J.S. (1997). *Drosophila* embryonic pattern repair: how embryos respond to bicoid dosage alteration. *Development* 124, 1393-1403.
- Ocorr, K., Akasaka, T., and Bodmer, R. (2007). Age-related cardiac disease model of *Drosophila*. *Mechanisms of ageing and development* 128, 112-116.
- Ohashi, M., and Huttner, W.B. (1994). An elevation of cytosolic protein phosphorylation modulates trimeric G-protein regulation of secretory vesicle formation from the trans-Golgi network. *J Biol Chem* 269, 24897-24905.

- Ohguro, H., Fukada, Y., Takao, T., Shimonishi, Y., Yoshizawa, T., and Akino, T. (1991). Carboxyl methylation and farnesylation of transducin gamma-subunit synergistically enhance its coupling with metarhodopsin II. *Embo J* 10, 3669-3674.
- Olson, E.N. (2006). Gene regulatory networks in the evolution and development of the heart. *Science* 313, 1922-1927.
- Pankratz, M.J., Busch, M., Hoch, M., Seifert, E., and Jackle, H. (1992). Spatial control of the gap gene knirps in the Drosophila embryo by posterior morphogen system. *Science* 255, 986-989.
- Park, M., Venkatesh, T.V., and Bodmer, R. (1998). Dual role for the zeste-white3/shaggy-encoded kinase in mesoderm and heart development of Drosophila. *Dev Genet* 22, 201-211.
- Park, M., Wu, X., Golden, K., Axelrod, J.D., and Bodmer, R. (1996). The wingless signaling pathway is directly involved in Drosophila heart development. *Dev Biol* 177, 104-116.
- Parks, A.L., Cook, K.R., Belvin, M., Dompe, N.A., Fawcett, R., Huppert, K., Tan, L.R., Winter, C.G., Bogart, K.P., Deal, J.E., *et al.* (2004). Systematic generation of high-resolution deletion coverage of the Drosophila melanogaster genome. *Nature genetics* 36, 288-292.
- Ponzielli, R., Astier, M., Chartier, A., Gallet, A., Therond, P., and Semeriva, M. (2002). Heart tube patterning in Drosophila requires integration of axial and

- segmental information provided by the Bithorax Complex genes and hedgehog signaling. *Development* *129*, 4509-4521.
- Raftery, L.A., and Sutherland, D.J. (1999). TGF-beta family signal transduction in *Drosophila* development: from Mad to Smads. *Dev Biol* *210*, 251-268.
- Ray, R.P., Arora, K., Nusslein-Volhard, C., and Gelbart, W.M. (1991). The control of cell fate along the dorsal-ventral axis of the *Drosophila* embryo. *Development* *113*, 35-54.
- Reiss, Y., Stradley, S.J., Gierasch, L.M., Brown, M.S., and Goldstein, J.L. (1991). Sequence requirement for peptide recognition by rat brain p21ras protein farnesyltransferase. *Proc Natl Acad Sci U S A* *88*, 732-736.
- Reynolds, N.K., Schade, M.A., and Miller, K.G. (2005). Convergent, RIC-8-dependent Galpha signaling pathways in the *Caenorhabditis elegans* synaptic signaling network. *Genetics* *169*, 651-670.
- Rivera-Pomar, R., Lu, X., Perrimon, N., Taubert, H., and Jackle, H. (1995). Activation of posterior gap gene expression in the *Drosophila* blastoderm. *Nature* *376*, 253-256.
- Rusch, J., and Levine, M. (1996). Threshold responses to the dorsal regulatory gradient and the subdivision of primary tissue territories in the *Drosophila* embryo. *Current opinion in genetics & development* *6*, 416-423.
- Sanford, J.L., Edwards, J.D., Mays, T.A., Gong, B., Merriam, A.P., and Rafael-Fortney, J.A. (2005). Claudin-5 localizes to the lateral membranes of

cardiomyocytes and is altered in utrophin/dystrophin-deficient cardiomyopathic mice. *Journal of molecular and cellular cardiology* 38, 323-332.

Santos, A.C., and Lehmann, R. (2004a). Germ cell specification and migration in *Drosophila* and beyond. *Curr Biol* 14, R578-589.

Santos, A.C., and Lehmann, R. (2004b). Isoprenoids control germ cell migration downstream of HMGCoA reductase. *Dev Cell* 6, 283-293.

Schaefer, M., Petronczki, M., Dorner, D., Forte, M., and Knoblich, J.A. (2001). Heterotrimeric G proteins direct two modes of asymmetric cell division in the *Drosophila* nervous system. *Cell* 107, 183-194.

Schneider, D.S., Jin, Y., Morisato, D., and Anderson, K.V. (1994). A processed form of the Spatzle protein defines dorsal-ventral polarity in the *Drosophila* embryo. *Development* 120, 1243-1250.

Schulz, S., Huber, A., Schwab, K., and Paulsen, R. (1999). A novel Ggamma isolated from *Drosophila* constitutes a visual G protein gamma subunit of the fly compound eye. *J Biol Chem* 274, 37605-37610.

Schwabe, T., Bainton, R.J., Fetter, R.D., Heberlein, U., and Gaul, U. (2005). GPCR signaling is required for blood-brain barrier formation in *drosophila*. *Cell* 123, 133-144.

Shishido, E., Ono, N., Kojima, T., and Saigo, K. (1997). Requirements of DFR1/Heartless, a mesoderm-specific *Drosophila* FGF-receptor, for the formation



of heart, visceral and somatic muscles, and ensheathing of longitudinal axon tracts in CNS. *Development* 124, 2119-2128.

Simard, A., Di Pietro, E., Young, C.R., Plaza, S., and Ryan, A.K. (2006).

Alterations in heart looping induced by overexpression of the tight junction protein Claudin-1 are dependent on its C-terminal cytoplasmic tail. *Mech Dev* 123, 210-227.

Simpson-Brose, M., Treisman, J., and Desplan, C. (1994). Synergy between the hunchback and bicoid morphogens is required for anterior patterning in *Drosophila*. *Cell* 78, 855-865.

Spradling, A.C., Stern, D., Beaton, A., Rhem, E.J., Lavery, T., Mozden, N., Misra, S., and Rubin, G.M. (1999). The Berkeley *Drosophila* Genome Project gene disruption project: Single P-element insertions mutating 25% of vital *Drosophila* genes. *Genetics* 153, 135-177.

Starz-Gaiano, M., Cho, N.K., Forbes, A., and Lehmann, R. (2001). Spatially restricted activity of a *Drosophila* lipid phosphatase guides migrating germ cells. *Development* 128, 983-991.

Struhl, G. (1989). Differing strategies for organizing anterior and posterior body pattern in *Drosophila* embryos. *Nature* 338, 741-744.

Struhl, G., Johnston, P., and Lawrence, P.A. (1992). Control of *Drosophila* body pattern by the hunchback morphogen gradient. *Cell* 69, 237-249.

- Tabata, T., Eaton, S., and Kornberg, T.B. (1992). The *Drosophila* hedgehog gene is expressed specifically in posterior compartment cells and is a target of engrailed regulation. *Genes & development* 6, 2635-2645.
- Tautz, D. (1988). Regulation of the *Drosophila* segmentation gene hunchback by two maternal morphogenetic centres. *Nature* 332, 281-284.
- Tepass, U. (1997). Epithelial differentiation in *Drosophila*. *Bioessays* 19, 673-682.
- Tepass, U., and Hartenstein, V. (1994). The development of cellular junctions in the *Drosophila* embryo. *Dev Biol* 161, 563-596.
- Tepass, U., Tanentzapf, G., Ward, R., and Fehon, R. (2001). Epithelial cell polarity and cell junctions in *Drosophila*. *Annual review of genetics* 35, 747-784.
- Thibault, S.T., Singer, M.A., Miyazaki, W.Y., Milash, B., Dompe, N.A., Singh, C.M., Buchholz, R., Demsky, M., Fawcett, R., Francis-Lang, H.L., *et al.* (2004). A complementary transposon tool kit for *Drosophila melanogaster* using P and piggyBac. *Nature genetics* 36, 283-287.
- Van Doren, M., Broihier, H.T., Moore, L.A., and Lehmann, R. (1998). HMG-CoA reductase guides migrating primordial germ cells. *Nature* 396, 466-469.
- Wang, H., Ng, K.H., Qian, H., Siderovski, D.P., Chia, W., and Yu, F. (2005). Ric-8 controls *Drosophila* neural progenitor asymmetric division by regulating heterotrimeric G proteins. *Nature cell biology* 7, 1091-1098.

Ward, E.J., and Skeath, J.B. (2000). Characterization of a novel subset of cardiac cells and their progenitors in the *Drosophila* embryo. *Development* *127*, 4959-4969.

Wessells, R.J., and Bodmer, R. (2007). Cardiac aging. *Seminars in cell & developmental biology* *18*, 111-116.

Wigglesworth, V.B. (1984). "Insect Physiology", 4th Ed. Chapman and Hall, London. "Insect Physiology", 4th Ed Chapman and Hall, London.

Wu, V.M., Schulte, J., Hirschi, A., Tepass, U., and Beitel, G.J. (2004). Sinuous is a *Drosophila* claudin required for septate junction organization and epithelial tube size control. *J Cell Biol* *164*, 313-323.

Wu, X., Golden, K., and Bodmer, R. (1995). Heart development in *Drosophila* requires the segment polarity gene wingless. *Dev Biol* *169*, 619-628.

Xu, X., Yin, Z., Hudson, J.B., Ferguson, E.L., and Frasch, M. (1998). Smad proteins act in combination with synergistic and antagonistic regulators to target Dpp responses to the *Drosophila* mesoderm. *Genes & development* *12*, 2354-2370.

Yarfitz, S., Niemi, G.A., McConnell, J.L., Fitch, C.L., and Hurley, J.B. (1991). A G beta protein in the *Drosophila* compound eye is different from that in the brain. *Neuron* *7*, 429-438.

Yi, P., Han, Z., Li, X., and Olson, E.N. (2006). The mevalonate pathway controls heart formation in *Drosophila* by isoprenylation of Ggamma1. *Science* *313*, 1301-1303.

Yin, Z., and Frasch, M. (1998). Regulation and function of tinman during dorsal mesoderm induction and heart specification in *Drosophila*. *Dev Genet* 22, 187-200.

Yu, F., Cai, Y., Kaushik, R., Yang, X., and Chia, W. (2003). Distinct roles of Galphai and Gbeta13F subunits of the heterotrimeric G protein complex in the mediation of *Drosophila* neuroblast asymmetric divisions. *J Cell Biol* 162, 623-633.

Zaffran, S., Astier, M., Gratecos, D., Guillen, A., and Semeriva, M. (1995). Cellular interactions during heart morphogenesis in the *Drosophila* embryo. *Biology of the cell / under the auspices of the European Cell Biology Organization* 84, 13-24.

Zaffran, S., and Frasch, M. (2002). Early signals in cardiac development. *Circ Res* 91, 457-469.

Zhang, N., Zhang, J., Purcell, K.J., Cheng, Y., and Howard, K. (1997). The *Drosophila* protein Wunen repels migrating germ cells. *Nature* 385, 64-67.

Zolk, O., Kouchi, I., Schnabel, P., and Bohm, M. (2000). Heterotrimeric G proteins in heart disease. *Canadian journal of physiology and pharmacology* 78, 187-198.

## VITAE

Peng Yi was born in the city of Jinan of Shandong province, People's Republic of China, on April 12, 1980, the son of Xianwei Yi and Guohua Ding. After completing his study at Shandong province experimental high school in 1998, he decided to go the University of Science and Technology of China to study molecular biology. From 1998 to 2003, he got his two major achievements, a bachelor degree in Molecular Biology and a beautiful girlfriend Wei Zhang. On Aug 13, Wei and Peng flied over the Pacific Ocean to United States and start their graduate study in the molecular biology department of UT Southwestern Medical Center at Dallas. In December 2003, he joined Dr. Eric Olson's lab to study *Drosophila* heart development. The year of 2006 has been the best year to him, in which he published his first paper on *Science* in September, and Wei finally agreed to marry him. They had a lovely wedding back in his hometown on May 6<sup>th</sup>, 2007.

Permanent Address: 8820 Southwestern Blvd.  
#905  
Dallas, TX, 75206  
U.S.A.